UNIVERSIDADE ESTADUAL DE PONTA GROSSA
PRÓ-REITORIA DE PESQUISA E PÓS-GRADUAÇÃO
PROGRAMA DE PÓS-GRADUAÇÃO EM ODONTOLOGIA

CAROLINA ALEJANDRA PARDO DÍAZ

AVALIAÇÃO DO EFEITO DE UM ADESIVO UNIVERSAL CARREGADO COM NANOPARTÍCULAS DE COBRE, ZINCO E VIDRO BIOATIVO (45S5), NA ATIVIDADE DAS MMPs 2 E 9, NA PERDA MINERAL E NAS PROPIEDADES MECÂNICAS DA INTERFACE EM DENTES RESTAURADOS COM RESINA COMPOSTA SUBMETIDOS A UM DESAFIO CARIOGÊNICO *IN VITRO*.

PONTA GROSSA
2026

CAROLINA ALEJANDRA PARDO DÍAZ

AVALIAÇÃO DO EFEITO DE UM ADESIVO UNIVERSAL CARREGADO COM NANOPARTÍCULAS DE COBRE, ZINCO E VIDRO BIOATIVO (45S5), NA ATIVIDADE DAS MMPs 2 E 9, NA PERDA MINERAL E NAS PROPIEDADES MECÂNICAS DA INTERFACE EM DENTES RESTAURADOS COM RESINA COMPOSTA SUBMETIDOS A UM DESAFIO CARIOGÊNICO *IN VITRO*.

Tese apresentada para obtenção do título de Doutora em Odontologia na Universidade Estadual de Ponta Grossa, Área de Dentística Restauradora

Orientador: Prof. Dr. Alessandro Dourado Loguercio.
Coorientador: Prof. Dr. Eduardo Fernández Godoy.

PONTA GROSSA
2026

Pardo Díaz, Carolina Alejandra

P226 Avaliação do efeito de um adesivo universal carregado com nanopartículas de cobre, zinco e vidro bioativo (45S5), na atividade das MMPs 2 e 9, na perda mineral e nas propriedades mecânicas da interface em dentes restaurados com resina composta submetidos a um desafio cariogênico in vitro / Carolina Alejandra Pardo Díaz. Ponta Grossa, 2026.

142f. :il.

Tese (Doutorado em Odontologia - Área de Concentração Dentística Restauradora), Universidade Estadual de Ponta Grossa.

Orientador: Prof. Dr. Alessandro Dourado Loguercio.
Coorientador: Prof. Dr. Eduardo Fernández Godoy

1.Adesivos dentinários. 2. Nanopartículas.3. Vidro bioativo. 4. MMPs. 5. Citotoxicidade. 6. União à dentina.I. Alessandro Dourado Loguercio. II. Eduardo Fernández Godoy. III. Universidade Estadual de Ponta Grossa. IV. Título.

CDD: 617.6

Ficha catalográfica elaborada por Maria Lúcia Madruga CRB9/952

CAROLINA ALEJANDRA PARDO DÍAZ

AVALIAÇÃO DO EFEITO DE UM ADESIVO UNIVERSAL CARREGADO COM NANOPARTÍCULAS DE COBRE, ZINCO E VIDRO BIOATIVO (45S5), NA ATIVIDADE DAS MMPs 2 E 9, NA PERDA MINERAL E NAS PROPIEDADES DA INTERFACE EM DENTES RESTAURADOS COM RESINA COMPOSTA SUBMETIDOS A UM DESAFIO CARIOGÊNICO *IN VITRO*.

Tese apresentada ao Programa de Pós-graduação Stricto sensu em Odontologia da Universidade Estadual de Ponta Grossa, como requisito parcial à obtenção do título de Doutor em Odontologia, área de concentração em Dentística Restauradora linha de pesquisa de Pesquisa Clínica em Odontologia.

Ponta Grossa, 11 de fevereiro de 2026.

gov.br Documento assinado digitalmente
ALESSANDRO DOURADO LOGUERCIO
Data: 13/05/2026 09:14:29-0300
Verifique em https://validar.iti.gov.br

Prof. Dr. Alessandro Loguercio Dourado
Universidade Estadual de Ponta Grossa

gov.br Documento assinado digitalmente
PAULO VITOR FARAGO
Data: 08/06/2026 17:33:21-0300
Verifique em https://validar.iti.gov.br

Prof. Paulo Vitor Farago
Universidade Estadual de Ponta Grossa

gov.br Documento assinado digitalmente
CESAR AUGUSTO GALVAO ARRAIS
Data: 08/06/2026 13:28:26-0300
Verifique em https://validar.iti.gov.br

Prof. Cesar Augusto Galvão Arrais
Universidade Estadual de Ponta Grossa

Prof. Cristian Bersezio Miranda
Universidade do Chile

Prof. Dr. Eduardo Fernández Godoy
Universidade do Chile

A Miguel e Lucas, minha inspiração constante.

AGRADECIMENTOS

Expresso minha mais profunda gratidão a todas as pessoas e instituições que, de forma direta ou indireta, contribuíram e apoiaram durante a realização deste trabalho.

Desejo agradecer ao Professor Dr. Eduardo Fernández Godoy, por sua confiança, orientação e paciência ao longo deste processo. Obrigada por acompanhar os momentos mais difíceis, desde o início em plena pandemia, passando pela dolorosa perda de meu pai, até a celebração pela chegada de meu filho. Seu apoio incondicional, seus valiosos conhecimentos e respeito foram fundamentais para a conclusão bem-sucedida deste trabalho.

Da mesma forma, agradeço ao Professor Dr. Alessandro D. Loguercio, por apoiar e prestigiar este trabalho e por me proporcionar a oportunidade de obter dupla titulação. Obrigada por seus ensinamentos e agradeço também, por sua humanidade e constante respeito.

Ao Laboratório de Nanobiomateriais da Universidade do Chile, dirigido pelo Professor Dr. Cristian Covarrubias, e ao seu coletivo, muito obrigada pela generosidade em compartilhar conhecimento e pelas trocas de ideias que enriqueceram esta pesquisa.

Aos pesquisadores do Brasil: ao Dr. Fabio Dupart Nascimento, por me receber na Universidade Estadual de São Paulo, e à Marina Chiari, pós-doutoranda. Agradeço a generosidade no ensino e por possibilitar o desenvolvimento de testes fundamentais para este projeto, além de engrandecer os resultados deste trabalho.

Ao grupo de pesquisa “Bleach & Bond” da Universidade Estadual de Ponta Grossa, por acompanhar as análises laboratoriais com dedicação, mesmo em dias de descanso, permitindo que eu aproveitasse ao máximo minhas estadias. Obrigada por me permitir fazer parte deste reconhecido grupo, caracterizado pelo seu empenho e dedicação.

À Universidade do Chile, por fornecer recursos, instalações e apoio necessários para a realização desta tese. Aos docentes do Comitê Acadêmico do Doutorado em Ciências Odontológicas.

À Universidade Estadual de Ponta Grossa (UEPG) por abrir suas portas e oferecer um ambiente acadêmico enriquecedor para o desenvolvimento desta pesquisa. A UEPG tornou-se parte fundamental deste caminho, contribuindo significativamente para meu crescimento pessoal, profissional e científico.

Finalmente, agradeço à minha família, pilar fundamental em cada etapa da minha vida. Ao meu pai, que me apoia desde o céu. À minha mãe, pela sua paciência e amor incondicional; por ser a melhor companheira nas minhas viagens e avó do Lucas. Ao meu esposo Miguel, pelo seu apoio constante, amor e paciência em todos os meus desafios profissionais. Ao meu filho Lucas, à minha irmã, Patricia, e aos meus sobrinhos, León e Pedro, por tornarem a minha vida mais doce. Aos meus amigos e a toda a minha família estendida, pela proximidade e apoio permanente.

A todas as pessoas que, de alguma forma, contribuíram com seu tempo, conhecimentos ou apoio nesta pesquisa. Sem a colaboração de vocês, esta conquista não teria sido possível.

Agradeço a Deus por sempre me mostrar o caminho certo.

RESUMO

Pardo-Díaz C. **Avaliação Do Efeito de um Adesivo Universal Carregado com Nanopartículas de Cobre, Zinco e Vidro Bioativo (45S5), na Atividade das MMPs 2 e 9, na Perda Mineral e nas Propiedades Mecânicas da Interface em Dentes Restaurados com Resina Composta Submetidos a um Desafio Cariogênico *in vitro*.** [Tese] Doutorado em Dentística Restauradora. Ponta Grossa: Universidade Estadual de Ponta Grossa; 2026.

Objetivo: Avaliar de forma abrangente o efeito de um adesivo universal modificado com nanopartículas de zinco e cobre (ZnO/Cu) e vidro bioativo (VB 45S5) sobre a estabilidade da união à dentina, considerando os mecanismos de citotoxicidade dos adesivos universais comerciais, suas propriedades biológicas e seu comportamento sob um desafio cariogênico in vitro. **Materiais e Métodos:** Inicialmente, foram investigados os mecanismos moleculares de citotoxicidade (apoptose e necrose) de adesivos universais comerciais em células osteoblásticas tipo Saos-2, a fim de estabelecer um panorama de segurança biológica. Posteriormente, sistemas adesivos experimentais contendo ZnO/Cu (0,2%/2,5%) e VB (5% e 10%) foram avaliados quanto à viabilidade celular (ensaio MTS), atividade antibacteriana (contagem de unidades formadoras de colônias, UFC), potencial de mineralização (ensaio em fluido corporal simulado, SBF; e espectroscopia de energia dispersiva de raios X, EDX), grau de conversão (espectroscopia Raman), atividade enzimática das MMPs (zimografia in situ) e resistência de união (μTBS), antes e após um desafio cariogênico in vitro. As análises estatísticas incluíram ANOVA de uma e duas vias, teste post-hoc de Tukey e teste t de Student ($\alpha=0,05$). **Resultados:** Os adesivos universais comerciais induziram morte celular por diferentes vias moleculares, destacando a importância de uma avaliação biológica prévia. A incorporação de VB, isoladamente ou em combinação com ZnO/Cu, reduziu significativamente a atividade bacteriana e aumentou a deposição de Ca e P, indicando efeito mineralizante ($p<0,05$). Nem a citocompatibilidade nem o grau de conversão foram afetados negativamente pela incorporação de nanopartículas ($p>0,05$). Apesar da persistência de elevada atividade das MMPs, os adesivos contendo 10% de VB — particularmente quando combinados com ZnO/Cu — demonstraram maior estabilidade da união após o desafio cariogênico, especialmente sob condições autocondicionantes. **Conclusão:** A incorporação de nanopartículas de vidro bioativo em adesivos universais modificados com ZnO/Cu melhora a estabilidade da união à dentina, principalmente por meio de mecanismos de remineralização e atividade antibacteriana, sem comprometer a citocompatibilidade ou o grau de conversão. No entanto, não promove inibição imediata da atividade das MMPs, sugerindo que a estabilidade interfacial está mais fortemente associada a processos de biomineralização do que à modulação enzimática direta.

Palavras-chave: Adesivos dentinários; Nanopartículas; Vidro bioativo; Citotoxicidade; MMPs; União à dentina.

ABSTRACT

Pardo-Díaz C. **Evaluation of the Effect of a Universal Adhesive Loaded with Copper, Zinc and Bioactive Glass (45S5) Nanoparticles on the Activity of MMPs 2 and 9, Mineral Loss and Mechanical Properties of the Interface in Teeth Restored with Composite Resin Submitted to an *in vitro* Cariogenic Challenge.** [Thesis] Doctorate in Restorative Dentistry. Ponta Grossa: State University of Ponta Grossa; 2026.

Objective: To comprehensively evaluate the effect of a universal adhesive modified with zinc and copper nanoparticles (ZnO/Cu) and bioactive glass (BG 45S5) on dentin bond stability, considering the cytotoxic mechanisms of commercial universal adhesives, their biological properties, and their behavior under an in vitro cariogenic challenge. **Materials and Methods:** Initially, the molecular mechanisms of cytotoxicity (apoptosis and necrosis) of commercial universal adhesives were investigated in Saos-2 osteoblast-like cells to establish a biological safety baseline. Subsequently, experimental adhesive systems containing ZnO/Cu (0.2%/2.5%) and BG (5% and 10%) were evaluated in terms of cell viability (MTS assay), antibacterial activity (colony-forming unit count, CFU), mineralization potential (simulated body fluid assay, SBF; and energy-dispersive X-ray spectroscopy, EDX), degree of conversion (Raman spectroscopy), MMP enzymatic activity (in situ zymography), and bond strength (μTBS) before and after an in vitro cariogenic challenge. Statistical analyses included one- and two-way ANOVA, Tukey's post-hoc test, and Student's t-test ($\alpha=0.05$). **Results:** Commercial universal adhesives induced cell death through distinct molecular pathways, highlighting the importance of prior biological assessment. The incorporation of BG, either alone or combined with ZnO/Cu, significantly reduced bacterial activity and increased Ca and P deposition, indicating a mineralizing effect ($p<0.05$). Neither cytocompatibility nor degree of conversion was adversely affected by nanoparticle incorporation ($p>0.05$). Despite persistently high MMP activity, adhesives containing 10% BG—particularly when combined with ZnO/Cu—demonstrated improved bond stability after cariogenic challenge, especially under self-etch conditions. **Conclusion:** The incorporation of bioactive glass nanoparticles into ZnO/Cu-modified universal adhesives enhances dentin bond stability primarily through remineralization and antibacterial mechanisms, without compromising cytocompatibility or degree of conversion. However, it does not promote immediate inhibition of MMP activity, suggesting that interfacial stability is more strongly associated with biomineralization processes than with direct enzymatic modulation.

Keywords: Dentin adhesives; Nanoparticles; Bioactive glass; Cytotoxicity; MMPs; Dentin bonding.

LISTA DE FIGURAS

Figura 1. Representative Flow Cytometry Images. (Artigo 1). 22
Figura 2. Inmunblot Analysis and Quantification of Activated Caspase-3. (Artigo 1). 23
Figura 3. Representative images of cell nuclei of Saos-2 cells treated with Universal Adhesives. (Artigo1). 24
Figura 4. Cell viability of Saos-2 cultured for 24 h with different universal adhesives. (Artigo 1). 24
Figura 5. Representative back-scattering SEM images of the resin–dentine interfaces. 46
Figura 6. EDX spectrum of the resin–dentine bonded interfaces 47
Figura 7. Representative flow diagram of the formation of the different groups 57
Figura 8. Nanoleakage representative scanning electron microscopy images of the resin–dentin interfaces. 66
Figura 9 Representative back-scattering scanning electron microscopy images and EDX spectra. 66
Figura 10. Confocal laser scanning microscopy (CLSM) images of the resin-dentin bonded interfaces 68
Figura 11. Field-Emission scanning electron microscopy (FE-SEM) images of zinc oxide (ZnO), copper (Cu), and bioactive glass (BG) nanoparticles. 84
Figura 12. FTIR–ATR spectrum of bioactive glass (BG) nanoparticles. 85
Figura 13. FE-SEM images of nanoparticle-modified adhesives after exposure to Streptococcus mutans. 86
Figura 14. Mineralization assessment of adhesive specimens immersed in simulated body fluid 88

LISTA DE TABELAS

Tabela 1. Manufacturer and Composition details of Universal Adhesives evaluated 18
Tabela 2. Percentages of viable cells, early apoptotic cells, late apoptotic cells, and necrotic cells obtained through flow cytometry. Ambar universal (AU), Single Bond Universal (SB), and Prime & Bond universal (PB). ([a]) 22
Tabela 3. Universal adhesive system (batch number), composition (∗) and application mode. 38
Tabela 4. Means and standard deviations of microtensile bond strength (MPa) obtained in each experimental condition with Prime&Bond Active. 43
Tabela 5. Fracture Pattern, pre-tested failures and number of resin-dentin sticks (n) tested in the microtensile bond strength test in each experimental condition with Prime&Bond Active (*) 43
Tabela 6. Means and standard deviations of microtensile bond strength (MPA) obtained in each experimental condition with Ambar Universal (*). 44
Tabela 7. Fracture pattern, pre-tested failures and number of resin-dentin sticks (n) tested in the microtensile bond strength test in each experimental condition. 44
Tabela 8. Means and standard deviations of nanoleakage (%) obtained in each experimental condition with Prime&Bond Active (*). 45
Tabela 9. Means and standard deviations of nanoleakage (%) obtained in each experimental condition with Ambar Universal (*). 45
Tabela 10. Zinc Oxide and copper nanoparticles manufacturer specifications. 58
Tabela 11. Materials, composition and application mode of the adhesive system and composite resin. (*) 60
Tabela 12. Failure pattern, mean and standard-deviation values of microtensile bond strength (μTBS; MPa)(DC;%) (*)., nanoleakage (NL;%) and in situ degree of conversion. 65
Tabela 13. Antibacterial activity against S. mutans for the experimental adhesive formulations. 86
Tabela 14. Cell viability of human gingival mesenchymal stem cells (hGMSCs) exposed to the adhesive formulations at 3 and 7 days (mean % ± SD relative to the positive control) 87
Tabela 15. Degree of Conversion of the experimental adhesive formulations (mean ± SD). 89
Tabela 16. Microtensile bond strength (μTBS, MPa; mean ± SD) of the experimental adhesives under self-etch (SE) and etch-and-rinse (E&R) strategies. 90
Tabela 17. Failure mode distribution (%) for each adhesive formulation under self-etch (SE) and etch-and-rinse (ER) strategies 90
Tabela 18. Universal adhesive system and batch number; composition and adhesive strategy. 104
Tabela 19. Microtensile bond strength **(**μTBS) at baseline and after cariogenic challenge 107
Tabela 20**.** Nanoleakage (NL) at baseline and after cariogenic challenge. 109

SUMÁRIO

1 INTRODUÇÃO 10
2 PROPOSIÇÃO 13
2.1 PROPOSIÇÃO GERAL 13
2.2 PROPOSIÇÃO ESPECÍFICA 13
3 MATERIAL E MÉTODOS 14
3.1 ARTIGO 1: MOLECULAR MECHANISMS OF CYTOTOXICITY IN SAOS-2 OSTEOBLAST-LIKE CELLS EXPOSED TO UNIVERSAL DENTAL ADHESIVES 14
3.2 ARTIGO 2: ADHESIVE PROPERTIES OF UNIVERSAL ADHESIVES SYSTEMS CONTAINING ZINC OXIDE AND COPPER NANOPARTICLES ON SOUND DENTINE: A 2-YEAR EVALUATION 33
3.3 ARTIGO 3: EVALUATION OF ADHESIVE PROPERTIES AND ENZYMATIC ACTIVITY AT THE HYBRID LAYER OF A SIMPLIFIED ADHESIVE LOADED WITH 0.2% CU AND 5% ZNO NANOPARTICLES: A RANDOMIZED CLINICAL TRIAL AND EX VIVO ANALYSIS 54
3.4 ARTIGO 4 - BIOACTIVE AND ANTIBACTERIAL UNIVERSAL ADHESIVES CONTAINING ZNO/CU AND BIOACTIVE GLASS NANOPARTICLES 75
3.5 ARTIGO 5 EFFECTS OF ZNO/CU AND BIOACTIVE GLASS-MODIFIED UNIVERSAL ADHESIVES ON BIOLOGICAL PROPERTIES, BOND STRENGTH, AND INTERFACIAL STABILITY UNDER CARIOGENIC CHALLENGE 98
4 DISCUSSÃO 121
5 CONCLUSÃO 133
REFERÊNCIAS 135
ANEXO A – APROVAÇÃO DO COMITÊ DE ÉTICA 140

1 INTRODUÇÃO

A cárie dentária permanece como uma das doenças crônicas mais prevalentes em nível mundial, com impacto significativo na saúde pública[1,2]. Apesar dos avanços nos materiais restauradores, a longevidade clínica das restaurações adesivas permanece limitada, sendo a degradação da interface resina–dentina um fator preponderante para o insucesso restaurador.[3-5]

O procedimento restaurador envolve a preparação da estrutura mineral do dente por meio de agentes ácidos, para que o adesivo resinoso possa selar a interface contra a infiltração de fluidos intraorais. Portanto, a fixação ao dente confere uma união micromecânica entre a resina composta e os tecidos duros do dente. Na dentina, essa camada de transição é denominada camada híbrida[6,7]. Embora a adesão ao esmalte seja previsível, a união à dentina é intrinsecamente mais complexa e suscetível à degradação[8,9].

A biocompatibilidade dos adesivos dentários constitui um requisito fundamental antes de qualquer modificação de formulação. A morte celular pode ser induzida por mecanismos como a necrose e a apoptose. A necrose é acompanhada de lise celular e resposta inflamatória[10-12]. Por outro lado, a apoptose é um processo de morte celular programada e, em condições fisiológicas não induz inflamação, embora sua desregulação possa comprometer os tecidos pulpares e periodontais adjacentes[12].

Diversas estratégias têm sido propostas para melhorar a estabilidade da interface adesiva, sendo as metaloproteinases da matriz (MMPs) fundamentais nesse processo[13]. Durante o procedimento adesivo, certas proteínas do colágeno permanecem desprotegidas e suscetíveis à degradação enzimática[13,14]. A liberação e ativação das MMPs durante esses procedimentos associa-se diretamente à degradação da interface adesiva[13]. Essa degradação contribui para o desenvolvimento de cárie secundária, favorecida pela invasão bacteriana presente no biofilme oral e pela produção de ácidos orgânicos que induzem a desmineralização dos tecidos adjacentes à restauração, comprometendo suas propriedades mecânicas e levando à falha do selamento adesivo e eventual fracasso da restauração[15,16].

Entre as estratégias investigadas para inibir as MMPs e prolongar a longevidade da camada híbrida, destaca-se a incorporação de nanopartículas (NPs)

metálicas.[17], As NPs de óxido de zinco (ZnO) e cobre (Cu) baseiam sua ação protetora na estabilização do colágeno dentinário: o zinco ocupa sítios de clivagem das MMPs nas moléculas de colágeno, promovendo resistência proteolítica e induzindo a formação de cristais de hidroxiapatita nas fibras colágenas; o Cu inibe a MMP-2 e estimula a secreção de inibidores teciduais de MMPs (TIMPs), além de ativar a enzima lisil-oxidase (LOX), favorecendo o entrecruzamento das fibras de colágeno.[17,18.] Além disso, NPs de cobre e óxido de zinco demonstraram melhorar as propriedades antimicrobianas quando incorporadas a adesivos universais[17-19]. Os principais efeitos tóxicos que as NPs metálicas induzem nas bactérias ocorrem pelo contato direto com a superfície celular, danificando-a e, portanto, aumentando a permeabilidade celular. Além disso, as NPs metálicas podem liberar íons no espaço extracelular, penetrando nas células e alterando seus processos biológicos, induzindo a produção de espécies reativas de oxigênio (ROS), que danificam as membranas celulares bacterianas sem afetar as células mamíferas[20]. Essa combinação resulta em um efeito sinérgico antibacteriano e potencializa o entrecruzamento da rede colágena[16], já que o cobre influencia indiretamente o entrecruzamento por meio da enzima lisil-oxidase (LOX), dependente de cobre[20,21]; enquanto o ZnO contribui a mineralização da dentina[19].

Contudo, a degradação da camada híbrida ainda não está completamente resolvida, o que impulsionou a exploração de materiais com propriedades remineralizantes. O Vidro Bioativo (VB), utilizado desde a década de 1960, destaca-se por sua capacidade de formar uma camada de hidroxiapatita que se liga a tecidos moles e duros[22]. Essas mudanças estão associadas a alterações no pH ambiental que promovem a liberação de íons cálcio e fosfato. Nos tecidos dentários, atua favorecendo a ação anticariogênica e o processo de remineralização[23]. Além disso, o VB, com sua capacidade de liberar outros íons, como íons Ca^{2+}, PO_4^{3-} e Na^{+}[22], é capaz de danificar as membranas celulares das bactérias, impedindo sua proliferação[22,23], promovendo um efeito antibacteriano. Na odontologia, o VB tem sido proposto como revestimento para implantes[22], em pastas ou géis remineralizantes[23], e como componente para adesivos e resinas compostas, avaliando sua capacidade de remineralizar a dentina e incorporar propriedades antibacterianas[24], melhorando as propriedades mecânicas e protegendo o colágeno da degradação proteolítica graças ao seu efeito mineralizante[25-27].

A biodegradação, inerente aos materiais resinosos dentro do ambiente oral[28], favorece que a comunidade microbiana, dominada por bactérias acidogênicas e

acidófilas, provoque a degradação da interface, bem como a perda mineral circundante à restauração, especialmente em indivíduos com alto risco de cárie[9,13,18]. Dada a complexidade da interação entre os materiais dentários e o ambiente biológico, é fundamental não apenas avaliar a eficácia de novas formulações em termos de suas propriedades mecânicas e bioativas, mas também compreender sua biocompatibilidade e os mecanismos de interação em nível celular[10,11]. A citotoxicidade dos adesivos dentários, mediada pela liberação de monômeros residuais, pode afetar a viabilidade das células pulpares, comprometendo a saúde dos tecidos adjacentes[10]. Portanto, qualquer estratégia para melhorar a longevidade das restaurações deve considerar a segurança biológica dos materiais incorporados.

Considerando que a cárie secundária é a principal causa de falha das restaurações, e que a combinação de VB com NPs de ZnO/Cu em adesivos dentais não havia sido explorada para melhorar a estabilidade da interface adesiva, esta tese propõe avaliar o efeito da incorporação de NPs de VB a um adesivo modificado com NPs de ZnO e Cu. As NPs de VB reduzem a perda mineral e promovem efeito antibacteriano, enquanto as NPs de As NPs de ZnO e Cu têm sido associadas à modulação do biofilme cariogênico e à redução da atividade proteolítica das MMPs em condições específicas, enquanto as NPs de VB podem reduzir a perda mineral e favorecer mecanismos de remineralização.[16,18,19,27] Essa estratégia apresenta-se como uma alternativa promissora para melhorar a estabilidade da união adesiva à dentina, aumentando a longevidade das restaurações.

Nesse contexto, a presente tese foi estruturada em cinco estudos complementares: (1) investigação dos mecanismos moleculares de citotoxicidade de adesivos universais comerciais em células osteoblásticas Saos-2;10 (2) avaliação do desempenho adesivo de longo prazo de sistemas modificados com ZnO/Cu em dentina hígida ao longo de dois anos; (3) análise da atividade enzimática e estabilidade interfacial em condições clínicas e ex vivo por meio de um ensaio clínico randomizado; (4) desenvolvimento e caracterização biológica de formulações adesivas bioativas contendo VB; e (5) avaliação da estabilidade da união e da perda mineral sob desafio cariogênico in vitro com as formulações que combinam VB e ZnO/Cu.27 Essa abordagem integrada e progressiva permite compreender, desde a segurança biológica até a estabilidade interfacial em condições adversas, o potencial das formulações propostas para melhorar a longevidade das restaurações adesivas.

2 PROPOSIÇÃO

2.1 PROPOSIÇÃO GERAL

Avaliar o efeito da incorporação de nanopartículas de vidro bioativo (VB) em um adesivo dental universal, modificado com nanopartículas (NPs) metálicas (ZnO, a 5 inicialmente e, 2,5% nos estudos finais; e Cu a 0,2%), na estabilidade da união adesiva à dentina em dentes restaurados com resina composta submetidos a um desafio cariogênico *in vitro*.

2.2 PROPOSIÇÃO ESPECÍFICA

Investigar os mecanismos de citotoxicidade (apoptose e necrose) de adesivos universais comerciais em células osteoblásticas tipo Saos-2 de origem humana, elucidando a indução diferencial das vias de apoptose e necrose.

Avaliar o efeito da adição de nanopartículas de óxido de zinco e cobre (ZnO/CuNp) a adesivos universais (UA) sobre a resistência de união à microtração (μTBS), a nanoinfiltração (NL) e a presença de ZnO/CuNp na camada híbrida, no tempo imediato (IM) e após 2 anos de armazenamento em água (2y).

Avaliar o efeito de um adesivo carregado com 0,2% de cobre (Cu) e 5% de nanopartículas de óxido de zinco (ZnO) sobre suas propriedades adesivas e a atividade enzimática na camada híbrida, ex vivo, em um modelo clínico randomizado.

Avaliar as propriedades biológicas, incluindo o efeito antibacteriano, citocompatibilidade e a capacidade mineralizante, de adesivos modificados com NPs de ZnO a 2,5% e Cu a 0,2%, e VB a 5 e 10%, em um modelo in vitro.

Avaliar o grau de conversão de adesivos modificados com NPs de ZnO a 2,5% e Cu a 0,2%, e VB a 5 e 10%, em um modelo in vitro.

Analisar o efeito nas propriedades biológicas, efeito mineralizante e na capacidade de inibição da atividade enzimática da degradação do colágeno na camada híbrida; e a resistência de união em dentes restaurados com resina composta utilizando adesivos modificados com NPs de ZnO a 2,5% e Cu a 0,2%, e VB a 5 e 10%, submetidos a um desafio cariogênico, em um modelo in vitro.

3 MATERIAL E MÉTODOS

DESCRIÇÃO DOS EXPERIMENTOS REALIZADOS

A descrição abrangente dos materiais e método utilizados em cada artigo pode ser encontrada na próxima seção de cada artigo individual, oferecendo aos leitores uma compreensão detalhada da metodologia empregada em cada estudo.

3.1 ARTIGO 1: MOLECULAR MECHANISMS OF CYTOTOXICITY IN SAOS-2 OSTEOBLAST-LIKE CELLS EXPOSED TO UNIVERSAL DENTAL ADHESIVES

STATUS: Publicado em 2025
REVISTA: International Journal of Adhesion and Adhesives
DOI: 10.1016/j.ijadhadh.2025.104101

Sonja Buvinic [a], Angelica Araya [b], Nadia Hernández [a], Javier Basualdo Allende [c], Carolina Pardo-Díaz [c d e], Gutiérrez Mario Felipe [f], Alessandro D. Loguercio [d], Eduardo Fernández [c g]

[a] Institute for Research in Dental Sciences, Faculty of Dentistry, Dental School, University of Chile, Santiago, 8380544, Chile

[b] Dental School, University of Chile, Santiago, 8380544, Chile

[c] Faculty of Dentistry, Dental School, University of Chile, Santiago, 8380544, Chile

[d] State University of Ponta Grossa, School of Dentistry, Ponta Grossa, PR, 84030-000, Brazil

[e] Department of Operative Dentistry, School of Dentistry, University of Valparaíso, Valparaíso, 2360004, Chile

[f] Faculty of Dentistry, Universidad de los Andes, Santiago, 7550000, Chile

[g] Department of Operative Dentistry, School of Dentistry and Instituto de Ciencias Biomédicas, Universidad Autónoma de Chile, Santiago, Chile

Alessandro Dourado Loguercio (Corresponding address)
Universidade Estadual de Ponta Grossa, Departamento de Odontologia
Av. Carlos Cavalcanti, 4748, Uvaranas, Zip-Code: 84030-000,
Ponta Grossa, PR, Brazil.
Email: aloguercio@hotmail.com

Abstract

Purpose: This study aimed to investigate the molecular mechanisms of cytotoxicity of three universal adhesives: Ambar Universal (AU), Single Bond Universal (SB), and Prime & Bond Universal (PB)-on human-derived Saos-osteoblast-like cells, elucidating the differential induction of apoptosis and necrosis pathways, contributing to a greater understanding of their biological effects. Methods: Saos-2 cells were incubated with 0.1 % v/v AU, SB, or PB during 2, 4, or 6 h. Populations of viable, early apoptotic, late apoptotic, and necrotic cells were estimated by cell sorting after Annexin V/Propidium Iodide staining. Apoptosis indicators, caspase-3 activation or nuclei fragmentation were addressed by immunoblot or immunofluorescence, respectively. Cytotoxicity was evaluated after 24 h incubation, using MTT Cell Proliferation Assay, with or without the apoptosis inhibitor Z-VAD-FMK. Results: SB exhibited a higher percentage of early apoptotic cells, and a significant increase in activated caspase-3 compared to control. AU and PB significantly increased necrosis, reducing cell viability by 100 %, compared to a 52 % reduction with SB. Immunofluorescence showed apoptotic nuclei morphology for SB, and necrotic characteristics for AU and PB. The apoptosis inhibitor Z-VAD-FMK only abolished SB-evoked cytotoxicity. Conclusion: The universal adhesives studied induced cell death in Saos-2 cells through different mechanisms. SB primarily evoked apoptosis, whereas AU and PB predominantly led to necrosis. These varying cytotoxic effects should be considered when selecting safer universal adhesives for clinical use. However, these findings should be interpreted with caution, as the exclusive use of the Saos-2 osteosarcoma cell line may not fully reflect the biological behavior of dental pulp cells or other oral tissues.

Keywords: Cytotoxicity, Dental adhesives, Apoptosis, Necrosis Osteoblast.

Introduction

Dental adhesives play a crucial role in clinical dentistry, bonding restorative materials to cavity preparations, aiming to enhance longevity of restorations through reduction of marginal leakage at dentin-resin interface, preserving healthy dental tissue, and effectively distributing occlusal stress [1]. Over the years, manufacturers have simplified the application steps and expanded the indications of these adhesives

by adjusting their components, which led to the introduction of Universal Adhesives (UAs). Also known as multimode adhesives, UAs can be used as self-etch, etch-and-rinse, or selective enamel etching adhesives [2,3]. Despite their advantages, current knowledge regarding the UAs cytocompatibility remains limited, particularly concerning their effects in human-derived cell lines.

The cytotoxicity of dental adhesives is primarily attributed to the release of residual monomers that are not incorporated into the polymer network. These unbound monomers may reach tissues surrounding and supporting the teeth, causing local adverse effects, or interact with body fluids, leading to systemic adverse effects, during restorative procedures. [4]. Furthermore, when adhesives are applied on cut and/or etched dentin, residual monomers can diffuse through dentinal tubules, ultimately reaching the pulp tissue and causing cellular damage [4,5]. Commonly used monomers, such as HEMA (2-hydroxyethyl methacrylate) and Bis-GMA (bisphenol A-glycidyl methacrylate), are known to activate cell death pathways by generating reactive oxygen species (ROS) and causing DNA damage [5–8].

Cell death can occur via two primary mechanisms: programmed (apoptosis, necroptosis, pyroptosis, ferroptosis and paraptosis) and nonprogrammed (necrosis). Apoptosis is the most studied mechanism of programmed cell death. It is a highly regulated, energy-dependent process characterized by several morphological and biochemical changes, including chromatin condensation, nuclear fragmentation, cell shrinkage, and the formation of apoptotic bodies [9,10]. This process involves the activation of a cascade of proteolytic enzymes known as caspases, which play a critical role in the execution phase of cell death. Particularly, caspase-3 is a key effector activated in response to apoptotic signals [9]. Apoptosis is essential for maintaining tissue homeostasis and eliminating damaged or harmful cells without eliciting an inflammatory response. In contrast, necrosis is a disorganized cell death that occurs in response to severe cellular injury [8]. It is characterized by irreversible changes in the cell nucleus, loss of cytoplasmic structure, mitochondrial dysfunction, increased cell volume, and subsequent cell lysis [9]. Unlike apoptosis, necrosis typically triggers an inflammatory response, leading to additional damage to surrounding tissues [10,11].

Identifying specific pathways and markers of cell death led by dental adhesives is mandatory to develop pharmacological strategies to mitigate these adverse effects and improve the biocompatibility of dental materials [4]. Despite certain limitations, cell

culture methodologies have been established to evaluate the biological responses of dental adhesives in vitro, using fibroblasts, pulpal cells, osteoblastic cells, and other cell types [5–8,11,12]. However, only a limited number of studies specifically address universal adhesives, and there remains a lack of consensus in the literature regarding their potential cytotoxicity [13–15].

Given the limited understanding of the molecular mechanisms underlying the cytotoxicity of UAs, and how variations on their formulations could impact their mechanism of cell death induction, this study aimed to address the induction of apoptosis and necrosis in Saos-2 cells, a human osteosarcoma cell line that serves as an osteoblast model. Three commercially available universal adhesives were tested: Ambar Universal (FGM Dental Products, Joinville, SC, Brazil), Single Bond Universal (Solventum, St Paul, MN, USA), and Prime & Bond Universal (Dentsply Sirona, Charlotte, NC, USA). These three universal adhesives—Ambar Universal, Single Bond Universal, and Prime & Bond Universal—were selected due to their widespread clinical application and distinct chemical compositions. Specifically, Ambar Universal features an optimized 10-MDP formulation with ethanol and water; Single Bond Universal includes 10-MDP and silane in an ethanol-water base; and Prime & Bond Universal contains the PENTA monomer with isopropanol and water. These differences in monomer type, hydrophilicity, and solvent polarity are likely to influence their cytotoxic potential and biological interactions, thereby justifying their selection for comparative evaluation. The null hypothesis was that universal dental adhesives promote cell death in Saos-2 cells through the same mechanisms.

Materials and Methods

This study adhered to biosafety guidelines for research involving cell lines. The Saos-2 cell line was obtained from ATCC, ensuring that all ethical and legal requirements for using human-derived cell lines were met.

2.1. Cell culture

The Saos-2 osteoblast-like cell line from ATCC HTB-8 was cultured in Dulbecco's Modified Eagle Medium (DMEM; Thermo Fisher Scientific, Dreieich, Germany) supplemented with 10 % fetal bovine serum (FBS; Thermo Fisher Scientific, Dreieich, Germany) and 1 % penicillinstreptomycin solution (Thermo Fisher Scientific, Dreieich, Germany). The cells were maintained at 37 ◦C in a humidified atmosphere

with 5 % CO2 and 95 % air. The culture medium was changed every 2–3 days, and cells were passaged upon reaching 80–90 % confluency using 0.05 % trypsin-EDTA (Thermo Fisher Scientific, Dreieich, Germany).

Preparation of adhesive solutions

Three UAs were evaluated: AU, Ambar Universal (FGM Dental Products; Joinville, SC, Brazil); SU, Single Bond Universal (Solventum, St. Paul, MN, USA); and PB, Prime & Bond Universal (Dentsply Sirona, Charlotte, NC, USA). The manufacturer and composition details of UAs are provided in Table 1. Each UA was diluted in autoclaved distilled water and then added directly to the cell culture medium, reaching a final dilution of 0.1 % v/v. This concentration was chosen based on previous studies demonstrating its cytotoxicity in Saos-2 cells [15]. The solutions were mixed thoroughly and stored at room temperature until use. Fresh adhesive solutions were prepared for each assay to ensure consistency and accuracy. A 0.1 % v/v concentration was selected based on previous studies reporting detectable cytotoxic effects in Saos-2 cells at this dilution [15]. Using a uniform concentration across all adhesives ensured standardized conditions for comparison, minimizing dose-dependent variability and isolating the influence of compositional differences on biological outcomes.

Tabela 1. Manufacturer and Composition details of Universal Adhesives evaluated

Commercial Name	Manufacturer	Composition
Ambar Universal (AU)	FGM Dental Products, Joinville, SC, Brazil	10-MDP, methacrylate monomers (UDMA, HEMA), photoinitiators, co-initiators, stabilizers. Inorganic filler (silica nanoparticles), solvent (ethanol).
Single Bond Universal (SB)	Solventum, St. Paul, MN, USA	10-MDP, HEMA, Bis-GMA, decamethylene dimethacrylate, 1,10-decanediol phosphate methacrylate, acrylic acid copolymer, itaconic acid, camphorquinone, N-dimethylbenzocaine. Inorganic filler (silica treated with silane), solvent (ethanol), water.
Prime & Bond Universal (PB)	Dentsply Sirona, Charlotte, NC, USA	10-MDP, PENTA, phosphoric acid modified with resin acrylate, multifunctional acrylates, bifunctional acrylates, acidic acrylates. Isopropanol, water, initiators, stabilizer.

Cell viability assays

A 24-h exposure period was selected based on prior cytotoxicity studies involving Saos-2 cells, which demonstrated that this duration is adequate for assessing mitochondrial activity and overall cell viability following chemical exposure [5,15]. Cell viability was assessed using a cell proliferation assay (Vybrant; Thermo Fisher Scientific, Dreieich, Germany). Saos-2 cells were seeded in 96-well plates at a density of 10, 000 cells per well in 100 µL of complete culture medium. After 24 h, cells were treated with 100 µL of adhesive solutions or control medium for 24 h. Following treatment, the medium was removed, and 10 µL of MTT stock solution (12 mM) was added to each well. Plates were incubated at 37 ◦C for 2 h to allow for the formation of formazan crystal. The reaction was stopped by adding 100 µL of SDS-HCl solution (0.01M HCl) to solubilize the formazan crystals. Absorbance was measured at 490 nm with a correction at 670 nm using a microplate reader (iMark; BioRad Laboratoires, CA, USA). Cell viability was calculated relative to control wells containing only medium. The apoptosis inhibitor Z-VAD-FMK (100 µM) was combined with the adhesives to confirm the involvement of apoptotic pathways. Saos-2 cells were pretreated with Z-VAD-FMK for 4 h before adding the adhesive solutions and then co-incubated for an additional 24 h. Cell viability was then assessed using the MTT assay as described above.

Apoptosis assays

All following assays were tested in triplicate. Each experiment included a negative control (cells treated with culture medium only) and a positive control for apoptosis (cells treated with 300 µM carbonyl cyanide m-chlorophenyl hydrazone).

Flow cytometry for phosphatidylserine exposure detection

Phosphatidylserine exposure to the extracellular medium, an early marker of apoptosis, was detected on the outer surface of the plasma membrane using annexin V staining. Propidium iodide (PI) staining was simultaneously used to test plasma membrane integrity. Saos-2 cells were seeded in 35 mm dishes at a density of 500,000 cells per dish and allowed to adhere for 24 h. Cells were then treated with UA solutions for 2, 4, or 6 h. After treatment, cells were harvested by trypsinization, washed with PBS, and resuspended in annexin V binding buffer (10 mM Hepes, 140 mM NaCl, 2.5 mM CaCl2, pH 7.4) at a concentration of 1 × 106 cells/mL. Cells were stained with annexin V-APC (1 µg/mL) and PI (10 µg/mL) and incubated at room temperature in the dark for 30 min, following a previously described protocol [11]. Samples were analyzed

using a flow cytometer (BD FACSCalibur; BD Biosciences, San Jose, CA, USA), and data were processed with FlowJo software (version 7.6.1). Viable cells (annexin V and PI negative), early apoptotic cells (annexin V positive and PI negative), late apoptotic cells (annexin V and PI positive), and necrotic cells (annexin V negative and PI positive) were expressed as a percentage of the total cells evaluated.

Detection of relative amounts of cleaved caspase-3 by Western blot

Activation of caspase-3, a key apoptosis effector, was assessed by Western blot. Saos-2 cells were seeded in 35 mm dishes at 200,000 cells per dish and treated with UA solutions for 2, 4, or 6 h. After treatment, cells were lysed in RIPA buffer (50 mM Tris-HCl, 150 mM NaCl, 1 % NP40, 0.25 % sodium deoxycholate, 1 % SDS, 1 mM EDTA, 1 mM EGTA, pH 7.4) supplemented with protease inhibitors (PMSF, AEBSF, aprotinin, bestatin, E− 64, leupeptin, pepstatin). Protein concentrations were determined using protein assay (Pierce Coomassie Plus; Thermo Fisher Scientific, Waltham, MA, USA). Equal amounts of protein (50 μg) were resolved by SDS-PAGE on 12 % polyacrylamide gels and transferred to PVDF membranes. Membranes were blocked with 5 % non-fat milk in TBS-T (20 mM Tris, 150 mM NaCl, 0.1 % Tween 20, pH 7.5) for 1 h and incubated overnight at 4 ◦C with anti-caspase-3 antibody (#9662; Cell Signaling Technology, MA, USA). After washing, membranes were incubated with HRP-conjugated secondary antibodies for 1 h at room temperature. Detection was performed using a reagent (RapidStep ECL Calbiochem; EMD medicals; CA, USA), and images were acquired with a specific system (Amersham Imager 600 RGB GE; Healthcare Life Sciences; IL, USA). Band intensities were quantified using a software (ImageJ, 2.0.0; National Institutes of Health, Bethesda, MD, USA). Tubulin protein was used as loading control (#3873; Cell Signaling Technology, MA, USA).

Analysis of chromatin condensation and nuclear fragmentation

Nuclear morphology was assessed using Hoechst 33342 staining and fluorescence microscopy. Saos-2 cells were seeded on glass coverslips in 35 mm dishes at a density of 20,000 cells per dish and treated with adhesive solutions for 2, 4, or 6 h. Following treatment, cells were fixed with 4 % paraformaldehyde in PBS for 30 min, washed with PBS, and permeabilized with 0.1 % Triton X-100 in PBS for 10 min. Cells were stained with Hoechst 33342 (10 μg/mL) in PBS for 30 min at room temperature in the dark. Coverslips were mounted with a reagent (Dako antifade; Dako, Denmark), and images were captured using a fluorescence microscope (Nikon TiE; Nikons instruments, Melville, NY, USA) with 40 × and 60 × objectives. Nuclear

morphology, including chromatin condensation and nuclear fragmentation, was analyzed using a software (ImageJ, 2.0.0; National Institutes of Health, Bethesda, MD, USA) based on a previously described protocol [12].

Statistical analysis

Results were expressed as mean ± standard error of the mean (SEM) from at least three independent experiments. Statistical comparisons between groups were made using the Mann-Whitney test for pairwise comparisons and the Kruskal-Wallis test, followed by Tukey's post-hoc test for multiple comparisons. A p-value of <0.05 was considered statistically significant. GraphPad Prism software (version 6, GraphPad Software, San Diego, CA, USA) was used for statistical analyses.

Results

Induction of apoptosis by universal adhesives Representative flow cytometry images for UAs evaluated at 2 and 6 h illustrate AU and PB's preference for necrosis and SB's tendency for early/late apoptosis at 6 h (Fig. 1). Viable cells, early apoptotic cells, late apoptotic cells, and necrotic cells quantitation obtained through flow cytometry were expressed as a percentage of the total cells evaluated. Comparison of the control at 6 h with the experimental groups revealed a significantly lower rate of late apoptosis for the SB at 2 h and for the PB in both 2 and 6 h ($p < 0.05$) (Table 2). Regarding necrosis, the AU caused a significant increase in necrotic cells at both 2 ($p < 0.01$) and 6 ($p < 0.001$) hours (Table 2). SB and PB showed a trend of increased necrosis at 6 h. Western blot analysis demonstrated the activation of caspase-3, a key effector protein in apoptosis, in Saos-2 cells treated with the adhesives. SB significantly increased the levels of cleaved caspase-3 at 4 h posttreatment, indicating activation of the apoptotic pathway (Fig. 2a). AU and PB exhibited less pronounced activation, which correlates with their higher necrotic effects (Fig. 2b). Fluorescence microscopy using Hoechst 33342 staining revealed distinct nuclear alterations in treated Saos-2 cells. After 4 h, cells treated with AU and PB exhibited smaller nuclei with less defined borders, indicative of necrotic nuclei. Conversely, SB-treated cells exhibited nuclear fragmentation and chromatin condensation, characteristic of apoptosis. Nuclear fragmentation began at 4 h, with apoptotic bodies showing intense staining due to DNA condensation, becoming evident by 6 h. Additionally, all treated groups exhibited a

decreased cell density compared to the control group, which displayed rounded and uniformly stained nuclei. Representative images are shown in Fig. 3.

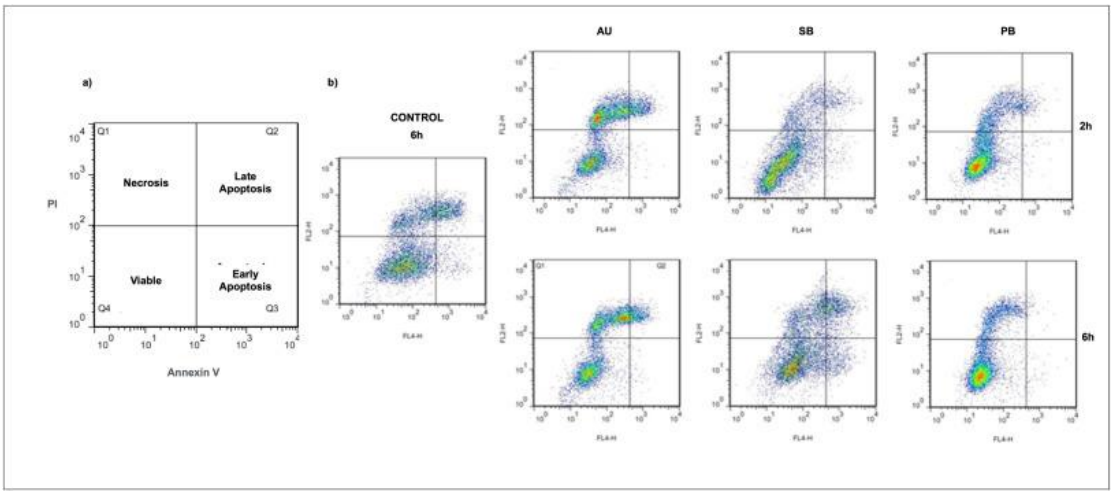

Figura 1. Representative Flow Cytometry Images. (Artigo 1).

a) Flow cytometry diagram illustrating the simultaneous measurement of two parameters through flow cytometry: Annexin V (X-axis) and propidium iodide (PI; Y-axis). This scatter plot shows the distribution of cells based on their apoptotic and necrotic states; b) Representative flow cytometry images for Ambar universal (AU), Single Bond Universal (SB), and Prime & Bond universal (PB) universal adhesives at 2 and 6 h.

Tabela 2. Percentages of viable cells, early apoptotic cells, late apoptotic cells, and necrotic cells obtained through flow cytometry. Ambar universal (AU), Single Bond Universal (SB), and Prime & Bond universal (PB). ([a])

	Viable (%)		Early Apoptosis (%)		Late Apoptosis (%)		Necrosis (%)	
Control	2h	6h	2h	6h	2h	6h	2h	6h
	–	63.8±6.3	–	3.7±1.3	–	18.9±5.1	–	13.5±3.6
AU	50.4±9.1	43.9±0.9	0.8±0.5	0.9±0.3	11.3±3.1	11.8±3.1	37.5±7.0**	43.2±3.1
SB	77.9±4.1	65.7±4.4	3.5±1.8	5.6±1.1	6.3±2.6[a]	9.4±2.6	12.2±0.3	19.1±1.5
PB	76.7±3.5	73.4±4.0	0.5±0.2	0.3±0.1	4.2±1.0[a]	3.3±2.6[a]	18.5±3.1	22.8±2.4

a Data are expressed as a percentage of the total cells evaluated. The mean ± standard error of the mean (M±SEM; n = 3) is shown. Results were analyzed using the Kruskal-Wallis test followed by Tukey's post-hoc test. *, $p < 0.05$; **$p < 0.01$; ***, $p < 0.001$ compared to control at 6h.

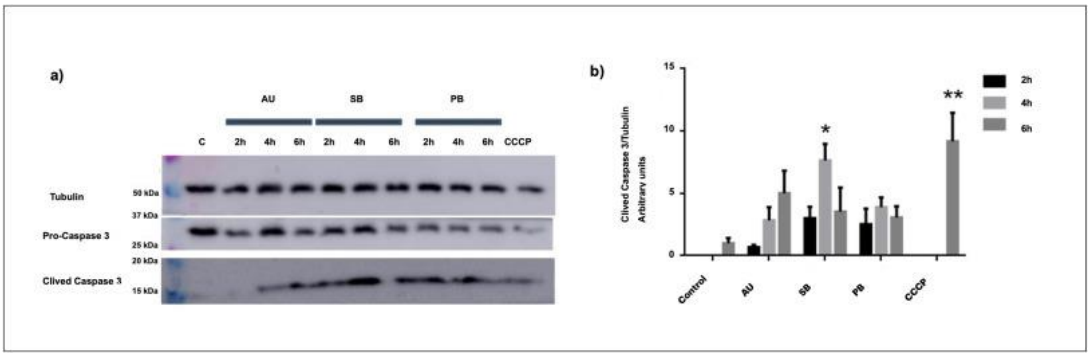

Figura 2. Inmunblot Analysis and Quantification of Activated Caspase-3. (Artigo 1)

a) Immunoblot analysis showing the activation of caspase-3 in Saos-2 cells treated with universal adhesives (Ambar universal, AU; Single Bond Universal, SB; Prime & Bond universal, PB) and carbonyl cyanide m-chlorophenyl hydrazone (CCCP) at 2, 4, and 6 h. The immunoblot visualizes the presence of cleaved caspase-3, indicating apoptotic activity; b) Graph depicting the relative quantification of activated caspase-3. Each sample was normalized to Tubulin. Values are presented as mean ± standard error of mean (n = 3). Statistical significance was assessed using the Mann-Whitney test. ∗, $p < 0.05$; ∗∗, $p < 0.01$ compared to control.

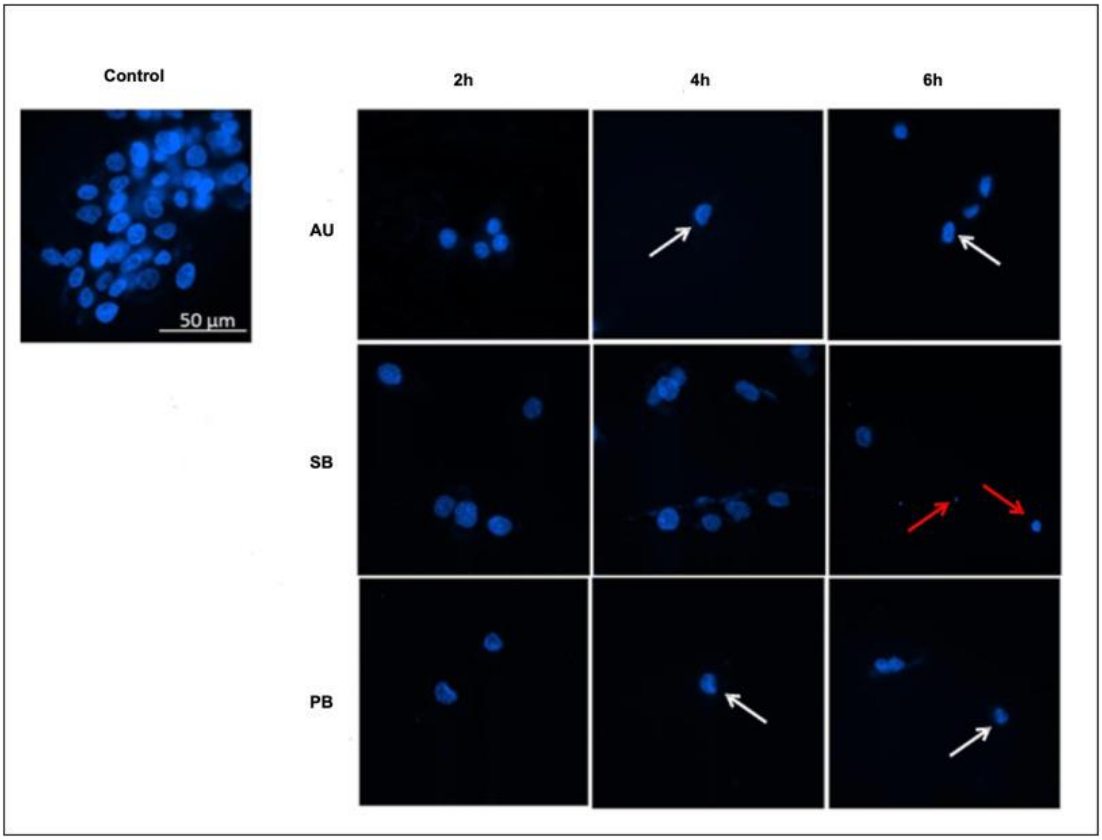

Figura 3. Representative images of cell nuclei of Saos-2 cells treated with Universal Adhesives. (Artigo1).

Cell Nuclei of Saos-2 cells treated with different universal adhesives (Ambar universal, AU; Single Bond Universal, SB; Prime & Bond universal, PB) for 2, 4, and 6 h, visualized by Hoechst 33342 staining (blue). White arrows highlight smaller, irregularly shaped nuclei indicative of necrotic cells, while red arrows point to apoptotic bodies characteristic of apoptosis. Images were captured using a Nikon Ti-E epifluorescence microscope (60X) and analyzed with ImageJ software.

Cell viability reduction by universal adhesives and dependence on apoptosis All adhesives showed a significant reduction of cell viability by MTT assay. SB exhibited the highest cell viability at 47.9 %, whereas AU and PB both reduced cell viability to nearly zero. Pretreatment with the apoptosis inhibitor Z-VAD-FMK significantly increased cell viability in SB-treated cells, indicating that apoptosis was the primary mode of cell death induced by this UA (Fig. 4). In contrast, Z-VAD-FMK did not significantly affect cell viability in AU or PB-treated cells, supporting that necrosis was the dominant form of cell death in these conditions.

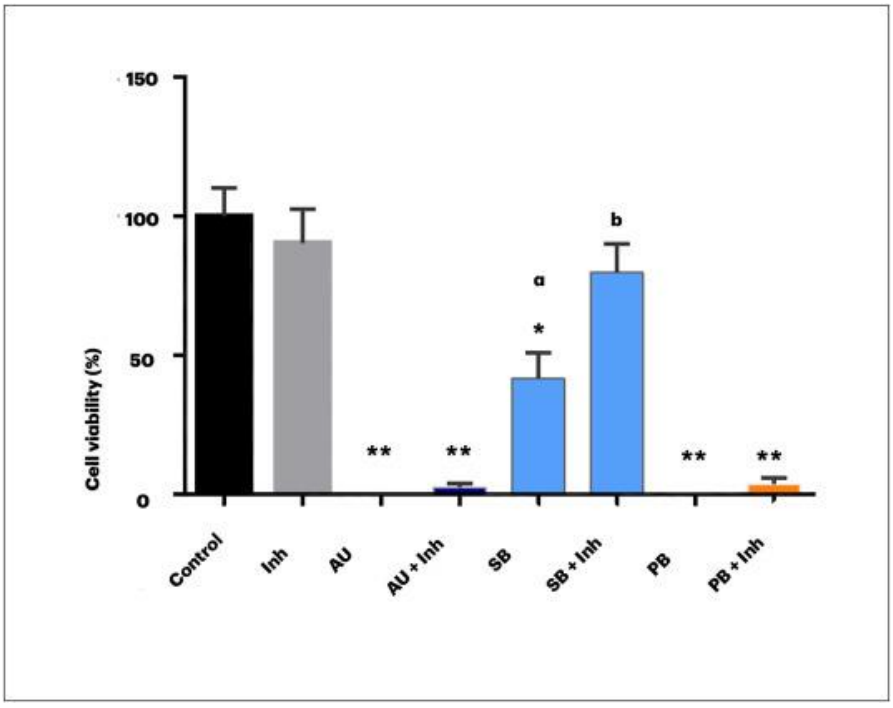

Figura 4. Cell viability of Saos-2 cultured for 24 h with different universal adhesives. (Artigo 1).

Cell viability of Saos-2 cultured for 24 h with different universal adhesives (Ambar universal, AU; Single Bond Universal, SB; Prime & Bond universal, PB), both alone and in combination with the apoptosis inhibitor Z-VAD-FMK (Inh). Data are presented as mean ± standard error of the mean (n = 6). Statistical analysis was performed using the Kruskal-Wallis test, followed by Tukey's post-hoc test. Different letters indicate significant differences between groups. ∗, $p < 0.05$; ∗∗, $p < 0.01$ compared to control.

Discussion

Understanding the cytotoxic mechanisms of dental adhesives is crucial, as these materials are routinely placed in close proximity to vital tissues such as the dental pulp and periradicular gingiva, and bone. This study investigated the cytotoxic effects and underlying cell death pathways of three universal adhesives (SB, AU, and PB) in Saos-2 osteoblast-like cells. The null hypothesis was rejected, as each adhesive elicited distinct cellular responses. SB primarily induced apoptosis—a controlled and energy-dependent form of cell death—whereas AU and PB predominantly caused necrosis, a passive process often associated with inflammation. These findings highlight the importance of characterizing the specific cytotoxic mechanisms of UAs to enhance the understanding of their cellular effects to enhance patient outcomes in clinical practice.

Phosphatidylserine translocation from the inner to the outer leaflet of the plasma membrane, facilitated by outer membrane translocase proteins, is a key marker for detecting apoptotic cells and aids in their removal by phagocytes [9,16]. Annexin V combined with PI is a qualitative method that distinguishes live cells from early apoptotic cells, late apoptotic cells, and necrotic cells. This technique has been widely applied to evaluate the effects of dental adhesives [17–20]. In this study, the flow cytometry assay for phosphatidylserine exposure revealed that AU significantly increased the necrotic cells compared to the control at both 2 and 6 h. PB also showed a trend toward increased necrosis, though this was not statistically significant, with lower percentages of early and late apoptosis at both time points. Both AU and PB adhesives caused substantial irreversible damage to the plasma membrane of Saos-2 cells, as indicated by PI staining. The minimal detection of phosphatidylserine for these adhesives suggests they primarily induce necrosis rather than apoptosis. In

contrast, SB adhesive exhibited similar levels of necrosis as the control but showed a higher percentage of phosphatidylserine exposure, indicating a predominant tendency toward programmed cell death (apoptosis). The latter suggests that SB induces apoptosis more effectively than AU and PB.

Apoptosis is a highly regulated process characterized by the activation of proteolytic enzymes known as caspases, with caspase-3 playing a pivotal role in the execution phase of apoptosis. Caspase-3 is crucial for the cleavage of key proteins, leading to DNA fragmentation and the eventual induction of apoptotic cell death [9,21]. Previous studies have used cleaved caspase-3 as a reliable marker for apoptosis induced by dental adhesives [17,19]. In this study, we observed activation of caspase-3 across all experimental conditions. Notably, a significant increase in cleaved caspase-3 levels was detected in the SB, supporting the flow cytometry data that indicated a trend toward apoptosis. This finding underscores the role of SB in promoting apoptotic cell death, consistent with its observed effects on phosphatidylserine exposure and nuclear morphology.

The analysis of nuclear morphology is a crucial parameter for identifying apoptotic cells and distinguishing them from necrotic cells, based on general morphological criteria [8,18]. In this study, nuclear morphology was assessed using fluorescence microscopy. All UAs reduced cell number, but distinct morphological patterns were observed. Cells treated with AU and PB displayed nuclei with necrotic characteristics, including poorly defined nuclear borders and less condensed DNA, indicative of necrotic cell death [22]. In contrast, the SB adhesive group exhibited nuclear fragmentation starting at 4 h, a hallmark of late apoptosis. By 6 h, apoptotic bodies were prominently observed, further confirming the tendency of SB to induce apoptotic cell death. The MTT assay, an enzymatic biosynthesis test for evaluating mitochondrial enzymatic activity, was employed to assess the cell viability and cytotoxicity of three UAs, both independently and in combination with the caspase inhibitor Z-VAD-PMK [23]. This assay measures cell viability by detecting the conversion of yellow MTT to blue formazan by mitochondrial dehydrogenases, indicating mitochondrial integrity [24].

The MTT assay has been widely utilized in previous studies to test the cytotoxicity of dental adhesives [6,19,25–29]. All three UAs significantly reduced cell viability, exceeding 30 %, demonstrating cytotoxicity as per ISO 10993–5:2019 standards. Among the UAs tested, SB showed the highest cell viability at 47.9 %,

consistent with prior studies that reported a 49–53 % reduction in the L929 fibroblast cell line [14]. Other investigations have shown that SB and AU exhibited better tolerance in the 3T3 fibroblast cell line, with viabilities of 97.4 % and 96 %, respectively [29]. Variations in findings may be attributed to differences in adhesive concentrations and the distinct cytotoxic responses of different cell lines [30]. Notably, combining SB with the caspase inhibitor Z-VAD-FMK significantly increased cell viability, suggesting that apoptosis is the primary cell death pathway induced by this adhesive. In contrast, AU and PB adhesives resulted in a nearly complete loss of cell viability, with no significant changes observed when the caspase inhibitor was present.

Numerous studies have established that dental adhesives induce cytotoxicity through apoptosis [7,9,17,31]. However, this study suggests that the specific adhesive evaluated can influence the predominant cell death pathway, potentially due to the distinct monomers present in their composition. For instance, several investigations have highlighted the cytotoxic effects of monomers such as HEMA, Bis-GMA, TEGMA, and UDMA. These monomers have been shown to generate reactive oxygen species (ROS) and decrease antioxidant levels, such as glutathione, leading to oxidative stress and cell death. [5,7,28,31]. Specifically, UDMA has been demonstrated to induce pathological changes and cell death at low concentrations [32]. On the other hand, all three UAs tested in this study contain 10-MDP, a monomer known for its toxicity even at low concentrations. 10-MDP has been shown to promote inflammatory responses and suppress odontoblastic differentiation in human dental pulp cells, similar to the effects of TEGMA [26]. Although the exact mechanisms of 10-MDP’s cytotoxicity remain unclear, it is hypothesized that its strong interaction with the phospholipid bilayer may lead to significant damage to the cell membrane [33]. While all UAs in this study share 10-MDP, their additional monomeric components differ: AU contains UDMA and HEMA, PB includes PENTA, and SB features HEMA and Bis-GMA. Notably, SB, which contains HEMA and Bis-GMA, was the least toxic among the evaluated UAs. HEMA, despite being generally regarded as the least toxic, can still suppress cell growth, delay cell cycle progression, increase ROS levels, and trigger apoptosis [31,34]. Conversely, Bis-GMA is considered highly toxic, altering the cell cycle and inducing apoptosis in a dose-dependent manner [15,19]. Considering that the interactions among various monomers within an adhesive formulation can significantly alter its cytotoxicity, potentially amplifying or diminishing individual toxicities [4,5,8,22], UAs differences in monomer composition can explain the varying

levels of cytotoxicity observed among them. The results of this study indicate that the combination of 10-MDP, HEMA, and Bis-GMA in the SB formulation was less toxic than other combinations, predominantly leading to apoptotic cell death, highlighting the importance of considering both the types and proportions of monomers when evaluating the cytotoxic profiles of dental adhesives.

Although our investigation did not directly explore cannabinoid compounds, the broader implications of how reactive monomers from dental adhesives influence intracellular signaling, oxidative stress, and cell death mechanisms resonate with findings from adjacent fields such as cancer biology. Valenti et al. [35] provides a comprehensive overview of cannabidiol (CBD)'s biological effects, including its modulation of redox homeostasis, mitochondrial dysfunction, and activation of both apoptotic and autophagic pathways in cancer cells. These effects are not strictly mediated by cannabinoid receptors but involve alternative routes such as the generation of reactive oxygen species, modulation of calcium homeostasis, and inhibition of pro-survival pathways like PI3K/Akt and ERK.

Such mechanisms are relevant in the context of dental adhesive toxicity, where unreacted monomers may similarly induce reactive oxygen species accumulation, mitochondrial depolarization, and caspase activation, ultimately triggering apoptosis or necrosis. Furthermore, Valenti et al. [35] highlight how intracellular damage and organelle stress can activate the NF-κB pathway and upregulate pro-inflammatory cytokines, including IL-6 and TNF-α—responses that mirror those observed following exposure to cytotoxic dental materials.

Importantly, beyond apoptosis, necrotic cell death induced by certain adhesive systems may result in the passive release of damage associated molecular patterns, further amplifying inflammation through Toll-like receptor pathways and inflammasome activation. Future research should therefore investigate whether specific adhesive formulations modulate these inflammatory axes, as understanding these molecular events may inform the development of safer biomaterials with reduced iatrogenic potential. Since dental adhesives have the potential to affect periodontal tissues, such as bone tissue, evaluating their cytotoxic effects on bone cells is significantly relevant [5]. This study evaluated Saos-2 cells, a human osteosarcoma cell line that serves as an osteoblast model. However, it is crucial to recognize that the harmful effects of the UAs are influenced by factors such as cell type and the concentration of residual monomer, and, in relation to dental tissues, the residual monomer diffusion through

dentinal tubules [4,22]. Future studies should consider more than one clinically relevant cell line, such as dental pulp cells, to better understand these mechanisms. The goal should be to develop pharmacological strategies to mitigate these effects and improve the biocompatibility of dental adhesives. Although Saos-2 cells offer a convenient and well-characterized osteoblast-like model for evaluating peri-radicular bone responses, they lack the biological and functional complexity of the dentin–pulp complex. Future studies should incorporate human dental pulp stem cells (hDPSCs) or primary pulp fibroblasts to more accurately reflect pulpal cytotoxic responses and enhance translational relevance [36]. In a recent in vitro investigation, Osorio et al. [36] demonstrated that hDPSCs exhibit pronounced sensitivity to inflammatory insults such as lipopolysaccharide, which significantly impaired their mineralization capacity, disrupted cytoskeletal organization, and altered the expression of key odontogenic genes. Notably, these detrimental effects were substantially mitigated by the application of tideglusib-doped nanoparticles (TDg-NPs), which promoted cell viability, preserved cytoskeletal integrity, and restored osteogenic differentiation markers—including ALP, RUNX2, and osteonectin—even under LPS-induced stress conditions.

These findings underscore the mechanistic and clinical value of using hDPSCs in dental biomaterial research, particularly when assessing inflammatory and regenerative responses. Moreover, Saos-2 cells—originating from osteosarcoma—may exhibit abnormal metabolic profiles and stress adaptation mechanisms, including elevated basal reactive oxygen species levels and enhanced resistance to apoptosis, which can skew toxicity assessments. Therefore, while Saos-2 cells remain useful for preliminary screening of osteogenic potential, their data should be complemented with non-transformed human cells, such as hDPSCs or pulp fibroblasts, to ensure a more physiologically relevant and clinically applicable evaluation of dental material biocompatibility and potential pulpal toxicity.

Additionally, it is important to acknowledge a conceptual limitation in interpreting the cellular mechanisms underlying the response to universal adhesives, particularly due to the use of a cancer-derived cell line. Saos-2 cells, originating from human osteosarcoma, may present altered metabolic characteristics that do not fully represent healthy oral cell physiology. These cells are known to exhibit features associated with the Warburg Effect—namely, increased glucose uptake and lactate production even in the presence of functional mitochondria. This metabolic reprogramming, often observed in malignant cells, is thought to support rapid

proliferation by promoting ATP synthesis, biosynthetic precursor generation, and redox balance. However, as Liberti and Locasale [37] have pointed out, many of these assumptions remain under debate, with some studies showing continued reliance on mitochondrial function and substantial carbon loss through lactate excretion. Moreover, the mechanistic models explaining the Warburg phenotype often lack experimental specificity, making it difficult to determine whether this metabolic shift is causative, adaptive, or simply a byproduct of oncogenic transformation. These uncertainties limit the extent to which findings in Saos-2 cells can be generalized to healthy, non-transformed cells. Therefore, while Saos-2 provides a consistent and well-characterized model for osteoblast-like responses, future studies should prioritize the use of primary, non-malignant cell types—such as human dental pulp stem cells or gingival fibroblasts—to enhance clinical relevance and more accurately assess the cytotoxic potential of dental adhesives.

Although this study offers valuable insights, it has limitations. Using a single cell line, Saos-2, limits the generalizability of our findings to other cell types relevant to dental tissue, such as dental pulp stem cells. Additionally, the in vitro conditions do not fully replicate the complex oral environment. Future research should include multiple cell lines and in vivo models to better assess the biocompatibility and cytotoxicity of dental adhesives. Efforts should also focus on developing new adhesive formulations with reduced cytotoxicity while maintaining or improving adhesive performance. Addressing these limitations will provide a more comprehensive understanding of the safety and efficacy of dental adhesives in clinical practice. In addition to pulp cells, other relevant oral cell types such as keratinocytes and gingival fibroblasts should be considered in future investigations, as they are frequently exposed to adhesive leachates and may exhibit distinct cytotoxic responses.

Conclusions

Universal dental adhesives tested in this study induced distinct cell death pathways in Saos-2 osteoblast-like cells.

Single Bond Universal primarily triggered apoptosis, whereas Ambar Universal and Prime & Bond Universal predominantly induced necrotic cell death.

These differences appear to be related to their respective monomeric compositions. • The results underscore the importance of evaluating adhesive systems not only for their mechanical performance but also for their biological compatibility.

Further investigations using multiple oral cell types and in vivo models are recommended to validate these findings.

References

[1] Nagarkar S, Theis Mahon N, Perdigão J. Universal dental adhesives: current status, laboratory testing, and clinical performance. J Biomed Mater Res B Appl Biomater 2019;107(6):2121–31. https://doi.org/10.1002/jbm.b.34305.
[2] Perdigão J, Sezinando A, Monteiro PC. Laboratory bonding ability of a multipurpose dentin adhesive. Am J Dent 2012;25(3):153–8. Erratum in: Am J Dent 2012;25(4):226. PMID: 22988685.
[3] Muñoz MA, Luque I, Hass V, Reis A, Loguercio AD, Bombarda NH. Immediate bonding properties of universal adhesives to dentine. J Dent 2013;41(5):404–11. https://doi.org/10.1016/j.jdent.2013.03.001.
[4] Caldas IP, Alves GG, Barbosa IB, Scelza P, de Noronha F, Scelza MZ. In vitro cytotoxicity of dental adhesives: a systematic review. Dent Mater 2019;35(2): 195–205. https://doi.org/10.1016/j.dental.2018.11.028.
[5] Kraus D, Wolfgarten M, Enkling N, Helfgen EH, Frentzen M, Probstmeier R, et al. In-Vitro cytocompatibility of dental resin monomers on osteoblast-like cells. J Dent 2017;65:76–82. https://doi.org/10.1016/j.jdent.2017.07.008.
[6] Gallorini M, Cataldi A, di Giacomo V. Hema-induced cytotoxicity: oxidative stress, genotoxicity and apoptosis. Int Endod J 2014;47(9):813–8. https://doi.org/ 10.1111/iej.12232.
[7] Kim EC, Park H, Lee SI, Kim SY. Effect of the acidic dental resin monomer 10-Methacryloyloxydecyl dihydrogen phosphate on odontoblastic differentiation of human dental pulp cells. Basic Clin Pharmacol Toxicol 2015;117(5):340–9. https://doi.org/10.1111/bcpt.12404.
[8] Accorinte Mde L, Loguercio AD, Reis A, Muench A, de Araújo VC. Adverse effects of human pulps after direct pulp capping with the different components from a totaletch, three-step adhesive system. Dent Mater 2005;21(7):599–607. https://doi. org/10.1016/j.dental.2004.08.008.
[9] Nuñez G, Benedict M, Hu Y, Inohara N. Caspases: the proteases of the apoptotic pathway. Oncogene 1998;17(25):3237–45. https://doi.org/10.1038/sj. onc.1202581.
[10] Green DR. The coming decade of cell death research: five riddels. Cell 2019;177(5): 1094–107. https://doi.org/10.1016/j.cell.2019.04.024.
[11] Crowley LC, Marfell BJ, Scott AP, Waterhouse NJ. Quantitation of apoptosis and necrosis by annexin V binding, propidium iodide uptake, and flow cytometry. Cold Spring Harb Protoc 2016;(11). https://doi.org/10.1101/pdb.prot087288.
[12] Crowley LC, Marfell BJ, Waterhouse NJ. Analyzing cell death by nuclear staining with hoechst 33342. Cold Spring Harb Protoc 2016;(9). https://doi.org/10.1101/ pdb.prot087205.
[13] Cardoso M, Coelho A, Marto C, Gonçalves AC, Paula A, Ribeiro ABS, et al. Effects of adper™ scotchbond™ 1 Xt, clearfil™ Se bond 2 and scotchbond™ universal in

odontoblasts. Materials 2021;14(21):6435. https://doi.org/10.3390/ma14216435. 2021.
[14] Wawrzynkiewicz A, Rozpedek-Kaminska W, Galita G, Lukomska-Szymanska M, Lapinska B, Sokolowski J, et al. The cytotoxicity and genotoxicity of three dental universal Adhesives-an in vitro study. Int J Mol Sci 2020;21(11):3950. https://doi. org/10.3390/ijms21113950.
[15] Gutiérrez M, Alegría L, Méndez L, Bermudez J, D´ avila A, Buvinic S, et al. Biological, mechanical and adhesive properties of universal adhesives containing zinc and copper nanoparticles. J Dent 2019;82:45–55. https://doi.org/10.1016/j. jdent.2019.01.012.
[16] Wisniewska-Jarosinska M, Poplawski T, Chojnacki CJ, Pawlowska E, Krupa R, Szczepanska J, et al. Independent and combined cytotoxicity and genotoxicity of triethylene glycol dimethacrylate and urethane dimethacrylate. Mol Biol Rep 2011; 38(7):4603–11. https://doi.org/10.1007/s11033-010-0593-1.
[17] Mantellini MG, Botero TM, Yaman Dennison JB, Hanks CT, Nor ¨ JE. Adhesive resin induces apoptosis and cell-cycle arrest of pulp cells. J Dent Res 2003;82(8):592–6. https://doi.org/10.1177/154405910308200804.
[18] El-kholany NR, Abbielhassan MH, Elembaby AE, Maria OM. Apoptotic effect of different self-etch dental adhesives on odontoblasts in cell cultures. Arch Oral Biol 2012;57(6):775–83. https://doi.org/10.1016/j.archoralbio.2011.11.019.
[19] Cort´es O, Alcaina A, Bernab´e A. Biocompatibility evaluation of four dentin adhesives used as indirect pulp capping materials. Acta Stomatol Croat 2007;51(2): 113–21. https://doi.org/10.15644/asc51/2/4. [
20] Catunda RQ, Vieira JR, Olivera de, da Silva EC, Brasil VL, Perez DC. Cytotoxicity evaluation of three dental adhesives on vero cells in vitro. J Clin Exp Dent 2017;9 (1):61–6. https://doi.org/10.4317/jced.53039.
[21] Chen RS, Liu CC, Tseng WY, Jeng JH, Lin CP. Cytotoxicity of three dentin bonding agents on human dental pulp cells. J Dent 2003;31(3):223–9. https://doi.org/ 10.1016/s0300-5712(02)00088-x.
[22] Goldberg M. In vitro and in vivo studies on the toxicity of dental resin components: a review. Clin Oral Invest 2008;12(1):1–8. https://doi.org/10.1007/s00784-007- 0162-8.
[23] Cao T, Saw TY, Heng BC, Liu H, Yap AU, Ng ML. Comparison of different test models for the assessment of cytotoxicity of composite resins. J Appl Toxicol 20005;25(2):101-108. https://doi.org/10.1002/jat.1041.
[24] Elmore S. Apoptosis: a review of programmed cell death. Toxicol Pathol 20007;35 (4):495-526. https://doi.org/10.1080/01926230701320337.
[25] Fujisawa S, Kadoma Y, Komoda Y. Hemolysis mechanism of dental adhesive monomer (Methacryloyloxydecyl dihydrogen phosphate) using a phosphatidylcholine liposome system as a model for biomembranes. Dent Mater J 1990;9(2):136–46. https://doi.org/10.4012/dmj.9.136.
[26] Imazato S, Horikawa D, Nishida M, Ebisu S. Effects of monomers eluted from dental resin restoratives on osteoblast-like cells. J Biomed Mater Res B Appl Biomater 2009;88(2):378–86. https://doi.org/10.1002/jbm.b.31067.
[27] Krifka S, Hiller KA, Spagnuolo G, Jewett A, Schmalz G, Schweikl H. The influence of glutathione on redox regulation by antioxidant proteins and apoptosis in macrophages exposed to 2-Hydroxyethyl methacrylate (Hema). Biomaterials 2012; 33(21):5177–86. https://doi.org/10.1016/j.biomaterials.2012.04.013.

[28] Ratanasathien S, Wataha JC, Hanks CT, Dennison JB. Cytotoxic interactive effects of dentin bonding components on mouse fibroblasts. J Dent Res 1995;74(9): 1602–6. https://doi.org/10.1177/00220345950740091601.
[29] Tuncer S, Demirci M, Schweikl H, Erguven M, Bilir A, Kara Tuncer A. Inhibition of cell survival, viability and proliferation by dentin adhesives after direct and indirect exposure in vitro. Clin Oral Invest 2012;16(6):1635–46. https://doi.org/ 10.1007/s00784-011-0669-x.
[30] Elias ST, Dos Santos AF, Garcia FC, Pereira PN, Hilgert LA, Fonseca-Bazzo YM, et al. Cytotoxicity of universal, self-etching and Etch-and-Rinse adhesive systems according to the polymerization time. Braz Dent J 2015;26(2):60–168. https://doi. org/10.1590/0103-6440201300294. 2015.
[31] Fadok VA, Bratton DL, Frasch SC, Warner ML, Henson PM. The role of phosphatidylserine in recognition of apoptotic cells by phagocytes. Cell Death Differ 1998;5(7):551–62. https://doi.org/10.1038/sj.cdd.4400404.
[32] Lee Y, An SY, Park YJ, Yu FH, Park JC, et al. Cytotoxic effects of one-step selfetching adhesives on an odontoblast cell line. Scanning 2016;38(1):36–42. https:// doi.org/10.1002/sca.21236.
[33] Li YC, Kuan YH, Huang FM, Chang YC. The role of DNA damage and caspase activation in cytotoxicity and genotoxicity of macrophages induced by Bisphenola-Glycidyldimethacrylate. Int Endod J 2012;45(6):499–507. https://doi.org/ 10.1111/j.1365-2591.2011.02001.x.
[34] Pupo YM, Bernardo CFF, de Souza FFFA, Mich´el MD, Ribeiro CNM, Germano S, et al. Cytotoxicity of Etch-and-Rinse, self-etch, and universal dental adhesive systems in fibroblast cell line 3T3. Scanning 2017:9650420. https://doi.org/ 10.1155/2017/9650420.
[35] Valenti C, Billi M, Pancrazi GL, Calabria E, Armogida NG, Tortora G, Pagano S, Barnaba P, Marinucci L. Biological effects of cannabidiol on human cancer cells.

3.2 ARTIGO 2: ADHESIVE PROPERTIES OF UNIVERSAL ADHESIVES SYSTEMS CONTAINING ZINC OXIDE AND COPPER NANOPARTICLES ON SOUND DENTINE: A 2-YEAR EVALUATION

STATUS: Publicado em 2025

REVISTA: International Journal of Adhesion and Adhesives

DOI: 10.1016/j.ijadhadh.2025.104023

Mario Felipe Gutiérrez [a b], Romina Aliaga-Gálvez [a], Carolina Pardo Diaz[c], Alejandra Nuñez [d e], Sofía Cavagnaro [a], Rocío Maturana [a], Alessandra Reis [d], Eduardo Fernández [b f], Alessandro D. Loguercio [d]

[a] Universidad de Los Andes, Chile. Facultad de Odontología. Santiago, Chile, Zip Code 7550000

[b] University of Chile, Department of Restorative Dentistry, Faculty of Dentistry, Santiago, Chile, Zip Code 8380544

[c] University of Valparaiso, Department of Operative Dentistry, School of Dentistry, Valparaíso, Chile, Zip Code 2360004

[d] State University of Ponta Grossa, Department of Restorative Dentistry, School of Dentistry, Ponta Grossa, Brazil, Zip Code 84030-900

[e] San Francisco de Quito University, Buonocore Dental Biomaterials Research Institute, Quito, Ecuador, Zip Code 170901

[f] Universidad Autónoma de Chile, Instituto de Ciencias Biomédicas, Santiago, Chile, Zip Code 7500912

Alessandro Dourado Loguercio (Corresponding author)

Universidade Estadual de Ponta Grossa, Departamento de Odontologia

Av. Carlos Cavalcanti, 4748, Uvaranas, Zip-Code: 84030-000,

Ponta Grossa, PR, Brazil.

Email: aloguercio@gmail.com

Abstract

Objectives: This study evaluated the effect of adding zinc oxide and copper nanoparticles (ZnO/CuNp) to universal adhesives (UA) on resin-dentine microtensile bond strength (μTBS), nanoleakage (NL), and the presence of ZnO/CuNp within the hybrid layer at immediate time (IM) and after 2 years of water storage (2y). Methods: ZnO/CuNp (commercial adhesive [control]; 5/0.1 and 5/0.2 wt%) were added to Prime&Bond Active (PBA) and Ambar Universal (AMB). The UAs were applied to flat dentine surfaces, followed by composite resin build-ups. These were then sectioned into resin–dentine bonded sticks. μTBS, NL and presence of ZnO/CuNp in the hybrid layer were evaluated at IM and after 2y. Data were analyzed with three-way ANOVA and Tukey's post hoc test ($\alpha = 0.05$). Results: The addition of ZnO/CuNp to UAs did not affect μTBS at IM ($p > 0.05$). After 2y, μTBS values were higher in the 5/0.1 and 5/0.2 wt% groups for AMB ($p < 0.05$), with values maintained for the PB ($p > 0.05$). All groups showed a decrease in μTBS over time ($p < 0.05$), except for the AMB-5/0.1 wt% group in etch-and-rinse mode. NL was lower in the ZnO/CuNp groups at both IM and 2y compared to control ($p < 0.05$). NL increased over time for all groups ($p < 0.05$). ZnO/CuNp remained in the hybrid layer after 2y. Conclusions: ZnO/CuNp improves adhesive interface stability and remains effective in the hybrid layer after 2 years of water storage.

Introduction

The longevity of tooth-coloured resin-based restorations is primarily influenced by the integrity of the resin-dentine bonding interface [1]. A critical component of this transition area is the hybrid layer (HL), which forms through the demineralisation of the dentine substrate, followed by the infiltration and polymerization of the adhesive monomers [2,3]. Ensuring the stability of the HL over time is essential for achieving a durable bond between the composite material and dentine [4].

Universal adhesives (UAs) represent the most advanced generation of bonding agents, designed as single-bottle materials that offer versatility in their application. They can be used in various modes: etchand-rinse (E&R) technique, where phosphoric acid is used to etch enamel and dentine; the self-etch (SE) technique, which simplifies the process by eliminating the need for a separate etching step; or a selective enamel etching approach that combines the benefits of both methods [5, 6]. This versatility makes UAs suitable for a wide range of clinical scenarios and adaptable to various substrates, ensuring reliable adhesion across diverse restorative procedures [7].

However, the bonding stability of UAS to dentine is significantly influenced by the materials used, as adhesion to dentine remains vulnerable to hydrolytic and enzymatic degradation [6,8]. Poorly infiltrated collagen and the hydrophilic components nature of dental adhesives contribute to water sorption, leading to degradation and reduced bond strength over time [9]. Enzymatic degradation of collagen structures is primarily linked to matrix metalloproteinases (MMPs), endogenous enzymes activated during the demineralisation process. Since dentine is a mineralised tissue predominantly composed of collagen, the activation of MMPs plays a crucial role in the deterioration of the HL [8]. This enzyme activation can occur during restorative procedures or be triggered by the acidic byproducts of bacterial activity associated with dental caries progression [10].

Degradation of HL often necessitates the replacement of dental restorations with more complex alternatives, resulting in the loss of sound tooth structure and increased dental care costs [11]. This highlights the urgent need for strategies to enhance the longevity of the bonded interface. To address this challenge, the independent incorporation of zinc oxide (ZnO) and copper (Cu) metallic nanoparticles (Np) into dental adhesives has been proposed due to their bactericidal properties and

ability to inhibit MMP activity. These Np have shown potential in enhancing the mechanical properties and degradation resistance of the adhesive interface [12–14].

Additionally, combining zinc oxide and copper nanoparticles (ZnO/ CuNp) has emerged as a promising approach to improve adhesive performance [15–17]. This synergy aims to optimise the protective effects on the HL and enhance the durability of dental restorations. However, despite these promising findings, the long-term effects of ZnO/CuNp on adhesive properties have not been comprehensively evaluated, necessitating further investigation.

This in vitro study aimed to evaluate the effect of incorporating different concentrations of zinc oxide and copper nanoparticles (ZnO/ CuNp) into universal adhesives on the resin-dentine microtensile bond strength, nanoleakage, and the presence of ZnO/CuNp within the hybrid layer on sound dentine immediately and after 2 years of water storage.

Thus, the following null hypotheses were tested: 1st) there is no significant differences in the adhesive properties evaluated (μTBS, NL and presence of ZnO/CuNp within the hybrid layer) among different adhesives; 2nd) there is no significant differences in the adhesive properties evaluated between the different adhesive strategies; and 3rd) there is no significant difference in the adhesive properties evaluated in the immediate time and after 2 years.

Material and methods

Formulation of the experimental adhesives Two UAs: Prime&Bond Active (Dentsply-Sirona, Konstanz, BadenWürttemberg, Germany) and Ambar Universal (FGM Dental Products, Joinville, SC, Brazil) were used to formulate six experimental UAs according to the addition of different concentrations of ZnONp (99.8 % pure, SkySpring Nanomaterials, Inc., Houston, TX, USA; www.ssnano. com) and CuNp (99.9 % pure, SkySpring Nanomaterials, Inc., Houston, TX, USA; www.ssnano.com) for each commercial UAs (Zn/Cu wt%): 5/0.1 % and 5/0.2 %. Additionally, the commercial adhesive (without modifications) was used as control. These concentrations were used based on previous literature [12–14,18]. The incorporation into the adhesive solution was done in a dark room with a motorised stirrer [14].

Teeth preparation and bonding procedures

Ninety-six caries-free extracted human third molars, collected from patients aged 18–35 years, were used after the approval from the Institutional Ethics Committee of the State University of Ponta Grossa/ PR/Brazil (Protocol 2.399.496). Teeth were disinfected in 0.5 % chloramine, stored in distilled water and used within 3 months after extraction. On each tooth, a flat dentine surface was exposed after wet grinding the occlusal enamel with 180-grit SiC paper (Buehler Ltd., Lake Bluff, IL, USA).

Bonding procedures

Before the bonding procedures, the surrounding enamel of all teeth was ground with a diamond bur nº 4137 (KG Sorensen, Barueri, SP, Brazil), until dentine was exposed. Then, the occlusal dentine surfaces were further polished with 600-grit silicon-carbide paper for 60 s to standardise the smear layer [17].

All UAs (with and without ZnO/CuNp) were applied in etch-andrinse (ER) or self-etch (SE) mode, as per manufacturer's instructions (Table 3) (n = 8) [19]. In ER mode, the dentine surface was acid etched with 37 % phosphoric acid for 15 s (Condac 37 %, FGM Dental Products, Joinville, SC, Brazil), water-rinsed for 15 s and air-dried keeping the dentine surface slightly wet. After the bonding procedures, resin composite (Opallis, FGM Dental Products, Joinville, SC, Brazil) was built up on the bonded surfaces in 3 increments of 1.0 mm thick each and each one was individually light-activated for 40 s at 1200 mW/cm2 (VALO, Ultradent Products, Salt Lake, UT, USA). A single operator carried out all bonding procedures in an environment with controlled temperature and humidity.

Tabela 3. Universal adhesive system (batch number), composition (∗) and application mode.

Universal adhesive system (manufacturer, batch number) and pH	Composition (∗)	Etch-and-rinse mode	Self-etch mode
Prime&Bond Active (PBA - Dentsply-Sirona, Konstanz, Baden-Württemberg, Germany) (1703000452) pH=~2.5	Phosphoric acid modified acrylate resin, multifunctional acrylate, bifunctional acrylate, acidic acrylate, isopropanol, water, initiator, Stabilizer (10-MDP and PENTA)	1 Apply phosphoric acid for 15s. 2 Remove gel with vigorous water spray and rinse conditioned areas thoroughly for 15s. 3 Remove rinsing water completely by blowing gently with an air syringe or blot dry. Do not desiccate dentin. 4 Apply adhesive to completely wet the surfaces to be treated. If necessary rewet applicator tip. Avoid pooling of the adhesive. 5 Keep the adhesive slightly agitated for 20s. 6 Disperse adhesive and remove solvent with clean, dry air from an air-water syringe. Treat every surface with a moderate air flow for at least 5s until a glossy and uniform layer result. 7 Light cure for 10s at 1200mW/cm^2	1 Apply adhesive to completely wet the surfaces to be treated. If necessary rewet applicator tip. Avoid pooling of the adhesive. 2 Keep the adhesive slightly agitated for 20s. 3 Disperse adhesive and remove solvent with clean, dry air from an air-water syringe. Treat every surface with a moderate air flow for at least 5s until a glossy and uniform layer result. 4 Light cure for 10s at 1200mW/cm^2
Ambar Universal (AMU - FGM Dental Products, Joinville, Santa Catarina, Brazil) (310516) pH=2.6–3.0	10-MDP, methacrylic monomers, photoinitiators, coinitiators, stabilizers, silica nanoparticles and ethanol	1 Apply phosphoric acid for 15s. 2 Wash the surface with plenty of water and dry the cavity so that the dentin does not get dehydrated, but without the accumulation of water on the	1 Apply a first layer vigorously rubbing the adhesive with the micro applicator for 10s. 2 Next, apply a second layer of adhesive for 10s, spreading the product.

		3	Evaporate excess solvent by thoroughly air-drying with an air syringe for 10s
3	Apply a first layer vigorously rubbing the adhesive with the micro applicator for 10s.	4	Light cure for 10s at 1200mW/cm^2
4	Next, apply a second layer of adhesive for 10s, spreading the product.		
5	Evaporate excess solvent by thoroughly air-drying with an air syringe for 10s		
6	Light cure for 10s at 1200mW/cm^2		

(∗) 10-MDP=methacryloyloxydecyl dihydrogen phosphate; PENTA=dipentaerythritol penta acrylate monophosphate.

After storage of the bonded teeth in distilled water at 37 ◦C for 24 h, they were longitudinally sectioned in both ‘‘x’’ and ‘‘y’’ directions across the bonded interface to obtain resin–dentine bonded sticks with a crosssectional area of approximately 0.8 mm2 . The number of premature failures (PF) during specimen preparation was recorded. The crosssectional area of each resin-dentine bonded stick was measured with the digital caliper to the nearest 0.01 mm and recorded for subsequent calculation of the microtensile bond strength values (Absolute Digimatic, Mitutoyo, Tokyo, Japan).

The resin–dentine bonded sticks originating from the same tooth were randomly divided and assigned to be tested immediately or after 2 years of storage in distilled water at 37 ◦C. The storage solution was not changed, and its pH was monitored monthly to ensure the medium remained close to a pH of 6.5. The pH was measured the same Eppendorf tube where each sample was stored, with a digital pH-meter (OneSense PH2500, Marte Cientifica, MG, Brazil).

The resin–dentine bonded specimens from each tooth were then divided as follows.

• Two resin–dentine bonded sticks for each tooth and at each storage period (16 per group) were used for nanoleakage evaluation.

• Two resin–dentine bonded sticks for each tooth and at each storage period (16 per group) were used for identification of the presence of zinc oxide and copper in the hybrid layer.

• Five resin–dentine bonded sticks for each tooth and at each storage period (40 per group) were submitted to μTBS test at each storage period.

Microtensile bond strength testing (μTBS)

Each resin–dentine bonded stick was attached to a modified device for μTBS test with cyanoacrylate resin (IC-Gel, bSi Inc., Atascadero, CA, USA) and subjected to a tensile force in a universal testing machine (Kratos, Sao ˜ Paulo, SP, Brazil) at 0.5 mm/min. The failure mode was evaluated under an optical microscope (SZH-131, Olympus; Tokyo, Japan) at 40x and classified as cohesive in dentine (failure exclusive within cohesive dentine – CD); cohesive in resin (failure exclusive within cohesive resin – CR); adhesive (failure at resin/dentine interface – A), or mixed (failure at resin/dentine interface that included cohesive failure of the neighbouring substrates, M). The number of premature failures (PF) was recorded, and it was not included in the average mean bond strength [20,21].

Nanoleakage evaluation (NL)

All resin–dentine bonded sticks selected for this test were coated with two layers of nail varnish applied up to within 1 mm of the bonded interfaces. The resin–dentine bonded sticks were immersed in 50 wt% ammoniacal silver nitrate solution in total darkness for 24 h, rinsed thoroughly in distilled water and immersed in photo-developing solution for 8 h under a fluorescent light to reduce silver ions into metallic silver grains within voids along the bonded interface [14].

Specimens (16 per group) were mounted on aluminium stubs, polished with 1000-, 1500-, 2000- and 2500-grit SiC paper and 1 and 0.25 μm diamond paste (Buehler Ltd., Lake Bluff, IL, USA). Then, they were ultrasonically cleaned, air-dried and gold-sputter coated (MED 010, Balzers Union, Balzers, Liechtenstein). The interfaces were observed in a scanning electron microscope in the backscattered mode at 12 kV (VEGA 3 TESCAN, Shimadzu, Tokyo, Japan).

To standardise image acquisition, five pictures were taken of each specimen. The first picture was taken in the centre of the resin–dentine bonded stick. The other four pictures were taken 0.3 and 0.6 mm to the left and right of the first one. Two resin–

dentine bonded sticks for each tooth and at each storage period were used for nanoleakage evaluation, totalling 80 images per group. A technician who was blinded to the experimental conditions under evaluation took them all. First, the adhesive layer was measured, which corresponds to the area of the adhesive between the resin and the dentine, including the hybrid layer. Secondly, the total infiltration area was measured (white areas within the hybrid layer). Then relative percentage of NL within the adhesive and hybrid layer areas was calculated in all pictures using the publicdomain ImageJ software, a Java-based image processing software package developed at the National Institutes of Health [22].

Identification of zinc oxide and copper within the hybrid layers by energy-dispersive X-ray

Two resin–dentine bonded sticks specimens for each tooth and at each storage period were used for identification of the presence of zinc oxide and copper within the hybrid layer. The analysis of the zinc oxide and copper content in each selected beam was performed by field emission scanning electron microscope (FE-SEM) (MIRA 3 TESCAN, Shimadzu, Tokyo, Japan) coupled with an energy-dispersive X-ray spectrometer (EDX). The bonding area was observed, and the analysis was focused on the middle of the hybrid layer. One site, randomly determined, per resin–dentine bonded stick was examined.

Statistical analysis

The data were first analyzed using the Kolmogorov-Smirnov test to assess whether the data followed a normal distribution, as well as Barlett's test for equality of variances to determine if the assumption of equal variances was valid. After confirming the normality of the data distribution and the equality of the variances, data for μTBS (MPa) and nanoleakage (%) of each UA were subjected to three-way ANOVA (adhesives vs. adhesive strategy vs. time). Tukey's post hoc test was used for pair-wise comparisons ($\alpha = 0.05$) using the Statistica for Windows software (StatSoft, Tulsa, OK, USA). The identification of zinc and copper within the hybrid layers by EDX was only qualitatively evaluated.

Results

Microtensile bond strength

For Prime&Bond Active, no significant differences were observed in μTBS among all groups at immediate time, in both adhesive strategies (Table 4; $p > 0.05$). Similarly, after 2 years, no significant differences were found in μTBS among all groups, regardless of the adhesive strategy (Table 4; $p > 0.05$). However, a significant difference in μTBS was observed between adhesive strategies, with the SE strategy showing lower μTBS values compared to the ER strategy (Table 4; $p < 0.05$). Furthermore, a significant decrease in μTBS was observed between immediate time and after 2 years for all groups, except for the 5/0.1 group in the ER strategy, where no significant change occurred (Table 4; $p > 0.05$). The predominant failure mode was adhesive for all groups, regardless of the main factors evaluated (Table 5).

For Ambar Universal, no significant differences were observed in μTBS among all groups at immediate time, regardless of adhesive strategy (Table 6; $p > 0.05$). After 2 years, the addition of ZnO/CuNp at 5/0.2 % resulted in higher μTBS values compared to the control, in both adhesive strategies (Table 6; $p < 0.05$). A significant difference was observed between adhesive strategies, with SE strategy showing lower μTBS values compared to the ER strategy (Table 6; $p < 0.05$). Additionally, a significant decrease in the μTBS was observed between immediate time and after 2 years for all groups, except for the 5/0.1 group in the ER strategy, where no significant change was found (Table 6; $p > 0.05$). The predominant failure mode was adhesive for all groups, regardless of the main factors evaluated (Table 7).

Tabela 4. Means and standard deviations of microtensile bond strength (MPa) obtained in each experimental condition with Prime&Bond Active.

Time	Etch-and-rinse			Self-etch		
	0 (control)	5/0.1	5/0.2	0 (control)	5/0.1	5/0.2
Immediate	51.2±4.1A	50.3±6.8 A	53.5±5.7 A	47.0±3.9 A	46.6±5.8 A	47.6±4.1 A
2-years	43.1±1.5 a,b	44.1±1.4 a	45.6±1.2 a	36.4±3.1 c	37.9±1.7 c	39.6±2.3 b,c
p-value	0.0036 *	0.0769	0.0157 *	0.0016 *	0.0126 *	0.0055 *

Comparisons are valid only within same row. Means identified with the same capital or lowercase letter are statistically similar. (Tukey's test, p≥0.05).

Comparisons are valid only within same column. Asterisk sign (*) identify means statistically different. (Tukey test,p<0.05).

Tabela 5. Fracture Pattern, pre-tested failures and number of resin-dentin sticks (n) tested in the microtensile bond strength test in each experimental condition with Prime&Bond Active (*)

ZnO/Cu concentration (%)	Immediate										
	Etch-and-rinse						Self-etch				
	Premature failure	n	Fracture pattern				Premature failure	n	Fracture pattern		
			CD	CR	A	M			CD	CR	A	M
0 (control)	1	40	2	2	36	0	0	40	2	3	35	0
5/0.1	0	40	1	0	39	0	0	40	1	0	38	1
5/0.2	0	40	0	1	38	1	0	40	0	0	40	0
2-years												
0 (control)	0	40	1	3	36	0	1	40	1	1	38	0
5/0.1	0	40	0	0	39	1	0	40	1	0	39	0
5/0.2	0	40	0	0	40	0	0	40	0	0	39	1

(*) Classification of fracture pattern: CD - cohesive dentin; CR – cohesive in resin; A - adhesive; and M–mixed.

Tabela 6. Means and standard deviations of microtensile bond strength (MPA) obtained in each experimental condition with Ambar Universal (*).

Time	Etch-and-rinse			Self-etch		
	0 (control)	5/0.1	5/0.2	0 (control)	5/0.1	5/0.2
Immediate	46.2±2.6 A	46.1±5.9 A	48.2±5.5 A	38.4±3.7 A	41.9±5.3 A	42.3±4.2 A
2-years	36.8±1.9 b,c	39.5±3.1 a,b	41.3±1.2 a	31.1±1.5 d	35.3±1.2 c,d	36.2±1.9 b,c
p-value	0.0078 *	0.0575	0.0273 *	0.0320 *	0.0254 *	0.0180 *

Comparisons are valid only within same row. Means identified with the same capital or lowercase letter are statistically similar. (Tukey's test, p≥0.05).

Comparisons are valid only within same column. Asterisk sign (*) identify means statistically different. (Tukey's test, p<0.05).

Tabela 7. Fracture pattern, pre-tested failures and number of resin-dentin sticks (n) tested in the microtensile bond strength test in each experimental condition.

ZnO/Cu concentration (%)	Immediate											
	Etch-and-rinse						Self-etch					
	Premature failure	n	Fracture pattern				Premature failure	n	Fracture pattern			
			CD	CR	A	M			CD	CR	A	M
0 (control)	2	40	3	0	37	0	1	40	1	0	39	0
5/0.1	0	40	0	0	40	0	0	40	1	3	36	0
5/0.2	0	40	1	1	38	0	0	40	0	0	40	0
2-years												
0 (control)	1	40	1	1	38	0	1	40	1	0	39	0
5/0.1	1	40	0	0	40	0	0	40	0	0	39	1
5/0.2	0	40	0	0	40	0	0	40	0	0	40	0

(*) Classification of fracture pattern: CD - cohesive dentin; CR – cohesive in resin; A - adhesive; and M–mixed.

Nanoleakage evaluation

For Prime&Bond Active, the addition of ZnO/CuNp resulted in significantly lower NL values compared to the control in both adhesive strategies at both the immediate time and after 2 years (Table 8; $p < 0.05$). No significant differences were observed between adhesive strategies, regardless different adhesive used (with or without different ZnO/CuNp evaluated), at either time point (Table 8; $p > 0.05$). A

significant increase in NL values was observed after 2 years all groups, irrespective of the adhesive strategy (Table 8; $p < 0.05$) (see Fig. 5).

Tabela 8. Means and standard deviations of nanoleakage (%) obtained in each experimental condition with Prime&Bond Active (*).

Time	Etch-and-rinse			Self-etch		
	0 (control)	5/0.1	5/0.2	0 (control)	5/0.1	5/0.2
Immediate	19.4±2.5B	12.3±2.3 A	10.3±2.2 A	18.1±4.5B	10.5±2.8 A	9.9±1.9 A
2-years	29.5±2.6 c	16.3±1.6b	14.3±0.7 a,b	29.6±2.3 c	15.2±2.5 a,b	12.9±1.1 a
p-value	0.0002 *	0.0014 *	0.0004 *	0.0002 *	0.0033 *	0.002 *

For Ambar Universal, the addition of ZnO/CuNp resulted in significantly lower NL values compared to the control in both adhesive strategies at both immediate time and after 2 years (Table 9; $p < 0.05$). No significant differences were observed between adhesive strategies, regardless different adhesive used (with or without different ZnO/CuNp evaluated), at either time point (Table 9; $p > 0.05$). A significant increase in NL values was observed after 2 years for all groups, irrespective of the adhesive strategy (Table 9; $p < 0.05$) (see Fig. 5).

Tabela 9. Means and standard deviations of nanoleakage (%) obtained in each experimental condition with Ambar Universal (*).

Time	Etch-and-rinse			Self-etch		
	0 (control)	5/0.1	5/0.2	0 (control)	5/0.1	5/0.2
immediate	15.5±4.8C	7.0±2.1 A	4.3±1.0 A	10.4±1.2B	6.6±0.9 A	6.9±0.6 A
2-years	25.1±2.4b	13.9±3.5 a	11.3±1.3 a	23.3±2.9b	11.2±3.7 a	11.0±1.9 a
p-value	0.0003 *	0.0005 *	0.0002 *	0.0002 *	0.0044 *	0.0002 *

Comparisons are valid only within same row. Means identified with the same capital or lowercase letter are statistically similar. (Tukey's test, $p \geq 0.05$).

Comparisons are valid only within same column. Asterisk sign (*) identify means statistically different. (Tukey's test, $p < 0.05$).

Identification of copper within the hybrid layers by EDX

The compositional analysis of the adhesive interface using EDX, conducted after 2 years, confirmed the presence of ZnO/CuNp within the hybrid layer in both

concentrations, across both adhesive strategies, and in both adhesive systems. (Fig. 5).

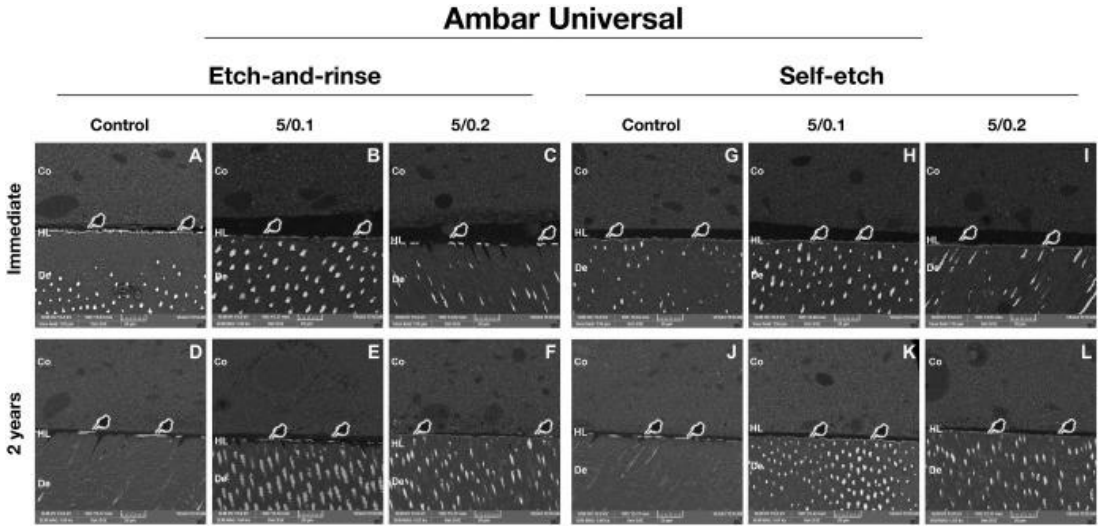

Figura 5. Representative back-scattering SEM images of the resin–dentine interfaces.

Representative back-scattering SEM images of the resin–dentine interfaces according to the different experimental conditions using Prime&Bond Active adhesive. In the ZnO/CuNp-containing adhesive groups (B-C and E-F for etch-and-rinse mode; H-I and K-L for self-etch mode) we can see lower silver nitrate deposition than the control groups (A and D for etch-and-rinse mode; G and J for self-etch mode) (white stains indicated by white pointer). (Co = composite; HL = hybrid layer and De = dentine).

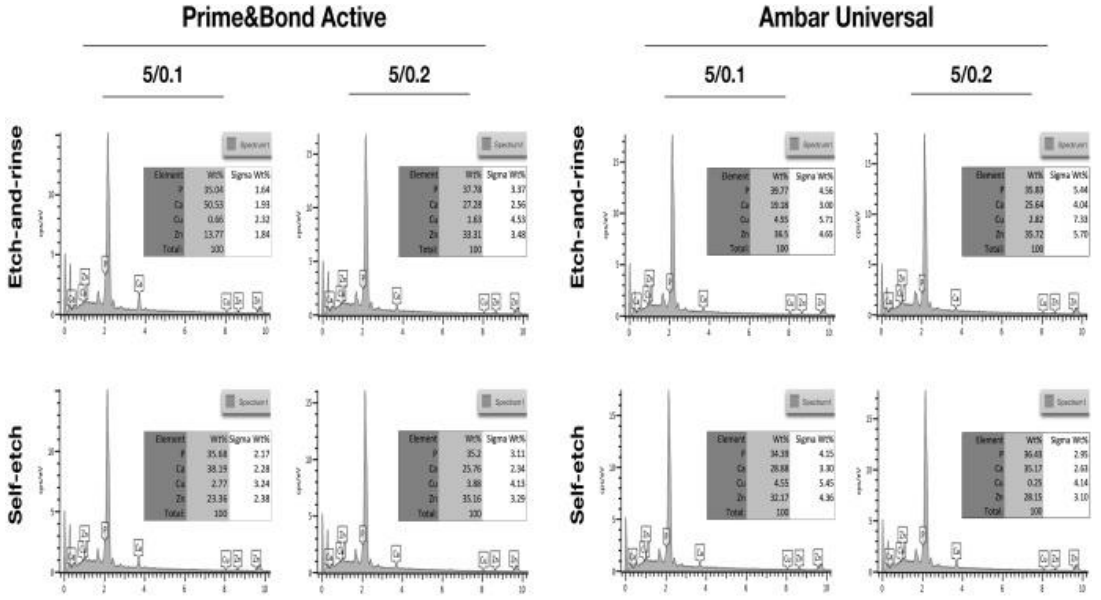

Figura 6. EDX spectrum of the resin–dentine bonded interfaces

EDX spectrum of the resin–dentine bonded interfaces after 2-year of water storage for 5.01 % and 5.02 % ZnO/CuNp-containing universal adhesives. The figure table summarizes the elemental composition of the sample outlined area.

Discussion

This in vitro study investigated the effects of incorporating of ZnO/ CuNp into two universal adhesives (Ambar Universal and Prime&Bond Active) by assessing their adhesive properties at the resin-dentine bonded interface. The results of the present study demonstrated that the addition of ZnO/CuNp positively impact the immediate bonding properties, with some variations between the adhesive strategies. Also, the results showed that adding ZnO/CuNp to universal adhesives would enhance the properties of the adhesive interface on sound dentine after 2 years of water storage. All these results lead the authors to reject the three null hypotheses of the present study.

The degradation of resin-dentine bonded interfaces in UAs primarily driven by hydrolysis and decline of bond strength over time [23]. This degradation is further exacerbated by the inclusion of hydrophilic monomers, which enhance initial bonding result but ultimately contribute to long-term reductions in bond strength [24]. In this study, bond strength decreased after the 2-year period for all groups, regardless of ZnO/CuNp incorporation, except for the 5/0.1 wt% groups, where resin-dentine bond strength remained stable. The observed reduction of bond strength over time for the other groups is likely due to the high hydrophilicity of the resin monomer, present in both Ambar Universal and Prime&Bond Active [17].

Notably, the addition of ZnO/CuNp to universal adhesives did not compromise the mechanical properties of the adhesive interface in terms of microtensile bond strength at both initial measurements and after two years. These findings align with previous studies, which have shown that adhesives modified with ZnO/CuNp at comparable concentrations retained their microtensile bond strength, even when applied to modified dentine substrate, albeit over shorter evaluation periods [15–17].

The addition of ZnO and CuNp to universal adhesives may help reduce matrix metalloproteinase (MMP) activity, thereby controlling collagen degradation [8]. Previous studies have shown that both Zn and Cu, either individually [25,26] or in

combination, can inhibit the activity of MMP-2, MMP-8, and MMP-9, enzymes that play a key role in collagen degradation during the demineralisation process [8]. The mechanism by which zinc oxide inactivates enzymes is not fully understood. However, it is hypothesized that metal ions bind to specific sites on the enzyme, inducing conformational changes that disrupt its catalytic function. For instance, zinc oxide may form a bridge between the catalytic zinc ion and a side chain within the enzyme's active site. In contrast, copper's inhibition of MMPs may occur through multiple mechanisms. One proposed mechanism involves the binding of copper ions to the zinc-binding site of MMPs, displacing the zinc ion that is essential for their catalytic activity. This displacement disrupts the enzyme's structure and function, leading to inhibition. Additionally, copper can modulate MMP activity at the transcriptional level by downregulating the expression of MMP genes, thereby reducing the overall production of these enzymes [27,28]. This suggests that the incorporation of ZnO/CuNp into adhesive systems could offer a protective effect against enzymatic breakdown of the hybrid layer, potentially improving the longevity and stability of the bond.

Specifically, microtensile bond strength was enhanced in the ZnO/ CuNp modified Ambar Universal groups at 2 years, while remaining stable in the Prime&Bond Active groups during the same period. The enhanced microtensile bond strength observed in ZnO/CuNp modified Ambar Universal groups can likely be attributed to the inclusion of ZnO/ CuNp, underscoring the importance of evaluating their effects over extended periods. Conversely, the stable microtensile bond strength in modified Prime&Bond Active groups may result from greater water sorption due to its distinct composition, which includes isopropanol, a highly water-soluble solvent [16]. This highlights the need to consider different formulations of universal adhesives. Application modes-etch-and-rinse and self-etch- exhibited varying outcomes at 2 year assessment, where self-etch yielding inferior results to etch-and-rinse, consistent with earlier findings [29]. Adhesive failure was the most common mode observed, emphasizing the critical role of adhesive interface integrity in bonding performance.

Bond failure often leads to nanoleakeage, which can be identified though silver tracer penetration observed via electron microscopy. Nanoleakeage indicates areas of increased water permeability, potentially compromising the restoration's integrity [30]. In this study, the addition of ZnO/CuNp reduced nanoleakeage values for both universal adhesives at both evaluation points, suggesting an improvement in adhesive performance. Additionally, the application mode did not significantly alter

nanoleakeage outcomes. One possible explanation for the observed nanoleakage results is the potential role of ZnO/CuNps in improving the structural integrity of the resin-dentine interface. CuNp may help stabilize the collagen matrix by promoting the cross-linking of collagen fibrils, which could improve the durability of the adhesive bond [13]. This is because copper is known to play a key role in the enzymatic activity of lysyl oxidase, an enzyme crucial for collagen cross-linking [31]. On the other hand, ZnO has been shown to contribute to the mineralization of dentine by inducing the formation of hydroxyapatite crystals on the collagen fibers [18], which may further strengthen the hybrid layer. Moreover, ZnO can chemically interact with various components of the adhesive resin, such as methacrylate and amide groups, enhancing the polymerization process and improving the overall adhesive properties by promoting stronger intermolecular bonds within the resin matrix [32,33].

However, all groups exhibited an increase in nanoleakeage at 2 years compared to immediate values, regardless of the presence of metallic nanoparticles. The observed increase in nanoleakeage and decrease in microtensile bond strength values over time suggests that while ZnO/ CuNp may enhance the longevity of the adhesive interface, they do not fully prevent degradation processes. Although we know that this decrease in adhesive properties is consistent with the long-term evaluation [2], the groups with ZnO/CuNps always had statistically higher values of microtensile bond strength and statistically lower values of nanoleakage than control, irrespective of universal adhesive and adhesive strategies.

Both microtensile bond strength (μTBS) and nanoleakage (NL) tests are widely employed in the scientific literature to evaluate the adhesive properties of dental adhesives. This likely explains why approximately 60 % of current studies assessing hybrid layer stability utilize the μTBS and NL approach [21]. However, the results of these tests should be interpreted with caution. Due to the high regional variability within the tooth, obtaining representative data on μTBS and nanoleakage remains challenging. Moreover, multiple studies have reported no correlation between nanoleakage and adhesive bond strength [34]. Thus, a relationship between these in vitro tests and the clinical behavior of these adhesives could be a challenge.

Nevertheless, a significant and reasonably strong correlation was observed between aged in vitro data and 5-year clinical performance [21]. Notably, some studies have pooled data from 500 thermocycles with 1-year water-storage results, despite the latter aging method likely inducing greater bond degradation than the former.

Conversely, as anticipated, the 5-year clinical data revealed a relationship between in vitro bond strength with clinical performance, that became statistically significant when non-aged bond strength data were excluded. Therefore, in addition to assessing the immediate bond strength of adhesives to dentin, evaluating aged bond strength is essential for predicting clinical effectiveness. In this study, specimens were aged for 2 years in water storage to address this critical aspect.

Compositional analysis of the adhesive interface through energy dispersive X-ray spectroscopy (EDX) offers critical insights into longterm stability and integration of nanomaterials within dental adhesives [35]. In this study, ZnO/CuNp were detected after 2 years of water storage, confirming their presence within the hybrid layer across both concentrations and adhesive strategies. The retention of ZnO/CuNp indicates its potential to serve as a long-term reservoir within universal adhesives [36]. Previous research has shown a controlled release of copper, with approximately half remaining after at least 1.3 year [17], Fig. 3. EDX spectrum of the resin–dentine bonded interfaces after 2-year of water storage for 5.01 % and 5.02 % ZnO/CuNp-containing universal adhesives. The figure table summarizes the elemental composition of the sample outlined area. M.F. Guti´errez et al. International Journal of Adhesion and Adhesives 140 (2025) 104023 7 supporting the idea of a slow, sustained release of ZnO and CuNp. This gradual release could provide ongoing reinforcement to the collagen fibrils in the hybrid layer, preventing premature degradation and maintaining bond stability over time. Such a mechanism may be potentially extending the longevity of adhesive restorations in clinical applications.

The successful incorporation and retention of ZnO/CuNp in the adhesive interface indicates that these nanoparticles can enhance the properties of the interface, potentially contributing to improved durability and performance over time. The consistent detection of ZnO/CuNp within the hybrid layer highlights their potential role in strengthening the mechanical and chemical stability of adhesive systems. These findings support the hypothesis that ZnO/CuNp can mitigate degradation processes, providing long-term benefits. Further research is needed to explore their specific functional contributions and overall impact on the longevity and clinical performance of dental adhesives.

This study provides evidence that the incorporation of ZnO/CuNp into two universal adhesive systems enhances the resin-dentine bond, particularly at the interface with caries-affected dentine, by reducing hybrid layer degradation over a 2-

year period. While this is the first study to assess the medium-term effects of ZnO/CuNp on bonding performance with sound dentine, the findings align with previous research, supporting the potential of these nanoparticles to improve adhesive stability [16,17]. However, as previous research has primarily focused on the clinical performance of CuNp in adhesives [37,38], further clinical studies are necessary to evaluate the impact of ZnO/CuNp on the long-term effectiveness and reliability of universal adhesives in real-world applications.

Despite the inherent limitations to in vitro studies-such as their inability to fully replicate the complex dynamics of the oral environment that influence the degradation of adhesive restorations-these findings underscore the potential of nanoparticle modifications to enhance adhesive durability over the long term. This emphasizes the need for further research aimed at optimizing the incorporation of nanoparticles into the adhesive formulations and investigating their specific contributions to the longevity and clinical performance of dental restorations.

Conclusion

The incorporation of zinc oxide and copper nanoparticles (up to 5/ 0.2 wt%) into two universal adhesive systems may enhance the integrity of the hybrid layer on sound dentine in comparison with the commercial adhesive (control), both immediately and after 2 years of water storage, regardless of the application mode.

References

[1] Tjaderhane L. Dentin bonding: can we make it last? Operat Dent 2015;40:4–18. [2] Betancourt DE, Baldion PA, Castellanos JE. Resin-dentin bonding interface: mechanisms of degradation and strategies for stabilization of the hybrid layer. Int J Biomater 2019;2019:5268342.
[3] Nakabayashi N, Kojima K, Masuhara E. The promotion of adhesion by the infiltration of monomers into tooth substrates. J Biomed Mater Res 1982;16: 265–73.
[4] Spencer P, Ye Q, Park J, Topp EM, Misra A, Marangos O, et al. Adhesive/Dentin interface: the weak link in the composite restoration. Ann Biomed Eng 2010;38: 1989–2003.
[5] Perdigão J, Swift Jr EJ. Universal adhesives. J Esthetic Restor Dent 2015;27:331–4.
[6] Nagarkar S, Theis-Mahon N, Perdigão J. Universal dental adhesives: current status, laboratory testing, and clinical performance. J Biomed Mater Res B Appl Biomater 2019;107:2121–31.

[7] Perdigão J, Araujo E, Ramos RQ, Gomes G, Pizzolotto L. Adhesive dentistry: current concepts and clinical considerations. J Esthetic Restor Dent 2021;33: 51–68.
[8] Mazzoni A, Tjaderhane L, Checchi V, Di Lenarda R, Salo T, Tay FR, et al. Role of dentin MMPs in caries progression and bond stability. J Dent Res 2015;94:241–51. [9] Pashley DH, Tay FR, Carvalho RM, Rueggeberg FA, Agee KA, Carrilho M, et al. From dry bonding to water-wet bonding to ethanol-wet bonding. A review of the interactions between dentin matrix and solvated resins using a macromodel of the hybrid layer. Am J Dent 2007;20:7–20.
[10] Tjaderhane L, Buzalaf MA, Carrilho M, Chaussain C. Matrix metalloproteinases and other matrix proteinases in relation to cariology: the era of 'dentin degradomics'. Caries Res 2015;49:193–208.
[11] Mjor IA, Moorhead JE, Dahl JE. Reasons for replacement of restorations in permanent teeth in general dental practice. Int Dent J 2000;50:361–6.
[12] Barcellos DC, Fonseca BM, Pucci CR, Cavalcanti B, Persici Ede S, Goncalves SE. Zndoped etch-and-rinse model dentin adhesives: dentin bond integrity, biocompatibility, and properties. Dent Mater 2016;32:940–50.
[13] Gutierrez MF, Malaquias P, Hass V, Matos TP, Lourenco L, Reis A, et al. The role of copper nanoparticles in an etch-and-rinse adhesive on antimicrobial activity, mechanical properties and the durability of resin-dentine interfaces. J Dent 2017; 61:12–20.
[14] Gutiérrez MF, Malaquias P, Matos TP, Szesz A, Souza S, Bermudez J, et al. Mechanical and microbiological properties and drug release modeling of an etchand-rinse adhesive containing copper nanoparticles. Dent Mater 2017;33:309–20.
[15] Basualdo Allende J, Nascimento FD, Damasceno ESCM, Aliaga-Galvez R, Naupari- ˜ Villasante R, Miranda CB, et al. Evaluation of adhesive properties and enzymatic activity at the hybrid layer of a simplified adhesive loaded with 0.2 % Cu and 5 % ZnO nanoparticles: a Randomized Clinical Trial and ex vivo analysis. J Dent 2024; 149:105283.
[16] Gutiérrez MF, Alegria-Acevedo LF, Mendez-Bauer L, Bermudez J, DavilaSanchez A, Buvinic S, et al. Biological, mechanical and adhesive properties of universal adhesives containing zinc and copper nanoparticles. J Dent 2019;82: 45–55.
[17] Gutierrez MF, Bermudez J, Davila-Sanchez A, Alegria-Acevedo LF, MendezBauer L, Hernandez M, et al. Zinc oxide and copper nanoparticles addition in universal adhesive systems improve interface stability on caries-affected dentin. J Mech Behav Biomed Mater 2019;100:103366.
[18] Toledano M, Sauro S, Cabello I, Watson T, Osorio R. A Zn-doped etch-and-rinse adhesive may improve the mechanical properties and the integrity at the bondeddentin interface. Dent Mater 2013;29:e142–52.
[19] S. Armstrong, L. Breschi, M. Ozcan, F. Pfefferkorn, M. Ferrari, B. Van Meerbeek Academy of Dental Materials guidance on in vitro testing of dental composite bonding effectiveness to dentin/enamel using micro-tensile bond strength (μTBS) approach. Dent Mater, 33 (2017), pp. 133-143.
[20] A. Mine, J. De Munck, M.V. Cardoso, K.L. Van Landuyt, A. Poitevin, T. Kuboki, et al. Bonding effectiveness of two contemporary self-etch adhesives to enamel and dentin. J Dent, 37 (2009), pp. 872-883.
[21] Van Meerbeek B, Peumans M, Poitevin A, Mine A, Van Ende A, Neves A, et al. Relationship between bond-strength tests and clinical outcomes. Dent Mater 2010; 26:e100–21.
[22] Schneider CA, Rasband WS, Eliceiri KW. NIH Image to ImageJ: 25 years of image analysis. Nat Methods 2012;9:671–5.

[23] Hashimoto M. A review–micromorphological evidence of degradation in resindentin bonds and potential preventional solutions. J Biomed Mater Res B Appl Biomater 2010;92:268–80.
[24] Frassetto A, Breschi L, Turco G, Marchesi G, Di Lenarda R, Tay FR, et al. Mechanisms of degradation of the hybrid layer in adhesive dentistry and therapeutic agents to improve bond durability–A literature review. Dent Mater 2016;32:e41–53.
[25] Osorio R, Yamauti M, Osorio E, Ruiz-Requena ME, Pashley DH, Tay FR, et al. Zinc reduces collagen degradation in demineralized human dentin explants. J Dent 2011;39:148–53.
[26] Jun SK, Yang SA, Kim YJ, El-Fiqi A, Mandakhbayar N, Kim DS, et al. Multifunctional nano-adhesive releasing therapeutic ions for MMP-deactivation and remineralization. Sci Rep 2018;8:5663.
[27] Alexandrova A, Bandˇzuchova ´ E, Kebis A, Kukan M, Kuba D. Copper decreases gene expression of TNF-α, IL-10, and of matrix metalloproteinases MMP-2 and MMP-9 in isolated perfused rat livers. Biologia 2007;62:365–9.
[28] de Souza AP, Gerlach RF, Line SR. Inhibition of human gingival gelatinases (MMP2 and MMP-9) by metal salts. Dent Mater 2000;16:103–8.
[29] Vieira BR, Dantas ELA, Cavalcanti YW, Santiago BM, Sousa FB. Comparison of selfetching adhesives and etch-and-rinse adhesives on the failure rate of posterior composite resin restorations: a systematic review and meta-analysis. Eur J Dermatol 2022;16:258–65.
[30] Tay FR, Pashley DH, Yoshiyama M. Two modes of nanoleakage expression in single-step adhesives. J Dent Res 2002;81:472–6.
[31] Vallet SD, Ricard-Blum S. Lysyl oxidases: from enzyme activity to extracellular matrix cross-links. Essays Biochem 2019;63:349–64.
[32] Soares R, Carone C, Einloft S, Ligabue R, Monteiro W. Synthesis and characterization of waterborne polyurethane/ZnO composites. Polym Bull 2014; 71:829–38.
[33] Rahman MM. Polyurethane/zinc oxide (PU/ZnO) composite-synthesis, protective propertyand application. Polymers 2020;12.
[34] Guzmán-Armstrong S, Armstrong SR, Qian F. Relationship between nanoleakage and microtensile bond strength at the resin-dentin interface. Operat Dent 2003;28: 60–6.
[35] Sarhan H, Mehesen R, Hamama H, Mahmoud SH. Elemental analysis and micromorphological patterns of tooth/restoration interface of three ion-releasing class V restorations. BMC Oral Health 2024;24:1221.
[36] Sabatini C, Mennito AS, Wolf BJ, Pashley DH, Renne WG. Incorporation of bactericidal poly-acrylic acid modified copper iodide particles into adhesive resins. J Dent 2015;43:546–55.
[37] Matos TP, Gutiérrez MF, Hanzen TA, Malaquias P, de Paula AM, de Souza JJ, et al. 18-month clinical evaluation of a copper-containing universal adhesive in noncarious cervical lesions: a double-blind, randomized controlled trial. J Dent 2019; 90:103219.
[38] Matos TP, Naupari-Villasante ˜ R, Kunz PVM, Hass V, Reis A, Gutiérrez MF, et al. 48- month clinical evaluation of a copper-containing universal adhesive in non-carious cervical lesions: a double-blind randomised clinical trial. Dent Mater 2023;39: 820–30.

3.3 ARTIGO 3: EVALUATION OF ADHESIVE PROPERTIES AND ENZYMATIC ACTIVITY AT THE HYBRID LAYER OF A SIMPLIFIED ADHESIVE LOADED WITH 0.2% CU AND 5% ZNO NANOPARTICLES: A RANDOMIZED CLINICAL TRIAL AND EX VIVO ANALYSIS

STATUS: Publicado em 2024
REVISTA: Journal of Dentistry
DOI: 10.1016/j.jdent.2024.105283

Javier Basualdo Allende[a,b] , Fabio Dupart Nascimento[c] , Marina Damasceno e Souza Chiari[c] , Romina Aliaga-Galvez[d] , Romina Ñaupari-Villasante[e] , Cristian Bersezio Miranda[a] , Carolina Pardo-Díaz[a,e,f] , Mario Felipe Gutièrrez [a,d] , Cristian Covarrubias[g] , Alessandro D. Loguercio[e] , Eduardo Fernández[a,h],*

[a] Universidad de Los Andes, Chile. Facultad de Odontología. Santiago, Chile, Zip Code 7550000
[b] University of Chile, Department of Restorative Dentistry, Faculty of Dentistry, Santiago, Chile, Zip Code 8380544
[c] University of Valparaiso, Department of Operative Dentistry, School of Dentistry, Valparaíso, Chile, Zip Code 2360004
[d] State University of Ponta Grossa, Department of Restorative Dentistry, School of Dentistry, Ponta Grossa, Brazil, Zip Code 84030-900
[e] San Francisco de Quito University, Buonocore Dental Biomaterials Research Institute, Quito, Ecuador, Zip Code 170901
[f] Universidad Autónoma de Chile, Instituto de Ciencias Biomédicas, Santiago, Chile, Zip Code 7500912

Abstract

Objective: The aim of this study was to evaluate the effect of an adhesive loaded with 0.2 % copper (Cu) and 5 % zinc oxide (ZnO) nanoparticles (Nps) on its adhesive properties and enzymatic activity at the hybrid layer *ex vivo* in a randomized clinical model. Methods: Fifteen patients participated in this study, and a total of 30 third molars were used. Occlusal cavities (4 × 4 × 2 mm) were made in each tooth, and randomly divided into 2 groups: (i) Experimental group: commercial adhesive loaded

with 0.2wt % CuNps and 5wt % ZnONps; and (ii) Control Group: non-loaded commercial adhesive. Teeth were restored with resin composite. Thirty days later, extractions were performed. Extracted teeth were longitudinally sectioned. Nps in powder were characterized by field emission scanning electron microscope (FE-SEM) and energy dispersive X-ray (EDX) analysis. Microtensile bond strength (μTBS), degree of conversion (DC), and nanoleakeage (NL) tests were executed. In situ zymography (Zym) was performed to evaluate the gelatinolytic activity at the hybrid layer. Student's *t*-test (α = 0.05) was applied for all tests. Results: μTBS and DC did not show significant differences ($p > 0.05$) between both groups. However, NL and gelatinolytic activity at the hybrid layer showed significant values ($p < 0.05$) for experimental group in comparison with control group. Conclusion: The addition of 0.2 % CuNps and 5 % ZnONps to a universal adhesive decreases NL and gelatinolytic activity at the hybrid layer, without jeopardizing its adhesive properties.

Introduction

Dental caries is one of the leading prevalent chronic oral diseases with an extensive socioeconomic impact throughout the world. It is promoted by acid demineralization and subsequent degradation of the organic matrix of the tooth which can result in cavities development [1].

In this context, composite resins are the main treatment for the consequences of dental caries, they offer advantages such as aesthetics and less invasive preparation techniques [2,3]. However, the lack of durability of resin-dentin bonds and secondary caries are considered the main problems with contemporary adhesive restorations, negatively affecting their clinical success [3,4]. Furthermore, constantly replacement of composite resins leads to loss of sound tooth structure, increasing cavity volume, and needing a more complex restoration [5]. This reduced longevity and replacement of these restorations for more complex ones, results in millions of dollars spent annually on dental care [6].

The adhesive/dentin interface can be considered the weakest point in the composite restoration [4], and factors related to adhesive/dentin interface degradation are mainly caused by hydrolytic degradation over time of the polymer present in the hybrid or adhesive layers, and a poorly infiltrated hybrid layer with unprotect collagen fibers, that could be hydrolyzed by host-derived matrix metalloproteinase (MMPs) and

cysteine-cathepsins (CTs) [7]. These enzymes are activated by pH changes relevant to the acid etching process and/or by an acidic pH brought about by lactate release from cariogenic bacteria, indicating the role of bacterial acids in the process [8,9,10].

Metallic nanoparticles (Nps) have been highlighted among the most promising agents with antibacterial properties, exhibiting biocidal activities even at low concentrations [11]. Copper nanoparticles (CuNps) have been shown to be effective against gram-positive and gram-negative bacteria [12]. Additionally, copper is a low-price compound, which makes the synthesis of copper nanoparticles economically relevant. Also, CuNps seems to be a potent inhibitor of dentin metalloprotease-2 (MMP-2), and stimulates the secretion of tissue inhibitors of MMPs, causing a decreased degradation pattern in the resin/dentin interface [13]. On the other hand, zinc oxide nanoparticles (ZnONps) can promote subtle conformational changes in collagenase cleavage sites in the collagen fibers that protect collagen from MMPs hydrolysis [14].

Recent in vitro studies have shown that the addition of CuNps at concentrations up to 0.1 wt % in the adhesive system provides antimicrobial properties and preserves the bonding to dentin after 1 and 2 years of water storage, without reducing the adhesive properties of the adhesive formulations [15,16] Likewise, the incorporation of ZnONps in an adhesive system preserves the bonding to dentin after 6 months, without reducing the mechanical properties of the adhesive [17]. To the best of our knowledge, no clinical study has been conducted to evaluate these properties using a combination of Cu and ZnO by ex vivo analysis. The aim of this randomized clinical study was to evaluate the adhesive properties and enzymatic degradation activity the behavior of a CuNps and ZnONps, 0.2wt % and 5wt % respectively, added to a universal adhesive in restored teeth after one month, by an ex vivo analysis. The tested hypothesis was that CuNps and ZnONps, 0.2wt % and 5wt % incorporated to a universal adhesive does not affect its adhesive properties and reduces enzymatic degradation activity of collagen at the hybrid layer.

Materials and methods

Ethics approval

This clinical study was conducted following the CONSORT recommendations and the ethical principles of the Helsinki Convention [18, 19]. Patients consent to their

participation was given in writing in a document reviewed and approved by the scientific ethical committee of the Faculty of Dentistry of local University.

Research design, patient selection, and randomization

This study was a randomized, split-mouth clinical trial, in which the clinical operator (J.B.), the evaluators (RNV and ADL) and the biostatistician (E.F) were blinded to the treatment assignment. Fifteen patients (average 28 years old), volunteers from the Orthodontic Dentistry Clinic at the local University were included, with at least an indication of two premolar and/or two third molar extraction, from right and left sides of the mouth for orthodontic reasons. Exclusion criteria: poor oral hygiene, untreated periodontal disease, and caries ongoing.

Teeth were randomly allocated into two groups (n = 15) for the resin-dentin adhesive tests according to the following variables: i) Experimental group: commercial adhesive loaded with 0.2wt % CuNps and 5wt % ZnONps; and (ii) Control Group: non-loaded commercial adhesive (Fig. 7). The adhesive bottles were labeled with letters A and B. Randomly generated intervention allocations using Excel software were given in a sealed opaque envelope to dental assistant The clinical operator received labeled bottles without knowing which adhesive was used, and the intervention allocations from the given envelope.

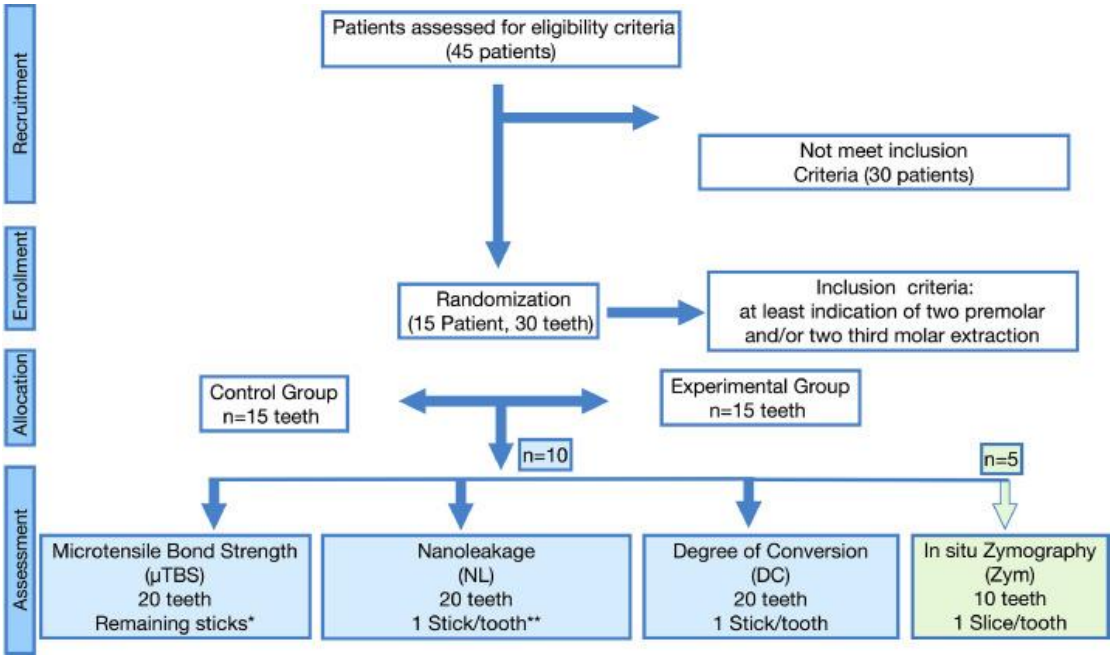

Figura 7. Representative flow diagram of the formation of the different groups

Representative flow diagram of the formation of the different groups. The light blue color corresponds to same teeth (*n* = 10). After specimen preparation, resin-

bonded sticks were allocated according to each test. The green color corresponds to teeth with different specimen preparation to perform the in situ zymography. *Remaining sticks analyzed for Microtensile bond strength (μTBS) were at least 6 per tooth. **Two sticks, one per group after nanoleakeage (NL) assessment were analyzed by energy-dispersive X-ray spectrometer (EDX).

Formulation of the experimental adhesive

Experimental adhesives were formulated using a simplified adhesive system: Ambar Universal (FGM Prod. Odont. Ltda, Joinville, SC, Brazil) with the addition 0.2wt % CuNps and 5wt % ZnONps Nps, as previously described [15,16]. The CuNps and ZnONps (SkySpring Nanomaterials, Inc., Houston, TX, USA; www.ssnano.com) were characterized by field emission scanning electron microscope (FE-SEM) and energy dispersive X-ray (EDX) analysis in previous studies [15,16]. Their manufacturer specifications are detailed in Table 10. These concentrations were based on previous in vitro studies [24,26]. The incorporation to the adhesive solution was done in a dark room with a motorized stirrer. For the Control group the commercial adhesive without any modification was used.

Tabela 10. Zinc Oxide and copper nanoparticles manufacturer specifications.

Type of particles/batch number/ manufacturer	**Specifications**
Copper nanoparticles (Cu) 0820XH Skyspring Nanomaterials, Inc*	Purity: 99.9 % trace metals basis Appearance: Black nanopowder APS: 40–60 nm SSA: ~12 m^2/g Morphology: spherical $_3$ Bulk density: 0.19 g/cm True density: 8.9 g/cm^3
Zinc oxide nanoparticles (ZnO) 8410DL Skyspring Nanomaterials, Inc*	Purity: 99.8 % trace metals basis Appearance: White yellow nanopowder APS: 10–30 nm SSA: 30–50 m^2/g

APS, Average Particle Size; SSA: Specific Surface Area.

Restorative procedure and specimen preparation

Before restorative procedures, local anesthesia was applied with a 3 % mepivacaine solution (Mepisv, Nova DFL, Rio de Janeiro, RJ, Brazil), and the rubber dam isolation was performed. Each tooth received a class I cavity (4 mm bucco-lingual width; 4 mm mesio-distal width; 2 mm depth in dentine), using a cylindrical flat end, medium grit diamond bur (60,730,025; 109/018 ISO number; DentsplySirona, Charlotte, NC, USA) under copious water coolant with a high-speed handpiece. Adhesives were applied in etch-and-rinse mode using 37 % phosphoric acid gel (Condac37, FGM, Joinville, SC, Brazil) for 15 s, water rinsed for 15 s and dried with absorbent paper. The adhesive system was applied according to the manufacturer's recommendations. Subsequently, the composite resin buildups (Opallis, FGM, Joinville, SC, Brazil) were placed in layers of 2 mm each. Each increment was light-cured for 40 s with an LED light-curing unit set at 1200 mW/cm2 (Valo, Ultradent, South Jordan, UT, USA). A single operator performed all the restorative procedures. The materials used, composition, and application modes are listed in Table 11.

Tabela 11. Materials, composition and application mode of the adhesive system and composite resin. (*).

Materials	Composition	Application technique
Condac 37 (FGM Dent Prod., Joinville, SC, Brazil)	37 % phosphoric acid	1. Apply etchant to the enamel (15 s), following to the dentin surfaces (more 15 s). 2. Rinsed with water for 30 s. 3. Gently air dry for 5 s using an air syringe held 10.0 cm away, while keeping the dentin surface slightly moist.
Ambar Universal (FGM Prod. Odont., Joinville, SC, Brazil) pH ≈ 2.6–3.0*	1. Commercial adhesive: UDMA, HEMA, 10-MDP, methacrylate hydrophilic monomers, methacrylate acid monomers, ethanol, ultrapure water, silanized silicon dioxide, camphorquinone, ethyl 4-dimethylamino-benzoate, surfactant, sodium fluoride.	1. Apply a first layer vigorously rubbing the adhesive with the Cavibrush (FGM Prod. Odont., Joinville, SC, Brazil) for 10 s. 2. Evaporate excess solvent by thoroughly air-drying with an air syringe for 10 s
	2. Commercial adhesive + 5wt % (ZnONp) and 0.2wt % (CuNp) (99.8 % pure, SkySpring Nanomaterials, Inc., Houston, TX, USA; www.ssnano.com ↗).	3. Apply a second layer of adhesive as described in 1. 3. Evaporate excess solvent as described in 3. 4. Light cure for 20 s at 1200 mW/cm^2 (Valo, Ultradent, South Jordan, UT, USA)

Opallis (FGM Dent. Prod., Joinville, SC, Brazil)	UDMA, Bis-GMA, Bis-EMA, TEGDMA, camphorquinone, co-initiator, silane, silanized barium aluminum silicate glass and pigments.	1. Placed in increments of 2 mm. 2. Light-curing for 10 s each layer at 1200 mW/cm^2 (Valo, Ultradent, South Jordan, UT, USA)

* UDMA, urethane dimethacrylate; HEMA, 2-hydroxyethyl methacrylate; 10-MDP, methacryloyloxydecyl dihydrogen phosphate; ZnONp: zinc oxide nanofiller; CuNp: copper nanofiller; Bis-GMA, bisphenol A-glycidyl methacrylate; Bis-EMA, bisphenol A ethoxylated dimethacrylate; TEGDMA, triethylene glycol dimethacrylate.

After 1 month of restorative procedure, 30 teeth extractions were performed. First, resin-dentin bonded sticks (cross-sectional area around 0.9 mm2) were prepared from 20 bonded teeth, 10 teeth for each group (Fig. 1), using a slow-speed diamond saw (Isomet, Buehler, Evanston, IL, USA). The number of resin-dentin bonded sticks showing premature failure (PF) during specimen preparation was recorded for each tooth. At least one resin-dentin bonded stick per tooth from each group was used to evaluate the in situ degree of conversion (DC) within the adhesive/ hybrid layers, as well as one resin-dentin bonded stick per tooth was used to evaluate nanoleakage (NL). Also, one stick per group used to evaluate NL was characterized by energy-dispersive X-ray spectrometer (EDX). After that, the remaining resin-dentin bonded sticks were measured by a digital caliper (Digimatic Caliper, Mitutoyo, Tokyo, Japan), tested for microtensile bond strength, and the bond strength in MPa was calculated. For the in situ zymography test (Zym), 10 bondedteeth, five for each group, were longitudinally cut into 1-mm-thick slabs using a slow-speed saw (Isomet) to expose the adhesive/dentin interfaces (Fig. 1) and stored in distilled water.

Microtensile bond strength (μTBS)

Resin-dentin bonded sticks were fixed to a special jig using cyanoacrylate glue and stressed under tension (Instron, Canton, MA, USA) at 1.0 mm/min until fracture occurred. The μTBS values (MPa) were derived by dividing the imposed force (N) by the resin-dentin bonded area. The fracture mode of the resin-dentin bonded sticks was examined with a light microscope at 100x magnification (Olympus SZ40, Tokyo, Japan) and categorized as adhesive (A/M, failure at the resin-dentin interface or with

partial cohesive failure of the neighboring substrates) or cohesive (C, failure exclusively within the dentin or the resin composite). Specimens with premature fracture (PF) were included in the tooth mean for statistical analysis.

Nanoleakage by scanning electron microscope (NL)

Resin-dentin bonded sticks were immersed in an aqueous solution of ammoniacal silver nitrate solution for 24 h, followed by 8 h in a photodeveloping solution under a fluorescent lamp [20]. The specimens were wetly polished using SiC paper and diamond paste (Buehler). The resin-dentin bonded interfaces were observed using a field-emission scanning electron microscope (VEGA 3 TESCAN, Shimadzu, Tokyo, Japan) at 15 kV in the backscattering mode. The amount of silver nitrate uptake within the adhesive layer and hybrid layer of each resin-dentin bonded stick was measured in three regions (5 × 5 μm) of the resin-dentin bonded stick [21]. The acquisition mode of the images and the percentage of silver nitrate uptake were calculated according to Hass et al. [22]. The ImageJ software was used to calculate the percentage of silver nitrate uptake within the hybrid layers in each specimen.

In situ degree of conversion (DC) by micro-Raman analysis

Resin-dentin bonded sticks were prepared as described by Hass et al. [22] and the in situ degree of conversion analysis was measured inside the hybrid layer of the adhesive interfaces using a dispersive micro-Raman spectrometer/microscope (XploRA ONETM Raman microscope, HORIBA Scientific, New Jersey, NY, USA). Previously, the micro-Raman spectrometer was calibrated to zero. The Raman spectrometer was configured to use with a 638-nm diode laser (1-μm spot diameter) at 100 mW, an X100/0.90 NA air objective, and 600 lines per millimeter of grating. The resin-dentin bonded interface was scanned from 400 to 2200 cm− 1 , with 30-s accumulation time with 6 co- additions The spectra were analyzed at three different sites for each specimen in the middle of the hybrid layer, and the values were averaged for statistical purposes. Post-processing of the spectra was performed using the Opus Spectroscopy Software version 6.5 (HORIBA Scientific, New Jersey, NY, USA). Additionally, spectra of the uncured adhesive were acquired with the method previously described.

The ratio of the double-bond content of the monomer to the polymer in the uncured and cured adhesive was quantified by calculating the ratio of the aliphatic C = C (vinyl) absorption (1638 cm-1) to the aromatic C = C absorption (1608 cm-1)

signals for both polymerized and unpolymerized samples. DC was calculated using the following formula:

DC (%) = (1 − [Rcured/Runcured]) × 100

Where “R” is the ratio of aliphatic and aromatic peak intensities at 1638 cm-1 and 1608 cm-1 in cured and uncured adhesives. In addition, more intense peaks were observed for all materials, and the corresponding chemical bonding was recorded. The average of the values was used for statistical analysis.

Identification of copper/zinc oxide within the adhesive/ hybrid layers by edx

Two resin-dentin bonded sticks from the NL assay randomly selected were used for the identification of the presence of copper and zinc at the adhesive/hybrid layer. The analysis of the Cu and Zn content in each resin-dentin bonded stick was performed by field emission scanning electron microscope (FE-SEM) (MIRA 3 TESCAN, Shimadzu, Tokyo, Japan) coupled with an energy-dispersive X-ray spectrometer (EDX). The bonding area was observed, and the analysis was focused on themiddle of the hybrid layer. One site, randomly determined, per resindentin bonded stick was examined.

In situ zymography

Ten teeth, restored as previously described, were sectioned perpendicularly to the bonded interface into 0.4-mm thick slices (Isomet 5000, Buehler) and polished with SiC abrasive papers (#1200 and #2400-griy) to obtain 300-μm thick slices. Then, in situ zymography was performed with quenched fluorescein-conjugated gelatin as the gelatinase substrate (EnzChek Gelatinolytic/Collagenolytic Assay Kit, E- 12,055, Thermo Fisher Scientific Inc.) as described Mazzoni et al. [10]. Two slices from each specimen were tested after seven days of incubation with the fluorescent-collagen solution. The hydrolysis of quenched fluorescein-conjugated gelatin substrate, indicative of endogenous gelatinolytic enzyme activity, was assessed by examination under a multiphoton confocal Scanning Laser microscope (CSLM; ex:488 nm and em:lp530nm; Leica TCS SP8 MP Multiphoton Microscope, Germany). Optical sections of 20 μm thick were acquired from different focal planes, and the images were analyzed, quantified, and processed with LAS X Life Science software (Leica, Germany). The mean fluorescence intensity emitted by ten slices from each experimental group in the same representative area was used to calculate the proteolytic activity inhibitory rate. 2.10.

Statistical analysis

Shapiro–Wilk test was used to assess whether the data from these tests followed a normal distribution. Bartlett's test was performed to determine the validity of the assumption of equal variances. The mean μTBS (MPa) of all resin-dentin bonded sticks from the same tooth were averaged for statistical purposes. Therefore, the experimental unit used in this study was the tooth. The value attributed to PFs specimens was 4.8 MPa, as indicated by previous studies [23]. The μTBS (MPa), NL (%), and in situ DC (%) means for both groups were calculated from the average of the teeth used per group. Once normal distribution and homoscedasticity of variances were confirmed, the μTBS (MPa), NL (%), in situ DC (%) and the proteolytic activity (AUF) were analyzed using Student's t-test (α=0.05). All analyses were performed using SPSS® (Statistical Package for the Social Science) version 17.0 (SPSS Inc., Chicago, IL, USA).

Results

Microtensile bond strength testing

There were no significant differences in Microtensile bond strength between both groups (p = 0.65). The most common failure pattern for both groups was the adhesive/mixed type (Table 3). The addition of CuNps and ZnONps did not influence the microtensile bond strength. 3.2. In situ degree of conversion within adhesive/hybrid layers For the in situ degree of conversion values, showed no significant differences between both groups were detected (p = 0.14, Table 12). The addition of CuNps and ZnONps did not influence the in situ degree of conversion.

Tabela 12. Failure pattern, mean and standard-deviation values of microtensile bond strength (μTBS; MPa)(DC;%) (*)., nanoleakage (NL;%) and in situ degree of conversion

Adhesives	Failure pattern (%)**			μTBS (MPa)	NL (%)	DC (%)
	A/M	CO	PF			
Control (w/o Cu + ZnONps)	90	00	10	37.1 ± 5.2 a	15.7 ± 1.3 B	44.9 ± 5.1 A
Experimental (w/ Cu + ZnONps)	93,3	00	6,7	38.1 ± 7.0 a	8.1 ± 2.2 A	48.9 ± 6.6 A

* Similar capital or lowercase superscript letters indicate no significant differences between groups ($p \geq 0.05$).

** A/M: adhesive/mixed failure; CO: cohesive (resin or dentin failures); PF: premature failure.

Nanoleakage evaluation For nanoleakage values, a significant difference between both groups were observed ($p < 0.0000002$, Table 12). Lower nanoleakage values were found in the experimental group when compared to the control group. Representative images from NL analysis are shown in Fig. 8; and Fig.9. EDX spectra of the hybrid layer from both groups detected the presence of CuNps and ZnONps, only in the experimental group (Fig. 9, E and F).

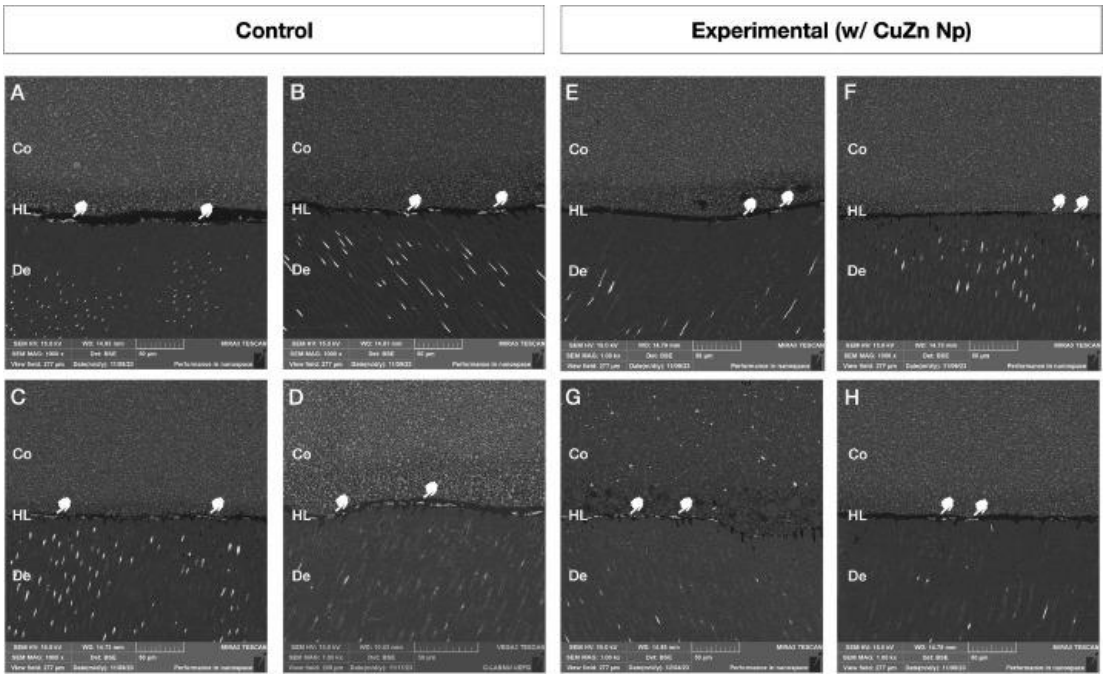

Figura 8. Nanoleakage representative scanning electron microscopy images of the resin–dentin interfaces.

Nanoleakage representative scanning electron microscopy images of the resin–dentin interfaces bonded with the control (A, B, C and D) and experimental adhesives (E, F,G and H). It is possible to observe lower silver nitrate deposition in the copper and zinc oxide nanoparticles (CuZnNp described in the image) containing group. Silver nitrate deposition is indicated at the images, and appears as white stains at the resin-dentin interphase. Co: composite; HL: hybrid layer; De: dentin.

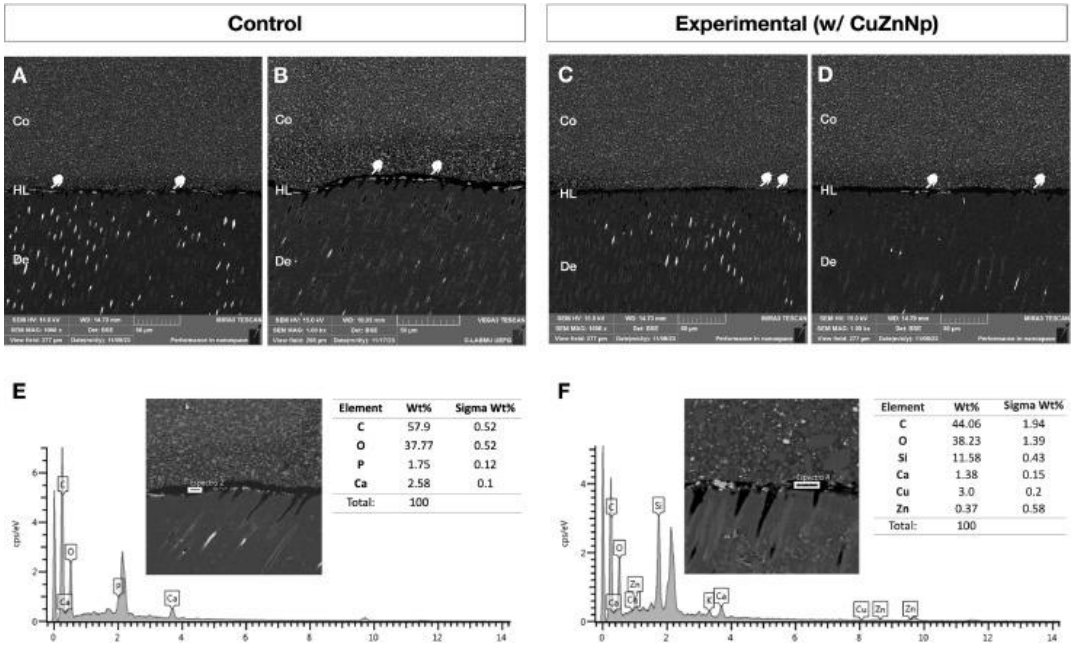

Figura 9 Representative back-scattering scanning electron microscopy images and EDX spectra.

Representative back-scattering scanning electron microscopy images (A to D) and EDX spectrum (E and F) of the resin–dentin interfaces bonded with the control (A, B and E) and experimental (C, D and F) adhesives. A significant amount of silver nitrate uptake was observed in the control group (without CuNps and ZnONps) when compared to experimental group (with CuNps and ZnONps). The EDX spectra from selected area of the hybrid layer was outlined by a magenta rectangle. The figure table summarizes the elemental composition of the sample area outlined. It is possible to observe the presence of CuNps and ZnONps only in the experimental group (F).

Enzymatic activity inhibition in the hybrid layer

The results of the Nps inhibitory profile on the gelatinolytic activity (AUF) in the hybrid layer showed significant difference in substrate hydrolysis between the Control and Experimental groups ($p < 0.004$). Lower enzymatic activity (AUF) inhibition in the hybrid layer were found in the experimental group when compared to the control group.

Micrographs of the in situ zymography assay for control adhesive and CuNps and ZnONps containing adhesive) are shown in Fig. 10. The images set corresponding to the optical density of the resin-dentin interface acquired using differential interference contrast are shown in panels A (control), and D (CuNps and ZnONps). Images showing the proteolytic activity (green fluorescence) in dentin tubules and within the hybrid layer in all tested groups are shown in panels B and E. This represents the MMPs activity in both groups. The merged images are shown in panels C and F. Panels G and H represent the three-dimensional reconstruction, and the quantification of the MMPs activity in both tested groups. The proteolytic inhibition promoted by Nps profile shown in the panel I. The in situ zymography evaluation indicates a significant reduction in the fluorescent intensity at the hybrid layer and within dentin in the CuNps and ZnONps group. CuNps and ZnONps containing adhesive successfully inhibited 60.32 % of the MMPs activity in the experimental group. The 3D projection further confirms these results and provides additional information on the position and depth of the proteolytic activity.

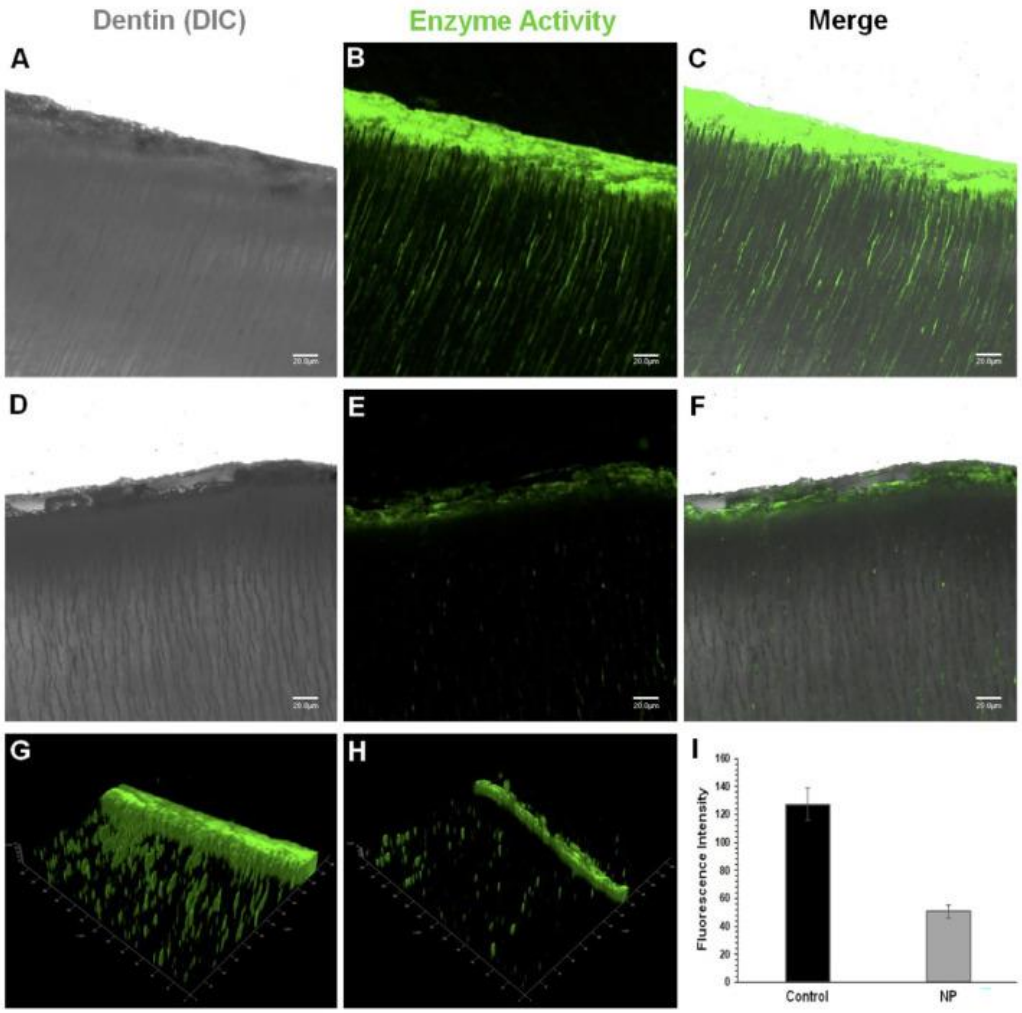

Figura 10. Confocal laser scanning microscopy (CLSM) images of the resin-dentin bonded interfaces

Confocal laser scanning microscopy (CLSM) images of the resin-dentin bonded interfaces after incubation with quenched fluorescein-labeled gelatin. Images of differential interference contrast (DIC) are presented in panels A (Control) and D (Experimental group; CuNps and ZnONps); panels B (Control) and E (CuNps and ZnONps) presents images acquired in the green channel (488 nm); and panels C (Control) and F (CuNps and ZnONps) presents images formed by merged images. The 3D projections from CSLM images are presented in panels G (Control) and H (CuNps and ZnONps). The panel I indicates the mean of the fluorescent intensity in both groups ($p \leq 0.005$).

Discussion

This randomized clinical trial evaluated the behavior of an adhesive loaded with 0.2 % CuNps and 5 % ZnO, on restored teeth ex vivo. The hypothesis of this study was that addition of 0.2 % CuNps and 5 % ZnO Nps to a universal adhesive does not affect its adhesive properties and reduces enzymatic degradation activity of collagen in the hybrid layer which was accepted.

Microtensile bond strength did not show significant differences between the control group (commercial adhesive) and the experimental group (adhesive with NPs). The average values were 38.1 MPa and 37.1 MPa for the experimental and control groups, respectively. Considering that it has been established in different publications [24,25,26] that for microtensile tests, values over 25 MPa [30] are acceptable, and that these study results obtained exceed that value in both groups (control and experimental), despite having been carried out ex vivo, microtensile bond strength results indicate that the addition of CuZnONps would not affect the mechanical properties in the hybrid layer and the adhesive layer, which is of vital importance in the longevity of esthetic restorations. Previous in vitro studies that evaluated the same commercial universal adhesive used in this study had values of 30.3 MPa and 18.9 MPa in etch-and-rinse and self-etch mode respectively, and when NPs were added at the same concentration as our study, the values described by Gutierrez et al. [24] were 33.6 MPa and 24.9 MPa in etch-and-rinse and self-etch mode, respectively. All in vitro results in accordance with this ex vivo analysis, confirming no clinical detrimental of mechanical properties with the addition of CuZnONps.

The NL results were 8.1 % and 15.7 % for the experimental and control groups, respectively, indicating significant differences. These results showed that CuNps and ZnONps increased the performance of the adhesive, achieving very good values for an ex vivo model. These values are similar to those reported previous studies [24] for the same commercial universal adhesive, which showed values of 13.2 % and 3.4 % for experimental and control, respectively. These in vitro results are in accordance with ex vivo results.

The significant reduction in nanoleakage for the experimental group of 0.2 % CuNps and 5 % ZnONps has several hypotheses that can help understand the results obtained. In addition to protection by reducing enzymatic activity, CuNps can increase the resistance of the collagen network, one of the components of the hybrid layer,

because the collagen cross-linking enzyme, lysyl oxidase (LOX), depends on Cu. Therefore, Cu has an indirect effect as a cross-linking agent [31,32]. Moreover, other studies have demonstrated that the incorporation of ZnO led to the formation of hydroxyapatite crystals on the collagen fibrils, favoring the mineralization of dentin and improving the cross-linking effect of collagen [33]. This cross-linking action of both CuNps and ZnONps alone can increase the resistance of collagen, leaving it less susceptible to the effects of proteolytic enzymes such as MMPs and CTs, indirectly decreasing immediate nanofiltration, as has been previously reported in an adhesive that contained only Cu Nps [15,16] and in an adhesive that contained only Zn [34] Nps. When dentin is remineralized in the presence of Zn scholzite is formed, which is more resistant than hydroxyapatite [35]. Although these mechanisms are well described after a month of follow-up, it is unlikely to find results of formation and even more of prevention of degradation.

The degree of conversion was 48.9 % for the experimental group and 44.9 % for the control group. This indicates that the addition of CuNps and ZnONps to the adhesive did not affect the degree of conversion. It should be noted that these values are also from cavities made in vivo. Therefore, similar results in both groups continue to support the hypothesis that CuNps and ZnONps in a neutral state would not influence the polymerization reaction of the adhesive, and in consequence the percentage of cured polymer would be similar in both groups, as previously observed [24].

Previous in vitro studies for the commercial universal adhesive used in this study had values of 63.4 % and 62.4 % in etch-and-rinse and selfetch mode respectively. When NPs were added at the same concentration as our study, the values described by Gutierrez et al. [24] were 65.2 % and 65.3 % in etch-and-rinse and self-etch modes, respectively. These results are closer to the ones obtained in this study.

Several studies have demonstrated the MMP inhibitory properties of Cu [27] and Zn [14], but only one study [26] has demonstrated the MMP inhibitory potential of the combination of both ions. Gutierrez et al. evaluated the anti-MMP activity previously finding significant differences in the inhibition of MMP-2, MMP-8, and MMP-9 when using same universal adhesive loaded with 0.2 % CuNps and 5 % ZnONps [26]. However, the property of inhibition of enzymatic activity in the hybrid layer with this experimental adhesive has never been evaluated by in situ zymography. The great

advantage is that it provides a direct visual image of the inhibition of enzymatic activity in the hybrid layer, through fluorescence (green), allowing us to directly appreciate the activity or not of the enzymes that degrade the collagen of the hybrid layer [10].

The results of in situ zymography showed that CuNps and ZnONps treated samples inhibited more than 60 % of the enzymatic activity in the hybrid-layer/dentin region. These findings align with the previouslyeported individual effects of CuNps [27] and ZnNps [14] in inhibiting MMP activity, demonstrating a synergistic effect when combined [26]. High concentrations of zinc prevent the breakdown of collagen in early dentin caries lesions by increasing collagen stability and inhibiting proteolytic activities. This can also provide a microenvironment that favors the remineralization process. Additionally, when adhesives bond to dentin, the zinc within the hybrid layer after the complete polymerization of resin monomers can provide the benefits of antibacterial properties and protect collagen fibrils from natural dentin enzymes [14].

The antimicrobial properties of CuNps and ZnNps have been widely documented, with their synergistic effect showing enhanced antibacterial activity against pathogens such as Streptococcus mutans [28], Pseudomonas aeruginosa, and Candida tropicalis [26,29]. This study used the same concentrations (0.2 % CuNps and 5 % ZnONps) as previous in vitro studies [24,26], which demonstrated significant antimicrobial effects. These properties are crucial for maintaining long-term antimicrobial activity at the adhesive interface, potentially extending the lifespan of restorations.

Furthermore, previous studies have shown that the incorporation of these nanoparticles does not negatively affect the cytotoxicity of the adhesive systems [26]. This suggests that the nanoparticles-controlled release does not result in a cytotoxic effect, maintaining the biocompatibility of the adhesive.

Among the limitations of this study are the inherent limitations of an in vivo study, including challenges related to patient recruitment and adherence. These factors contributed to a decreased patients cohort size. Besides, performing standardized restorations even with defined protocols and then extracting and processing teeth for samples could increase the error bias at any stage.

Studies that have compared in vitro versus in vivo samples have found significantly lower values or in vivo tests. In the present study, the values obtained were lower in the bond strength, degree of conversionand nanoleakage test compared to in vitro studies [36]. This could be explained by the fact that one of the major

differences between vital and extracted teeth is the presence of live odontoblastic processes, fluid in the dentinal tubules, and intrapulpal pressure [37], which could influence the adhesive properties of dentine-bonding interphase.

Currently, there are no similar studies to compare these results, giving significant clinical value to this study. Future work should be conducted to create more evidence in the area, such as, longitudinal studies should be performed to evaluate the longevity of restorations using this adhesive system and validate its effect on increasing the lifespan of restorations.

Conclusion

According to the results obtained, it is possible to conclude that the addition of 0.2 % CuNps and 5 % ZnONps to a universal dental adhesive does not compromise its adhesive properties and decreases the enzymatic activity of degradation and nanoleakeage of the adhesive-collagen hybrid layer, in a randomized ex vivo clinical model.

References

[1] N.B. Pitts, D.T. Zero, P.D. Marsh, et al., Dental caries, Nat. Rev. Dis. Primers. 3 (2017) 17030, https://doi.org/10.1038/nrdp.2017.30.
[2] G.J. Christensen, Should Resin-Based composite dominate restorative dentistry today? J. Am. Dent. Assoc. 141 (2010) 1490–1493, https://doi.org/10.14219/jada.archive.2010.0112.
[3] A. ´ Astvaldsd ´ ottir, ´ J. Dagerhamn, J.W. van Dijken, et al., Longevity of posterior resin composite restorations in adults – a systematic review, J. Dent. 43 (2015) 934–954, https://doi.org/10.1016/j.jdent.2015.05.001.
[4] P. Spencer, Q. Ye, J. Park, et al., Adhesive/Dentin interface: the weak link in the composite restoration, Ann. Biomed. Eng. 38 (2010) 1989–2003, https://doi.org/10.1007/s10439-010-9969-6.
[5] A.R. Hunter, E.T. Treasure, A.J. Hunter, Increases in cavity volume associated with the removal of class 2 amalgam and composite restorations, Oper. Dent. 20 (1) (1995) 2–6.
[6] Deligeorgi V., Mjor ¨ I.A., Wilson N.H. An overview of reasons for the placement and replacement of restorations. Prim Dent Care. 8 (2001) 5–11. https://doi.org/10.1308/135576101771799335.
[7] F.D. Nascimento, C.L. Minciotti, S. Geraldeli, et al., Cysteine cathepsins in human carious dentin, J. Dent. Res. 90 (2011) (2011) 506–511, https://doi.org/10.1177/0022034510391906. [8] F. Femiano, R. Femiano, L. Femiano, et al., Dentin caries progression and the role of metalloproteinases: an update, Eur. J. Paediatr. Dent. 17 (2016) 243–247. htt ps://pubmed.ncbi.nlm.nih.gov/27759416/.

[9] L. Tjäderhane, M.A. Buzalaf, M. Carrilho, et al., Matrix metalloproteinases and other matrix proteinases in relation to cariology: the era of ’dentin degradomics, Caries Res. 49 (2015) 193–208, https://doi.org/10.1159/000363582.
[10] A. Mazzoni, F.D. Nascimento, M. Carrilho, et al., MMP activity in the hybrid layer detected with in situ zymography, J. Dent. Res. 91 (2012) 467–472, https://doi.org/10.1177/0022034512439210.
[11] H. Palza, Antimicrobial polymers with metal nanoparticles, Int. J. Mol. Sci. 16 (2015) 2099–2116, https://doi.org/10.3390/ijms16012099.
[12] A.M. Schrand, M.F. Rahman, S.M. Hussain, et al., Metal-based nanoparticles and their toxicity assessment, Wiley. Interdiscip. Rev. Nanomed. Nanobiotechnol. 2 (2010) 544–568, https://doi.org/10.1002/wnan.103.
[13] A.P. de Souza, R.F. Gerlach, S.R. Line, Inhibition of human gingival gelatinases (MMP-2 and MMP-9) by metal salts, Dent. Mater. 16 (2000) 103–108, https://doi.org/10.1016/s0109-5641(99)00084-6.
[14] R. Osorio, M. Yamauti, E. Osorio, et al., Zinc reduces collagen degradation in demineralized human dentin explants, J. Dent. 39 (2011) 148–153, https://doi.org/10.1016/j.jdent.2010.11.005.
[15] M.F. Guti´errez, P. Malaquias, V. Hass, et al., The role of copper nanoparticles in an etch-and-rinse adhesive on antimicrobial activity, mechanical properties and the durability of resin-dentine interfaces, J. Dent. 61 (2017) 12–20, https://doi.org/10.1016/j.jdent.2010.11.005.
[16] M.F. Guti´errez, P. Malaquias, T.P. Matos, et al., Mechanical and microbiological properties and drug release modeling of an etch-and-rinse adhesive containing copper nanoparticles, Dent. Mater. 33 (2017) 309–320, https://doi.org/10.1016/j.dental.2016.12.011. [17] D.C. Barcellos, B.M. Fonseca, C.R. Pucci, et al., Zn-doped etch-and-rinse model dentin adhesives: dentin bond integrity, biocompatibility, and properties, Dent. Mater. 32 (2016) 940–950, https://doi.org/10.1016/j.dental.2016.04.003.
[18] R. Sarkis-Onofre, M.S. Cenci, F.F. Demarco, et al., Use of guidelines to improve the quality and transparency of reporting oral health research, J. Dent. 43 (2015) 397–404, https://doi.org/10.1016/j.jdent.2015.01.006.
[19] World Medical Association, World Medical Association Declaration of Helsinki. Ethical principles for medical research involving human subjects, Nurs. Ethics 9 (2002) 105–109, https://doi.org/10.1001/jama.2013.281053.
[20] F.R. Tay, D.H. Pashley, B.I. Suh, et al., Single-step adhesives are permeable membranes, J. Dent. 30 (2002) 371–382, https://doi.org/10.1016/s0300-5712(02)00064-7.
[21] A. Reis, R.H. Grande, G.M. Oliveira, et al., A 2-year evaluation of moisture on microtensile bond strength and nanoleakage, Dent. Mater. 23 (2007) 862–870, https://doi.org/10.1016/j.dental.2006.05.005.
[22] V. Hass, M. Dobrovolski, C. Zander-Grande, et al., Correlation between degree of conversion, resin-dentin bond strength and nanoleakage of simplified etch-andrinse adhesives, Dent. Mater. 29 (2013) 921–928, https://doi.org/10.1016/j.dental.2013.05.001.
[23] A. Reis, A. Pellizzaro, K. Dal-Bianco, et al., Impact of adhesive application to wet and dry dentin on long-term resin-dentin bond strengths, Oper. Dent. 32 (2007) 380–387, https://doi.org/10.1016/j.jdent.2013.03.001. [24] M.F. Guti´errez, J. Bermudez, A. Davila-S ´ anchez, ´ et al., Zinc oxide and copper nano

particles addition in universal adhesive systems improve interface stability on caries-affected dentin, J. Mech. Behav. Biomed. Mater. 100 (2019) 103366, https://doi.org/10.1016/j.jmbbm.2019.07.024.
[25] M.A. Muñoz, I. Luque, V. Hass, et al., Immediate bonding properties of universal adhesives to dentine, J. Dent. 41 (5) (2013) 404–411, https://doi.org/10.1016/j. jdent.2013.03.001.
[26] M.F. Gutiérrez, L.F. Alegría-Acevedo, L. Méndez-Bauer, et al., Biological, mechanical and adhesive properties of universal adhesives containing zinc and copper nanoparticles, J. Dent. 82 (2019) 45–55, https://doi.org/10.1016/j. jdent.2019.01.012.
[27] S.K. Jun, S.A. Yang, Y.J. Kim, et al., Multi-functional nano-adhesive releasing therapeutic ions for MMP-deactivation and remineralization, Sci. Rep. 8 (2018) 5663, https://doi.org/10.1038/s41598-018-23939-6.
[28] C. Covarrubias, D. Trepiana, C. Corral, Synthesis of hybrid copper-chitosan nanoparticles with antibacterial activity against cariogenic Streptococcus mutans, Dent. Mater. J. 37 (2018) 379–384, https://doi.org/10.4012/dmj.2017-195.
[29] P. Kaali, M.M. Perez-Madrigal, E. Stromberg, et al., The influence of Ag+, Zn2+ and Cu2+ exchanged zeolite on antimicrobial and long-term in vitro stability of medical grade polyether polyurethane, Express. Polym. Lett. 5 (2011) 1028–1040, https://doi.org/10.3144/expresspolymlett.2011.101.
[30] B.O. Sahadi, M. Sebold, C.B. Andr´e, et al., Effect of experimental dentin etchants on dentin bond strength, metalloproteinase inhibition, and antibiofilm activity, Dental Mater. 40 (2024) e12–e23, https://doi.org/10.1016/j.dental.2024.02.017.
[31] B. Marelli, D.L. Nihouannen, S.A. Hacking, et al., Newly identified interfibrillar collagen crosslinking suppresses cell proliferation and remodelling, Biomaterials 54 (2015) 126–135, https://doi.org/10.1016/j.biomaterials.2015.03.018.
[32] J.L. Chitty, Y.F.I. Setargew, T.R. Cox, Targeting the lysyl oxidases in tumour desmoplasia, Biochem. Soc. Trans. 47 (2019) 1661–1678, https://doi.org/ 10.1042/BST20190098.
[33] M. Toledano, S. Sauro, I. Cabello, et al., A Zn-doped etch-and-rinse adhesive may improve the mechanical properties and the integrity at the bonded-dentin interface, Dental Mater. 29 (2013) e142–e152, https://doi.org/10.1016/j. dental.2013.04.024.
[34] M. Toledano, R. Osorio, E. Osorio, et al., A zinc chloride-doped adhesive facilitates sealing at the dentin interface: a confocal laser microscopy study, J. Mech. Behav. Biomed. Mater. 74 (2017) 35–42, https://doi.org/10.1016/j.jmbbm.2017.04.030.
[35] R. Osorio, E. Osorio, A.L. Medina-Castillo, et al., Polymer nanocarriers for dentin adhesion, J. Dent. Res. 93 (2014) 1258–1263, https://doi.org/10.1177/ 0022034514551608.
[36] A.C. Chibinski, R. Stanislawczuk, D.A. Roderjan, et al., Clinical versus laboratory adhesive performance to wet and dry demineralized primary dentin, Am. J. Dent. 24 (2011) 221–225. https://pubmed.ncbi.nlm.nih.gov/22016916.
[37] J. Perdigão, Dentin bonding—variables related to the clinical situation and the substrate treatment, Dental Mater. 26 (2010) e24–e37, https://doi.org/10.1016/j. dental.2009.11.

3.4 ARTIGO 4 - BIOACTIVE AND ANTIBACTERIAL UNIVERSAL ADHESIVES CONTAINING ZNO/CU AND BIOACTIVE GLASS NANOPARTICLES

STATUS: Publicado em 2026

REVISTA: Journal of Dentistry

DOI: 10.1016/j.jdent.2026.106524

Carolina Pardo-Díaz[abc], Gabriel Cochinski[b], Pedro Moreira[b], Fabio Dupart Nascimento[d], Marina Damasceno e Souza Chiari[de], Joatan Costa[f], Cristian Covarrubias[g], Mario Felipe Gutiérrez[h], Alessandro D. Loguercio[b*], Eduardo Fernández[af]

[a] Faculty of Dentistry, Dental School, University of Chile, 8380544, Santiago, Chile.

[b] Department of Restorative Dentistry, School of Dentistry, State University of Ponta Grossa, 84030-900, Ponta Grossa, Brazil.

[c] Department of Operative Dentistry, School of Dentistry, University of Valparaíso, 2360004, Valparaíso, Chile.

[d] Molecular Biology Division, Department of Biochemistry, Paulista Medical School, Federal University of São Paulo, 04044-020, São Paulo, Brazil

[e] Dental Research Division, Paulista University, 04026-002, São Paulo, Brazil

[f] Instituto de Ciencias Biomédicas, Universidad Autónoma de Chile, Santiago, Chile

[g] Laboratory of Nanobiomaterials, Institute for Research in Dental Sciences, Faculty of Dentistry, University of Chile, Santiago, Chile

[h] Faculty of Dentistry, Universidad de los Andes, Santiago, Chile

Alessandro Dourado Loguercio (Corresponding author)

Universidade Estadual de Ponta Grossa, Departamento de Odontologia

Av. Carlos Cavalcanti, 4748, Uvaranas, Zip-Code: 84030-000,

Ponta Grossa, PR, Brazil.

Email: aloguercio@hotmail.com

Abstract

Objectives: To evaluate the antibacterial activity, cytocompatibility, mineralizing potential, degree of conversion (DC), enzymatic activity, and resin-dentin microtensile bond strength (μTBS) of a universal adhesive modified with zinc oxide (ZnO), copper (Cu), and bioactive glass (BG) nanoparticles. Methods: Five adhesive formulations

were evaluated: control (0 wt %); ZnO/Cu (0.2 wt % Cu + 2.5 wt % ZnO); 5 wt %BG + ZnO/Cu; 10 wt %BG + ZnO/Cu; and 10 wt %BG. Antibacterial activity against Streptococcus mutans was quantified by colony-forming unit counts. Cytocompatibility was assessed using human gingival stem cells (MTS assay, 3 and 7 days). Mineralization was evaluated after immersion in simulated body fluid (7 and 28 days) via FE-SEM and EDX. The DC was measured by Raman spectroscopy. Resin-dentin μTBS was tested under self-etch (SE) and etch-and-rinse (ER) strategies. MMPs activity was assessed by in situ zymography. Data were analyzed with ANOVA and Tukey tests (α = 0.05). Results: BG nanoparticles significantly enhanced antibacterial and mineralizing responses. The 10 wt %BG and 10 wt %BG + ZnO/Cu groups achieved >80 % bacterial inhibition and marked Ca-P deposition after 28 days. All adhesives exhibited cytocompatibility (>80 % viability) and DC values >60 %. A slight reduction in μTBS was observed for 10 wt %BG groups under the ER strategy. High gelatinolytic activity was detected across all groups, with reduced fluorescence only for the ZnO /Cu group under ER strategy.

Conclusions: Incorporating BG nanoparticles into a ZnO/Cu-modified universal adhesive improved antibacterial and mineralizing properties without impairing cytocompatibility, polymerization, without critically compromising bond strength. MMP activity varied with bonding strategies, with no consistent inhibitory effect observed.

Clinical relevance: Universal adhesives modified with bioactive glass and ZnO/Cu nanoparticles exhibited enhanced antibacterial and mineralizing properties while maintaining cytocompatibility and degree of conversion, without critically compromising bond strength. Although, no immediate inhibition of MMP activity was observed, this multifunctional approach may contribute to more stable adhesive interfaces and improved long-term performance of composite restorations.

Keywords: Antibacterial activity; Bioactive glass; Bond strength; Copper; Cytocompatibility; MMPs; Mineralization; Universal adhesive; Zinc oxide.

Introduction

Resin composites are the primary materials for restoring cavitated carious lesions, as they combine esthetics, conservative tooth preparation, and satisfactory mechanical performance [1]. However, the long-term survival of resin-based restorations remains limited, with average clinical lifespans of approximately 7–10 years. This limitation is primarily attributed to the instability of dentin bonding and the gradual degradation of the resin-dentin interface over time [2,3].

The clinical success of resin composite restorations largely depends on the integrity of the resin–dentin interface [4]. This interface is established through partial demineralization of dentin and subsequent infiltration of adhesive monomers into the exposed collagen network, forming the hybrid layer [5,6]. While enamel bonding is relatively predictable, dentin bonding is more challenging due to its higher organic content, tubular structure, and inherent moisture. These features make dentin more susceptible to hydrolytic and enzymatic degradation mediated by intrinsic dentin proteases that can be activated by acidic monomers or bacterial-derived acids, such as matrix metalloproteinases (MMPs) and cysteine cathepsins [6]. Moreover, cariogenic biofilms accelerate interface deterioration by releasing organic acids that demineralize adjacent dentin and promote microleakage. This dual degradation pathway compromises the adhesive seal, facilitates bacterial penetration, and ultimately contributes to restoration failure [6,7].

Several strategies have been proposed to enhance hybrid layer durability, including enzymatic inhibitors (e.g., chlorhexidine, ethylenediaminetetraacetic acid, or tetracyclines), collagen cross-linking, and alternative conditioning protocols. Nevertheless, their long-term effectiveness remains limited [8,9].

Nanotechnology has introduced new approaches for tailoring adhesive formulations [10]. Metallic nanoparticles (Nps), particularly zinc oxide (ZnO) and copper (Cu), have attracted considerable interest to their multifunctional properties [11]. ZnO and Cu Nps exert potent antibacterial effects through mechanisms such as disruption of bacterial membranes, ion release, and generation of reactive oxygen species. Notably, these effects can be selective toward bacteria without significant cytotoxicity to mammalian cells when used at appropriate concentrations [11,12]. Zn can also bind to collagen at proteolytic cleavage sites, protecting the fibrillar network from enzymatic degradation and facilitating mineral nucleation within collagen fibrils

[12,11]. Cu has been shown to inhibit MMP-2 activity and upregulate tissue inhibitors of metalloproteinases, further enhancing matrix stability [13].

The combination of ZnO and Cu Nps has demonstrated synergistic antimicrobial activity, producing stronger antibacterial effects and more stable adhesive performance than unmodified adhesives [11,14,15]. However, metallic Nps alone may not completely prevent hydrolytic and enzymatic degradation, nor do they provide sustained remineralization at the adhesive interface.

Bioactive glass (BG), originally developed in the 1960s, is a silica-based material widely studied for its ability to induce mineralization and bond to both hard and soft tissues [16]. In aqueous environments, BGs undergoes surface reactions that led the release of calcium, phosphate, and sodium, increasing local pH [16]. This ionic exchange promotes the precipitation of hydroxycarbonate apatite, chemically similar to natural tooth mineral [17]. In dentistry, BG has been incorporated into toothpastes, desensitizing agents, liners, composites, and implant coatings. Its sustained release of calcium and phosphate ions makes it a promising additive for enhancing the remineralization potential of dental adhesives [17]. Additionally, BG can exert antibacterial activity by raising local pH and disrupting bacterial membranes [16].

Universal adhesives provide an ideal platform for these modifications. Their simplified protocols and versatility, allowing the use in etch-and-rinse (ER), self-etch (SE), or selective enamel etching, have contributed to their widespread clinical adoption [18]. Incorporating BG Nps into universal adhesives may complement the properties of ZnO and Cu Nps, yielding a multifunctional system with antibacterial, remineralizing, and potentially bioactive characteristics. However, despite these advantages, the combined incorporation of metallic Nps and BG into universal adhesives remains scarcely investigated.

Therefore, the aim of this in vitro study was to evaluate the biological properties of a universal adhesive modified with ZnO and Cu Nps in combination with BG Nps. The null hypothesis was that incorporating ZnO/Cu Nps and BG Nps into a universal adhesive would not significantly affect: (i) antibacterial activity against Streptococcus mutans (S. mutans); (ii) cytocompatibility with human gingival stem cells; (iii) mineralizing potential, as indicated by calcium and phosphate deposition; and (iv) degree of monomer conversion, (v) enzymatic activity withing the hybrid layer; and (vi) resin-dentin microtensile bond strength, compared with a unmodified universal adhesive.

Methods And Materials

This in vitro experimental study investigated the biological properties of a universal adhesive modified with zinc oxide (ZnO) and copper (Cu) Nps in combination with bioactive glass (BG) Nps. The study was approved by the Ethics Committee of State University of Ponta Grossa, PR/Brazil (Protocol No. 5.395.921).

Sample sizes were determined based on previous literature [14] and Academy of Dental Materials guidelines for in vitro adhesive testing [19,20]. A minimum of three replicates per group was used for characterization and biological tests, while four replicates per group were included for cytocompatibility. This design ensured adequate statistical power (β = 0.80, α. = 0.05) to detect differences among groups.

Nanoparticles and characterization

Commercial Nps of ZnO (Skyspring Nanomaterials Inc., Houston, TX, USA), Cu (Skyspring Nanomaterials Inc.) and BG Nps (Nanomaterials Laboratory, Faculty of Dentistry, University of Chile) were used. Nps samples were dried at 37°C for 24 h in a silica-gel desiccator to remove moisture, mounted on an aluminum stub, sputter-coated with gold, and analyzed using field-emission scanning electron microscopy (FE-SEM; MIRA3 LM, Tescan, Czech Republic). Particle size (< 100 nm) was confirmed using the MiraTC software (Tescan, Czech Republic) to verify nanoscale classification and suitability for adhesive modification.

The chemical structure of BG was confirmed using attenuated total reflectance Fourier-transform infrared spectroscopy (ATR-FTIR; Cary 630, Agilent Technologies, Santa Clara, CA, USA), identifying characteristic Si–O–Si vibrational peaks.

Preparation of experimental adhesives

Experimental adhesives were prepared by incorporating Nps into a commercial universal adhesive (Ambar Universal, FGM Dental Group, Joinville, SC, Brazil). The mixture was continuously stirred and sonicated for 10 min at 25°C to ensure homogeneous dispersion. Five experimental groups were prepared (w/w): unmodified adhesive (0 % NP), Control; 2.5 % ZnO + 0.2 % Cu, ZnO/Cu; 5 % BG + ZnO/Cu, 5 %BG+ZnO/Cu; 10 % BG + ZnO/Cu, 10 %BG+ZnO/Cu; and 10 % BG, 10 %BG.

Nps concentrations were selected based on previous studies demonstrating effective antibacterial activity and enzymatic modulation while maintaining polymerization efficiency and cytocompatibility [11,14,15,21].

Nps were incorporated under controlled lighting conditions within a light-shielded dark chamber by mechanical stirring followed by sonication for 10 min at 25°C to ensure homogeneous dispersion and minimize agglomeration. Adhesives were kept in opaque containers at room temperature until specimen fabrication to prevent premature photopolymerization. Immediately after preparation and before application, the modified adhesives were visually inspected to confirm the absence of phase separation, sedimentation, or macroscopic segregation, as evidenced by the lack of visible layer formation.

Sample Preparation

Adhesive disks were fabricated using a polyvinyl siloxane mold (6 mm diameter; 0.15 mm thickness). Each cavity was filled with different experimental adhesives, and the solvent was evaporated with an air syringe for 40 s at a distance of 10 mm. Specimens were then light-cured for 60 s using a LED curing unit (VALO, Turbo mode, Ultradent Products, Salt Lake City, UT, USA) at an irradiance of 1000 mW/cm². A polyester strip was placed over the surface during polymerization.

After curing, the discs were carefully removed from the mold, trimmed with a scalpel, and stored at 37°C for 24 h before testing. The thin disc thickness (0.15 mm) was selected to approximate the clinical adhesive layer and to ensure adequate light transmission and polymerization.

Antibacterial Activity

The antibacterial activity on the adhesive surface was evaluated against Streptococcus mutans (ATCC 25175). The bacteria were cultured in Brain Heart Infusion (BHI) broth at 37°C under anaerobic conditions. Cultures were adjusted to a 0.5 McFarland standard (≈1–5 × 10^6 CFU/mL) using a spectrophotometer (Halo RB-10 UV-VIS, Dynamica Scientific, UK).

For each group (n = 3), adhesive disks were immersed in 3 mL of the bacterial suspension and incubated anaerobically for 48 h at 37°C. After incubation, the disks were rinsed with 10 mL of sterile saline and immersed in a surfactant solution (0.9 % NaCl + 1 % Tween 80) for 20 minutes to detach adherent bacteria. Serial dilutions (10^{-1}, 10^{-2}, and 10^{-3}) were plated on TYC agar (tryptone–yeast–cysteine–sucrose) and incubated for 48 h at 37°C. Colony forming units (CFUs) were then counted using a colony counter (CC-1, Boeco, Hamburg, Germany).

CFU counts obtained from the unmodified adhesive group (0 % Nps) were used as the reference for calculating antibacterial inhibition. The unmodified adhesive

(0 % Nps) served as the antibacterial control group. Antibacterial performance was expressed as percentage inhibition relative to this control, as absolute CFU thresholds for acceptable antibacterial performance on adhesive surfaces are not universally established in the literature.

Antibacterial activity expressed as percent inhibition relative to the control group was calculated as follows:

$$\text{Inhibition Percentage (n\%)} = \frac{[\text{CFU(Control)} - \text{CFU(Experimental adhesive group)}] \times 100}{\text{CFU(Control)}}$$

Representative disks from each group were dehydrated, sputter-coated with gold, and examined under SEM (JSM-IT300LV, JEOL, Japan) to visualize bacterial adherence and morphological changes.

Cytocompatibility

This study adhered to institutional biosafety and ethical guidelines for research involving human-derived primary cells. All ethical and legal requirements for the use of human-derived biological materials were fulfilled. Human gingival mesenchymal stem cells (hGMSCs) were harvested from healthy donors (retromolar gingiva), after obtaining informed consent. Cells were cultured in high glucose Dulbecco's Modified Eagle Medium (DMEM) supplemented with 10 % fetal bovine serum and antibiotics (gentamicin, penicillin-streptomycin, and amphotericin B). For each group (n = 4), 10,000 cells per well were seeded into 96-well plates and exposed to adhesive disks. Two assay controls were included: positive control (cells without adhesive) and negative control (Pb^{2+} 2000 ppm). Cell viability was assessed at 3 and 7 days using a CellTiter 96® AQueous One Solution Cell Proliferation Assay (Promega, USA), following the manufacturer's protocol. Absorbance was measured at 490 nm using a microplate reader (ELISA). Results were expressed as viability percentages relative to the positive control.

Mineralizing potential

Adhesive disks (n = 3/group) were immersed in 10 mL of simulated body fluid (SBF), prepared according to previous study [22]. Samples were incubated at 37°C for 7 and for 28 days. After immersion, disks were rinsed in distilled water, dried, and examined by SEM (JSM-IT300LV, JEOL, Japan) for surface deposits. Elemental analysis was performed with energy dispersive X-ray spectroscopy (EDX) to quantify calcium and phosphorus content. Data were reported as mean weight percentages.

Degree of conversion (DC)

To verify that nanoparticle incorporation did not impair polymerization, Raman spectroscopy (Senterra, Bruker Optik GmbH, Ettlingen, Germany) was used. Adhesive samples (5 mm × 2 mm, n = 3/group) were polymerized under the same conditions previously described. Spectra were acquired using a 532 nm laser at 5 mW with 20 × magnification. The ratio of aliphatic (1639 cm^{-1}) to aromatic (1609 cm^{-1}) C=C peaks was compared between unpolymerized and polymerized states. DC was calculated as:

$$DC\ (\%) = \left(1 - \left[\frac{Rp}{Rnp}\right]\right) \times 100$$

Where R is the ratio of the intensities of the aliphatic and aromatic peaks of the adhesives, with (p) and without (np) polymerization.

Teeth preparation and bonding procedures

Eighty sound human third molars (extracted within the previous 6 months) were disinfected with 0.5 % chloramine and stored in distilled water. Occlusal enamel was removed with 180-grit SiC paper under water irrigation to expose flat dentin. Lateral enamel was eliminated using a #4137 cylindrical diamond bur (KG Sorensen, Barueri, SP, Brazil) to expose dentin [14].

Teeth were randomly assigned to two bonding strategies: etch-and-rinse (ER) or self-etch (SE) (n = 10). The adhesive was applied according to the manufacturer's instructions and light-cured for 20 s using an LED curing unit (1000 mW/cm²; VALO, Ultradent, USA), in accordance with the assigned bonding strategy. Restorations were built using a microhybrid resin composite (Opallis, FGM Dental Products, Joinville, SC, Brazil) in 1-mm increments, each light-cured for 40 s [14]. A single operator performed all bonding procedures under controlled temperature and humidity. A schematic illustration of tooth preparation, bonding strategies, and restorative build-up is provided in the Supplementary Material.

Microtensile bond strength (μTBS)

After 24 h of storage in distilled water at 37°C, the bonded teeth were sectioned longitudinally in both "x" and "y" directions across the bonded interface using a diamond saw under water cooling. Resin-dentin bonded sticks with a cross-sectional area of approximately 0.8 mm² were obtained. The number of premature failures per tooth was recorded. The cross-sectional area of each stick was measured with a digital caliper (Mitutoyo, Tokyo, Japan) and recorded for the subsequent calculation of microtensile bond strength. Each stick was attached to a modified μTBS testing jig

using cyanoacrylate adhesive and subjected to a tensile force at 0.5 mm/min in a universal testing machine.

Failure mode was assessed under an optical microscope at 40 × magnification and categorized as follows: cohesive (C), when the failure occurred exclusively within dentin or within the resin composite; adhesive (A), when the failure occurred at the resin-dentin interface; or mixed (M), when the failure at the resin-dentin interface was accompanied by cohesive failure of the adjacent substrate. Premature failures (PF) were recorded but not included in the calculation of mean μTBS values.

Inhibition of Proteolytic Activity (Matrix metalloproteinases, MMPs)

In situ zymography was performed to evaluate the inhibition of endogenous dentinal proteolytic activity after application of the experimental adhesive formulations. Adhesive discs (bonded specimens; n = 3 teeth per group per adhesive strategy), were prepared according to either the SE or ER protocol described above. After 24 h of storage in distilled water at 37°C, the specimens were sectioned perpendicular to the bonded interface using a low-speed diamond saw (Isomet 5000, Buehler, IL, USA) to obtain discs approximately 0.4 mm thick. The discs were subsequently polished under water cooling to a final thickness of approximately 300 μm.

Proteolytic activity was assessed using fluorescein-conjugated gelatin as a substrate (EnzChek Gelatinolytic/Collagenolytic Assay Kit, Thermo Fisher Scientific, Eugene, OR, USA) by incubating the discs for 7 days at 37°C in a dark and humid environment to prevent photobleaching and dehydration, following the protocol previously described by Mazzoni et al. [23]. Gelatin hydrolysis by endogenous dentin matrix metalloproteinases resulted in the release of fluorescent fragments, indicating gelatinolytic activity, which was analyzed using multiphoton confocal laser scanning microscopy (CLSM; Leica TCS SP8 MP, Leica Microsystems, Wetzlar, Germany). Fluorescence images were acquired using an excitation wavelength of 488 nm and emission detection above 530 nm. Optical sections with a thickness of 20 μm were obtained across the resin–dentin interface, encompassing both the hybrid layer and underlying dentin.

Fluorescence intensity, expressed as arbitrary units of fluorescence (AUF per pixel/mm²), was quantified using LAS X software (Leica Microsystems, Wetzlar, Germany). For each experimental group, measurements from eight discs were averaged to obtain a mean fluorescence value representative of gelatinolytic activity. Untreated dentin surfaces were included as internal negative controls during CLSM

acquisition. All imaging parameters, including detector gain, laser power, and acquisition settings, were kept standardized for all specimens to allow valid intergroup comparisons and quantitative analysis of MMP-related proteolytic activity.

Statistical analysis

Normality and homoscedasticity were assessed using the Shapiro–Wilk and Levene tests, respectively. One-way ANOVA with Tukey's post-hoc test was used for single-factor outcomes (Antibacterial activity). Two-way ANOVA was applied for outcomes involving multiple factors (cytocompatibility, mineralization, μTBS and in situ zymography). Statistical significance was set at $\alpha = 0.05$, and analyses were performed using SPSS 28.0 (IBM Corp., Armonk, NY, USA).

Results

Nanoparticle Characterization

Figure 11 shows FE-SEM images at different magnifications (74, 110, and 127 kx), confirming that the analyzed BG Nps exhibited a nanometric size (<100 nm). The average particle sizes were 78 nm for BG Nps, 56.4 nm for Cu Nps, and 45.9 nm for ZnO Nps.

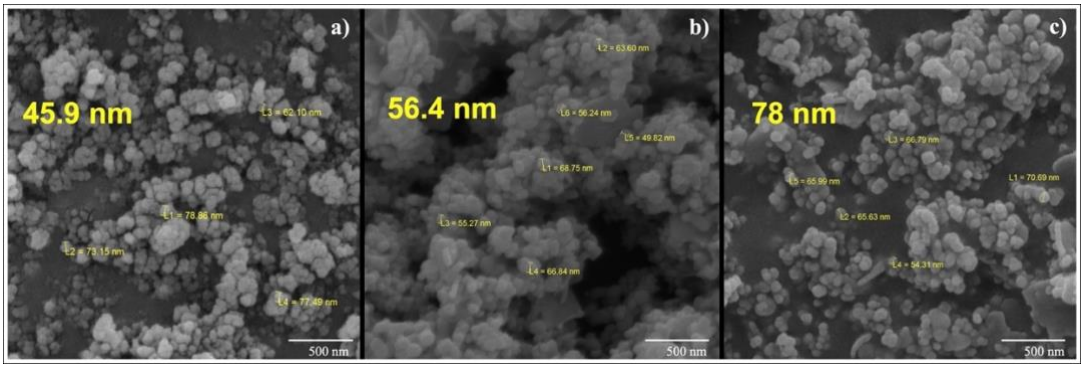

Figura 11. Field-Emission scanning electron microscopy (FE-SEM) images of zinc oxide (ZnO), copper (Cu), and bioactive glass (BG) nanoparticles.

Field-Emission scanning electron microscopy (FE-SEM) images of zinc oxide (ZnO), copper (Cu), and bioactive glass (BG) nanoparticles. (a) BG nanoparticles (BG Nps); (b) Cu nanoparticles (Cu Nps); (c) ZnO nanoparticles (ZnO Nps). Yellow larger represent the mean particle size for each nanoparticle group. FE-SEM analysis confirmed that all nanoparticles exhibited nanometric dimensions (<100 nm).

Figure 12 shows the infrared spectrum corresponding to the BG Nps. Characteristics peaks were observed at 1058 cm^{-1}, 798 cm^{-1}, and 443 cm^{-1}, associated with the vibrational modes of Si–O–Si bonds in the silica network of the BG.

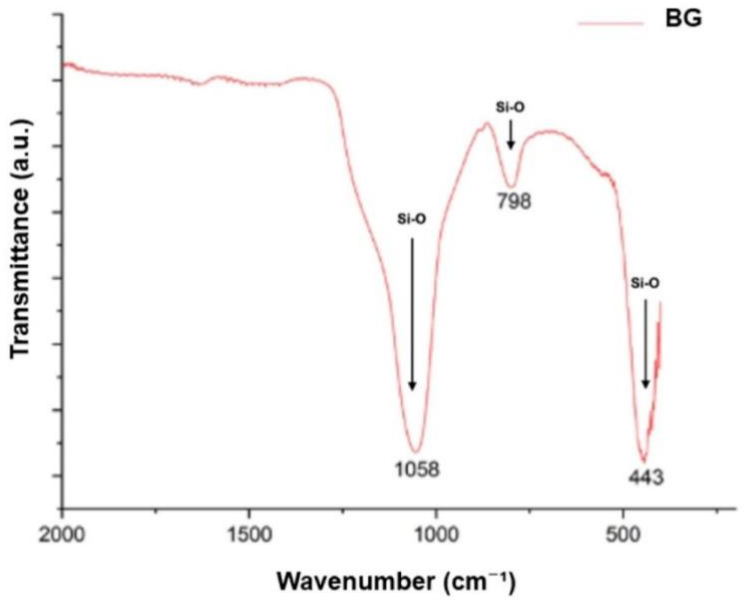

Figura 12. FTIR–ATR spectrum of bioactive glass (BG) nanoparticles.

FTIR–ATR spectrum of bioactive glass (BG) nanoparticles. Characteristics Si–O–Si vibrational bands are highlighted. The absorption peak between 1000-1100 cm^{-1} corresponds to asymmetric stretching, the band near ~799 cm^{-1} corresponds to symmetric stretching, and the band between 400-500 cm^{-1} corresponds to bending vibrations of the Si–O–Si network.

Antibacterial Activity

Colony-forming unit (CFU) counts revealed significant differences among groups ($p < 0.05$). Adhesives containing BG demonstrated a pronounced reduction in bacterial growth compared with the control and ZnO/Cu groups. The 10%BG and 10%BG+ZnO/Cu adhesives presented the lowest CFU values, corresponding to inhibition rates above 80%. The 5%BG+ZnO/Cu formulation showed intermediate antibacterial activity, while the ZnO/Cu-only group exhibited the weakest effect among the modified adhesives (Table 13).

Tabela 13. Antibacterial activity against S. mutans for the experimental adhesive formulations.

Group	CFU (log_{10}/mL, mean ± SD)	Inhibition (%)
Control	6.35 ± 0.12 A	–
ZnO/Cu	5.89 ± 0.15 B	21.8% A
5%BG+ZnO/Cu	**5.21 ± 0.18** C	43.8% B
10%BG+ZnO/Cu	**4.02 ± 0.14** D	83.7% C
10%BG	**3.98 ± 0.11** D	84.4% C

Values are expressed as mean ± standard deviation (CFU log_{10}/mL) and corresponding inhibition percentages. **Different uppercase letters within each column indicate statistically significant differences among groups** ($p < 0.05$).

Representative SEM images confirmed dense biofilm formation on the control specimens, characterized by “pearl chain” arrangements of coccoid *S. mutans.* In contrast, BG-containing adhesives showed sparse bacterial colonization and surface deposits of Nps embedded within the adhesive matrix (Fig. 13).

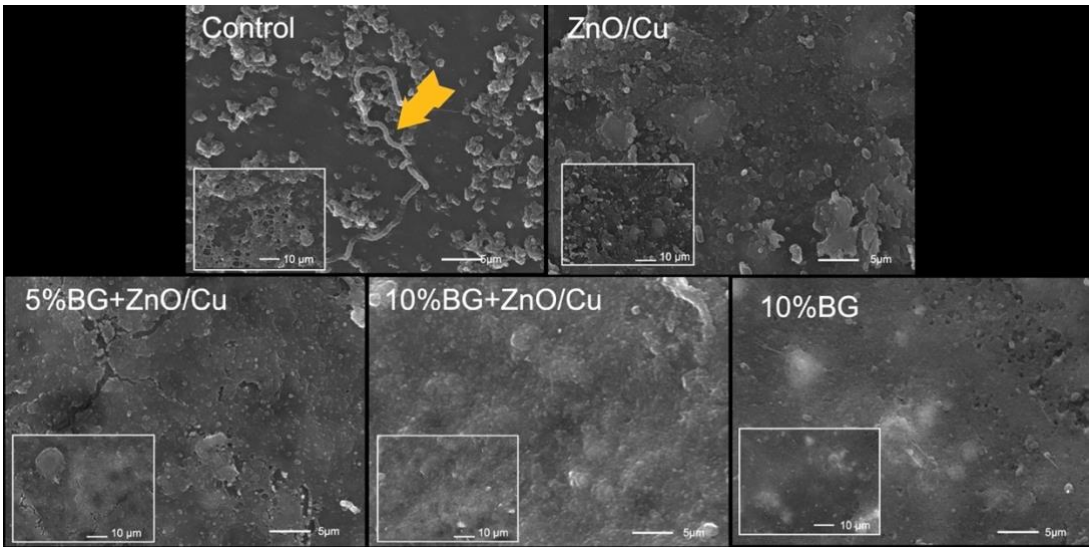

Figura 13. FE-SEM images of nanoparticle-modified adhesives after exposure to Streptococcus mutans*.*

FE-SEM images of nanoparticle-modified adhesives after exposure to *Streptococcus mutans*. Images acquired at 2000× and 3000× magnification show adhesives containing nanoparticles (NPs) following exposure to *S. mutans* broth culture. In the control group, a dense biofilm was observed at lower magnification

(2000×), while higher magnification (3000×) revealed *S. mutans* arranged in a characteristic “pearl-chain” formation (highlighted in yellow). Experimental groups containing NPs exhibited a marked reduction in bacterial number and density, demonstrating the antibacterial effect of the nanoparticles on adhesive surfaces.

Cytocompatibility

The MTS assay demonstrated that all experimental adhesives, maintained cell viability above 80% relative to the positive control. No statistically significant differences were observed among groups at either 3 or 7 days ($p > 0.05$). A slight reduction in viability was observed over time for all groups, consistent with the expected aging behavior of polymer-based materials. The negative control (Pb^{2+} exposure) confirmed assay sensitivity, showing viability below 20% (Table 14).

Tabela 14. Cell viability of human gingival mesenchymal stem cells (hGMSCs) exposed to the adhesive formulations at 3 and 7 days (mean % ± SD relative to the positive control).

Group	3 days	7 days
Control	97.4 ± 3.1	90.6 ± 4.2
ZnO/Cu	95.9 ± 2.8	88.2 ± 3.5
5%BG+ZnO/Cu	96.8 ± 3.0	87.6 ± 3.9
10%BG+ZnO/Cu	94.5 ± 3.7	86.9 ± 4.1
10%BG	95.2 ± 3.4	87.3 ± 3.7
Positive Control	100.0 ± 0.0	100.0 ± 0.0
Negative Control	19.8 ± 2.1	18.5 ± 2.3

No statistically significant differences were detected among the adhesive groups at either time point ($p > 0.05$). Viability values >80% meet ISO 10993 biocompatibility criteria.

Mineralizing Potential

SEM analysis after immersion in SBF revealed mineral deposition in the BG-containing groups. At 7 days, small spherical Ca–P clusters were observed on 5%BG+ZnO/Cu and 10%BG specimens; by 28 days, these clusters had increased in density and coalesced into apatite-like layers. EDX spectra confirmed the presence of Ca and P peaks in BG-containing adhesives, whereas no such deposits were detected in the control or ZnO/Cu groups (Fig.14a)

Quantitative analysis showed significant increases in Ca and P content at 28 days in the BG-modified groups ($p < 0.05$), with the 10%BG+ZnO/Cu and 10%BG formulations exhibited the highest mineral deposition (Fig. 14b).

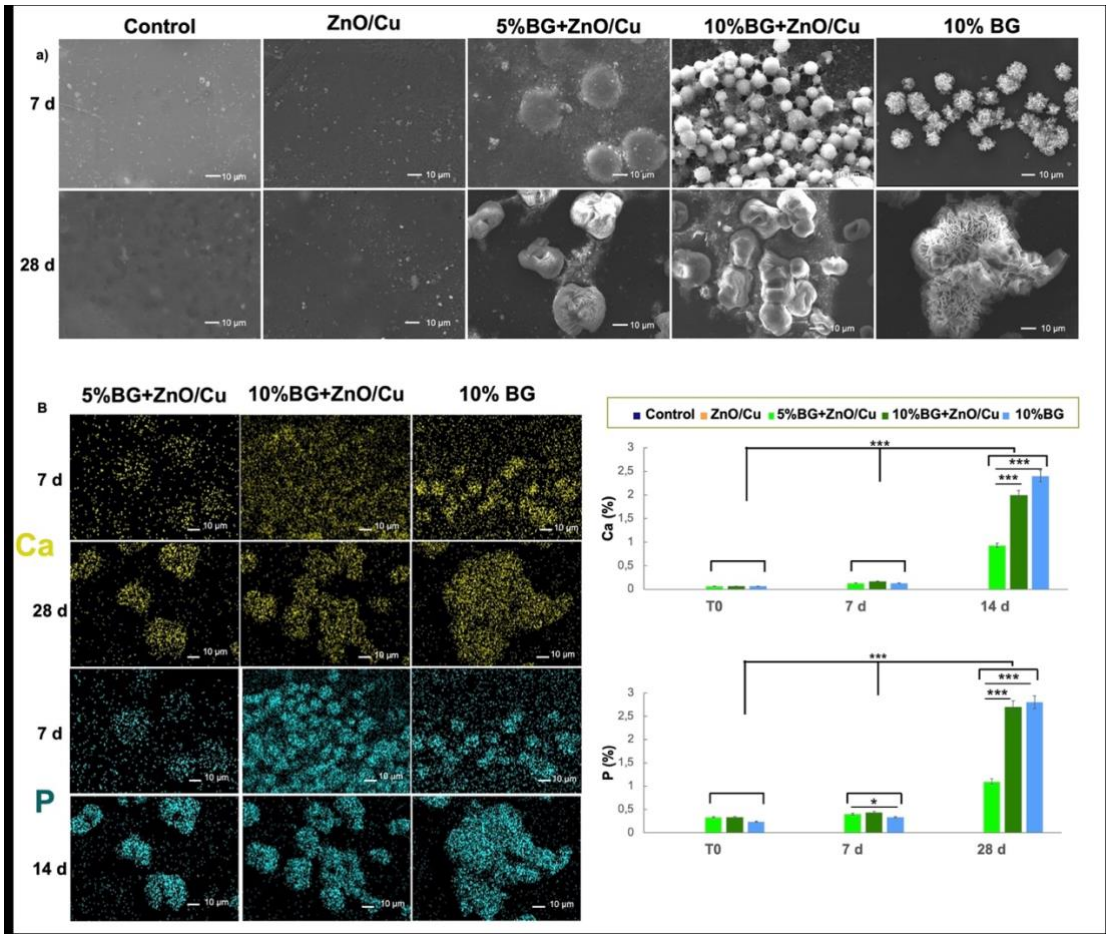

Figura 14. Mineralization assessment of adhesive specimens immersed in simulated body fluid.

Mineralization assessment of adhesive specimens immersed in simulated body fluid. (a) FE-SEM images of adhesive disks after immersion for 7 and 28 days; (b) Energy-dispersive X-ray spectroscopy (EDX) analysis showing Ca and P. Bar graphs on the right panel represent mean (±SD) elemental composition (n = 3). Significant increases in Ca and P were observed at 28 days compared with baseline (T_0) and 7 days, and among BG-modified groups within each time point ($p < 0.05$*, $p < 0.0001$**; Student's *t*-test). Elemental maps indicate Cain yellow and P in turquoise. Degree of Conversion (DC).

Raman spectroscopy showed that all groups achieved DC values above 60%, indicating effective polymerization [9]. The control and ZnO/Cu groups demonstrated

similar DC values (~72%). The 10%BG adhesive exhibited the highest DC (~79%), significantly higher than the 10%BG+ZnO/Cu formulation (~70%, $p < 0.05$). No significant differences were observed among the remaining groups (Table 15).

Tabela 15. Degree of Conversion of the experimental adhesive formulations (mean ± SD).

Group	DC (%)
Control	71.8 ± 2.4 A
ZnO/Cu	72.4 ± 2.2 A
5%BG+ZnO/Cu	70.3 ± 2.7 A
10%BG+ZnO/Cu	**69.5 ± 2.6** AB
10%BG	**79.1 ± 2.8** AC

Different uppercase letters indicate statistically significant differences among groups ($p < 0.05$).

Microtensile bond strength

All experimental adhesives produced measurable μTBS values. For the SE strategy, no significant differences in μTBS were found among groups ($p > 0.05$), with mean values ranging from 37.41 ± 3.8 MPa in the 5%BG+ZnO/Cu group to 49.1 ± 2.9 MPa in the 10%BG+ZnO/Cu group. In contrast, under the ER strategy, the 10%BG and 10%BG+ZnO/Cu adhesives demonstrated significantly lower μTBS values compared with the control ($p < 0.05$). Mean values ranged from 51.9 ± 5.9 MPa in the ZnOCu group to 35.2 ± 3.7 MPa in the 10%BG+ZnO/Cu group. No significant differences were observed between the SE and ER strategies ($p > 0.05$; Table 16). Failure mode was predominantly adhesive (Table 17)

Tabela 16. Microtensile bond strength (μTBS, MPa; mean ± SD) of the experimental adhesives under self-etch (SE) and etch-and-rinse (E&R) strategies.

Group	μTBS (Mpa)	
	SE	E&R
Control	40 ± 1.47 A	44,8 ±0.52 A
ZnO/Cu	44.1 ± 11 A	51,9 ± 5,9 A
5%BG+ZnO/Cu	49,1 ± 2.9 A	46.8 ± 2.4 A
10%BG+ZnO/Cu	37.4 ± 3.8 A	35.2 ± 3.7 B
10%BG	39.9 ± 1.3 A	37.2 ± 2.2 B

Different uppercase letters within each column indicate statistically significant differences among groups ($p < 0.05$). No significant differences were found between SE and E&R strategies ($p > 0.05$).

Tabela 17. Failure mode distribution (%) for each adhesive formulation under self-etch (SE) and etch-and-rinse (ER) strategies

Group	Failure Pattern (%)					
	SE			ER		
	A/M	C	PF	A/M	C	PF
Control	8	2	0	94	6	0
ZnO/Cu	88	8	4	88	12	0
5%BG+ZnO/Cu	92	8	0	98	2	0
10%BG+ZnO/Cu	84	8	8	92	6	2
10%BG	96	4	0	88	6	6

SE = self-etch; ER = etch-and-rinse/ Failure mode categories: A/M = adhesive or mixed failure; C = cohesive failure; PF = premature failure.

MMP inhibition

In situ zymography revealed distinct patterns of gelatinolytic activity at the resin–dentin interface depending on adhesive formulation and bonding strategy. Overall, high enzymatic activity was detected across all groups. Under SE strategy, none of the groups showed significantly lower enzymatic activity than the control. Under the ER strategy, only ZnO/Cu exhibited lower fluorescence intensity within the

hybrid layer and adjacent dentin compared with the control. None of the experimental formulations completely suppressed MMP activity, irrespective of the dentin conditioning strategy. (Fig. 5).

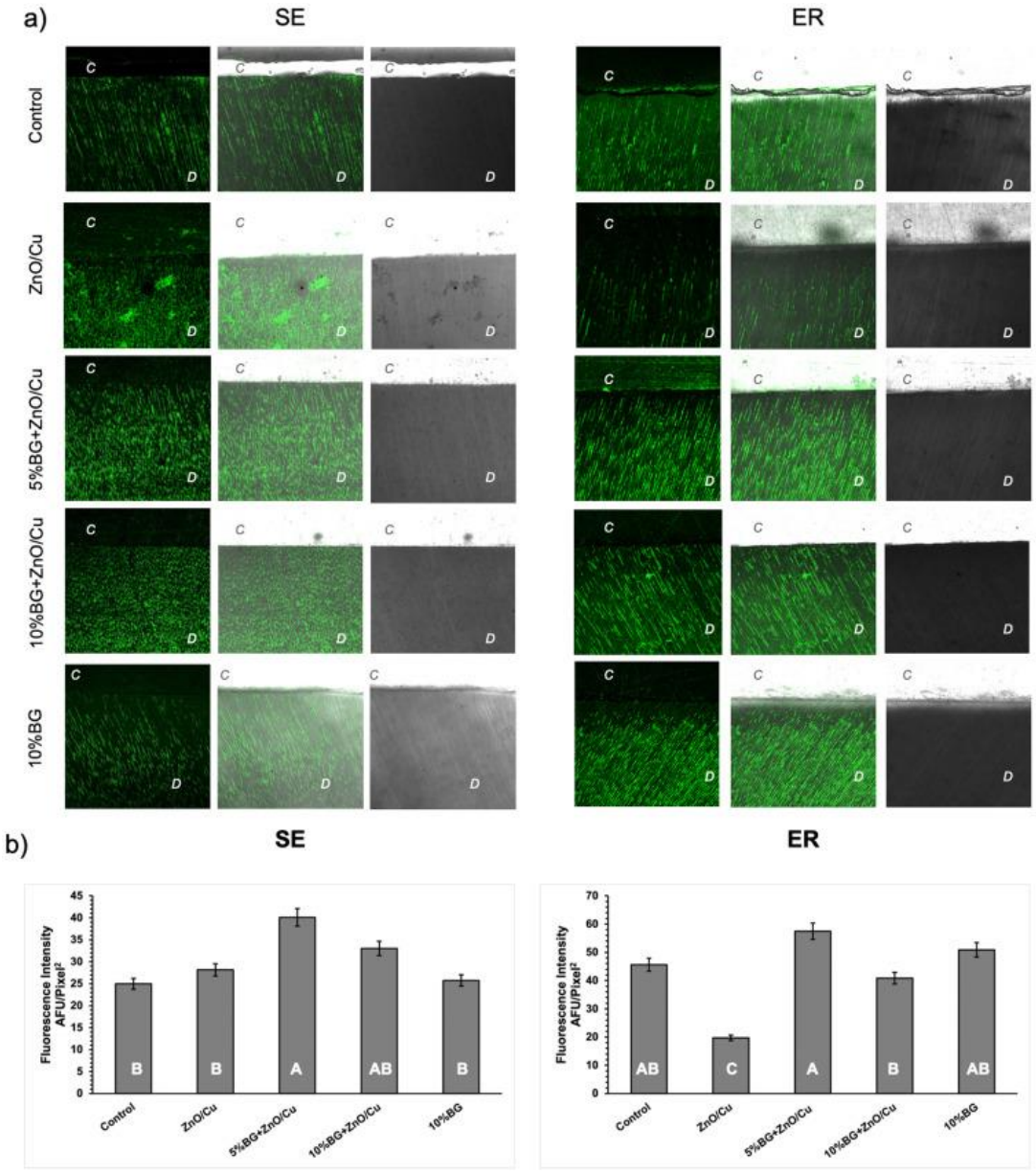

Figura 15. In situ zymography.

Confocal laser scanning microscopy (CLSM) images of resin–dentin adhesive interfaces after in situ zymography. (a) Representative CLSM images obtained after 7 days of incubation in fluorescein-labeled gelatin. Two bonding strategies were evaluated: self-etch (SE) and etch-and-rinse (ER). The left column shows green fluorescence indicating gelatinolytic activity, the right column presents differential interference contrast (DIC) images identifying dentin morphology, and the middle

column shows merged images. High enzymatic activity was observed in all groups; however, under ER strategy, lower fluorescence intensity within the hybrid layer and adjacent dentin was observed for the ZnO/Cu group. c: resin composite; d: dentin; the adhesive layer I located between them. (b) Quantitative analysis of fluorescence intensity expressed as arbitrary fluorescence units (AFU) normalized by area (pixels/mm²). Data are presented as mean ± standard deviation. Different uppercase letters indicate significant differences among the groups within each adhesive strategy ($p < 0.005$).

Discussion

This study evaluated the antibacterial activity, cytocompatibility, mineralizing potential, degree of conversion, enzymatic activity, and resin-dentin μTBS of a universal adhesive modified with ZnO, Cu, and BG Nps. The findings rejected allthe null hypotheses. Adhesives containing 10 wt %BG demonstrated significantly enhanced antibacterial activity against S. mutans and pronounced mineralizing potential. Although all formulations maintained cytocompatibility and acceptable polymerization performance, a slight reduction in μTBS was observed under ER for the 10 %wt BG-containing groups. MMPs activity varied according to the bonding strategy; however, no consistent inhibitory effect was detected. Overall, these results highlight the potential of multifunctional Np-modified adhesives to improve the biological performance of the resin-dentin interface, although minor trade-offs in initial bond strength may occur at higher BG concentrations.

Nanoparticle characterization confirmed that Cu, ZnO and BG were <100 nm, ensuring nanoscale classification and favoring high chemical reactivity [10]. BG Nps were amorphous, supporting their mineralizing potential and bioactivity [14,17].

Although ZnO/Cu nanoparticles have demonstrated antibacterial effects in previous studies [24], the present results indicate that BG was the dominate contributor to antibacterial performance in this model. Adhesives containing 10 wt %BG, with or without ZnO/Cu, achieved comparable inhibition levels (>80 %), suggesting that BG-driven alkalinization and sustained ionic release predominated in bacterial suppression under the experimental conditions tested. Accordingly, ZnO/Cu should be interpreted as providing complementary rather than essential antibacterial effects.

The reduced apparent contribution of Cu at higher BG concentrations may be partially explained by ionic interactions between Cu^{2+} and the silanol-rich surface of BG Nps, as well as coordination with oxygen-containing functional groups within the adhesive matrix. These interactions may promote transient coordination complexes, potentially limiting the immediate bioavailability of Cu ions and attenuating their biological reactivity without eliminating its stabilizing effects. Notably, the intermediate response observed in the 5 %BG+ZnO/Cu group supports a dose-dependent effect, consistent with the findings of Jun et al. [25]. Clinically, sustained antibacterial activity at the adhesive interface may contribute to the prevention of secondary caries, a major cause of resin restoration failure [3].

All adhesives maintained >80 % cell viability at both time points, fulfilling ISO 10993 requirements. These findings align with Catunda et al. [26], who reported although resin adhesives release cytotoxic monomers, they remain compatible with oral cells at clinical levels. The absence of significant cytotoxicity increase confirms the biological safety of the Np concentrations used. The slight time-dependent decrease in viability is consistent with monomer elution [1]. Previous studies suggest that ZnO Nps may mitigate oxidative stress and support biocompatibility [12], which aligns with our findings.

A key finding of this study was the mineralizing capability of BG-containing adhesives. After immersion in SBF, FE-SEM/EDX analyses showed progressive deposition of Ca–P clusters, with the 10 %BG+ZnO/Cu and 10 %BG groups exhibiting the most extensive mineralization after 28 days. These results corroborate evidence that BG releases Ca^{2+} and PO_4^{3-} ions that facilitate apatite formation at the material surface. However, although FE-SEM/EDX confirmed Ca–P deposition, the crystalline nature of these deposits could not be determined. Therefore, they are described as apatite-like rather than confirmed hydroxyapatite, and further crystallographic analyses, such as X-ray diffraction, are required to verify hydroxyapatite formation [27].

From a clinical perspective, the capacity to form apatite-like layers may reinforce the hybrid layer against acid challenge and bacterial infiltration, thereby enhancing interfacial stability. Abuna et al [17] similarly reported improved bonding to demineralized dentin in BG-containing adhesives, supporting the concept of biomimetic repair of compromised substrates. The current results extend that evidence, demonstrating that BG-maintains its mineralization potential even when combined with metallic Nps [28].

All adhesives achieved DC exceeding 60 %, indicating acceptable polymerization performance [20]. The highest DC observed for the 10 %BG formulation may be attributed to enhanced light scattering, which can improve polymerization depth [29]. The slight decrease in DC observed for the 10 %BG+ZnO/Cu formulation, which contained the highest Nps loading, may be related to particle agglomeration or ion-mediated interference with polymerization kinetics [21]. Because BG releases ions (e.g., Ca^{2+}, Na^{+}) during aqueous exposure, future studies combining ion-release quantification with real-time kinetic analyses are warranted to determine whether such ions interact with the photoinitiator system or radical propagation. Importantly, this potential effect did not compromise overall curing performance.

The combined use of ZnO, Cu, and BG Nps provides complementary biological mechanisms. Zn^{2+} ions stabilize collagen by occupying MMP-sensitive sites and promoting mineral nucleation, while Cu^{2+} ions inhibit MMP-2 and enhance collagen cross-linking through lysyl oxidase activation [14]. BG continuously releases Ca^{2+} and PO_4^{3-} ions, which promote remineralization and create a high-pH environment unfavorable to bacteria growth and MMP activity. In this study, BG exerted the dominant effect on antibacterial and mineralizing properties, whereas ZnO/Cu contributed moderately without compromising cytocompatibility or polymerization. Optimizing the nanoparticle ratio may further enhance these synergistic outcomes. The limited antibacterial performance of ZnO/Cu alone may be attributed to suboptimal concentrations, as previous studies have employed higher loadings (e.g., 5 %ZnO and 0.5 %Cu) to achieve greater efficacy [14]. Future research should focus on fine-tuning Nps proportions to maximize the multifunctional performance of these adhesives.

In situ zymography revealed high gelatinolytic activity across all formulations. Under ER conditions, ZnO/Cu demonstrated partial suppression of fluorescence, whereas BG-containing formulations did not exhibit consistent inhibition. These findings suggest that short-term ionic release and pH modulation were insufficient to suppress MMP activity within the evaluated timeframe. Because enzyme modulation is both concentration- and time-dependent, longer aging periods or sustained ion delivery may be required to achieve measurable enzymatic inhibition [30]

The mechanical behavior of adhesive systems is influenced by filler content, particle morphology, and bonding strategy [21]. The ER strategy is more sensitive to changes in adhesive composition due to deeper dentin demineralization and increased reliance on adequate resin infiltration and polymer network integrity [5,7]. Higher BG

loadings may hinder optimal infiltration and stress distribution, particularly because BG particles do not chemically bond to the resin matrix. Conversely, SE bonding produced more consistent μTBS values, indicating lower technique sensitivity [11].

Although reductions in bond strength of approximately 20–30 % were observed for 10 wt %BG-containing formulations under ER conditions, the values remained above commonly reported in vitro thresholds associated with clinically acceptable dentin bonding [31]. Nevertheless, these reductions should be interpretated caustiously, as long-term fatigue loading, thermocycling, and enzymatic degradation may further compromise interfacial over time [32].

Overall, the incorporation of BG into ZnO/Cu-modified universal adhesives represents a promising strategy to address the multifactorial degradation of the resin–dentin interface. BG was the primary contributor to mineralization and antibacterial effects, while ZnO and Cu provided complementary protection without impairing polymerization or cell compatibility. This synergy suggests that optimized nanoparticle formulations could extend adhesive performance beyond that of conventional systems. These attributes are particularly relevant for patients at high risk of caries. Sustained antibacterial activity may limit bacterial colonization at restoration margins, while ongoing remineralization reinforces the hybrid layer against acid-mediated degradation. Together with preserved polymerization efficiency and cytocompatibility, these properties suggest that multifunctional universal adhesives could improve restoration longevity, reduce replacement frequency, and enhance cost-effectiveness in restorative dentistry.

Several limitations should be acknowledged. All experiments were performed in vitro and evaluated short-term outcomes only, without mechanical aging or thermocycling. The antibacterial model was restricted to S. mutans, whereas clinical biofilms are multispecies and structurally complex. Mineral deposition was assessed by FE-SEM/EDX, which provides elemental but not crystallographic confirmation. Enzymatic activity was evaluated only at early time points, limiting inference regarding long-term modulation. Future studies should incorporate aging protocols, multispecies biofilms, quantitative ion-release analysis, crystallographic validation, and in situ or in vivo models to strengthen translational relevance.

Conclusion

Within the limitations of this in vitro study, incorporating bioactive glass nanoparticles into a zinc oxide and copper-modified universal adhesive improved antibacterial and mineralizing performance while maintaining cytocompatibility and adequate polymerization. Although higher bioactive glass loadings slightly reduced bond strength under the etch-and-rinse strategy and no immediate reduction in matrix metalloproteinases activity was observed, bond strength values remained within commonly reported in vitro ranges. These findings support the potential of multifunctional nanoparticle-modified adhesives to enhance the biological performance of the resin–dentin interface; however, long-term aging studies are required to confirm durability.

References

1. Ferracane JL. Resin composite - State of the art. Dent Mater. 2011;27(1):29–38. https://doi.org/10.1016/j.dental.2010.10.020.
2. Askar H, Krois J, Göstemeyer G, & Schwendicke F. Secondary caries risk of different adhesive strategies and restorative materials in permanent teeth: Systematic review and network meta-analysis. J Dent. 2021;104:103541. https://doi.org/10.1016/j.jdent.2020.103541.
3. Demarco FF, Collaresa K, Coelho-de-Souza FH, Correa MB, Cenci MS, Moraes RR, Opdam NJM, & A. Anterior composite restorations: A systematic review on long-term survival and reasons for failure. Dent Mater. 2015;31:1214–1224. https://doi.org/10.4103/jcd.jcd_527_21.
4. Breschi L, Mazzoni A, Ruggeri A, Cadenaro M, Di Lenarda R, De Stefano Dorigo E. Dental adhesion review: aging and stability of the bonded interface. Dent Mater. 2008;24(1):90-101. https://doi.org/10.1016/j.dental.2007.02.009
5. Pashley DH, Tay FR, Breschi L, Tjäderhane L, Carvalho RM, Carrilho M, A Tezvergil-Mutluay. A state of the art etch-and-rinse adhesives. Dent Mater. 2011;27(1):1–16. https://doi.org/10.1016/j.dental.2010.10.016.
6. A. Mazzoni, L. Tjäderhane, V. Checchi, R. Di.Lenarda, T. Salo, F.R. Tay, D.H. Pashley, L. Breschi. Role of dentin MMPs in caries progression and bond stability. J. Dent. Res., 94 (2015), pp. 241-251, 10.1177/0022034514562833
7. Van Meerbeek B, Yoshihara K, Van Landuyt K, Yoshida Y, & Peumans M. From Buonocore's Pioneering Acid-Etch Technique to Self-Adhering Restoratives. A Status Perspective of Rapidly Advancing Dental Adhesive Technology. J Adhes Dent. 2020;22(1):7–34. https://doi.org/10.3290/j.jad.a43994.
8. Mazzoni A, Tjäderhane L, Checchi V, Di Lenarda R, Salo T, Tay FR, Pashley DH, Breschi L. Role of dentin MMPs in caries progression and bond stability. J Dent Res 2015;94(2):241–251. https://doi.org/10.1177/0022034514562833.
9. Breschi, L., Mazzoni, A., Nato, F., Carrilho, M., Visintini, E., Tjäderhane, L., Ruggeri, A., Jr, Tay, F. R., Dorigo, E.deS., Pashley, D. H. Chlorhexidine

stabilizes the adhesive interface: A 2-year in vitro study. Dent Mater. 2010;26(4):320–325. https://doi.org/10.1016/j.dental.2009.11.153.
10. Cadenaro M, Josic U, Maravić T, Mazzitelli C, Marchesi G, Mancuso E, Breschi L, A Mazzoni. Progress in Dental Adhesive Materials. J Dent Res. 2023;102(3):254-62. https://doi.org/10.1177/00220345221145673
11. Jandt KD, Watts DC. Nanotechnology in dentistry: Present and future perspectives on dental nanomaterials. Dent Mater. 2020;36(11):1365–1378, https://doi.org/10.1016/j.dental.2020.08.006.
12. Gutiérrez MF, Bermudez J, Dávila-Sánchez A, Alegría-Acevedo LF, Méndez-Bauer L et al. Zinc oxide and copper nanoparticles addition in universal adhesive systems improve interface stability on caries-affected dentin. J Mech Behav Biomed Mater. 2019;103366. https://doi.org/10.1016/j.jmbbm.2019.07.024.
13. Toledano M, Yamauti M, Ruiz-Requena ME, Osorio R. A ZnO-doped adhesive reduced collagen degradation favoring dentine remineralization. J Dent. 2012;40(9):756-65. https://doi.org/10.1016/j.jdent.2012.05.007
14. Vidal O, de Paris Matos T, Núñez A, Méndez-Bauer L, Sutil E, Ñaupari-Villasante Ret al. A universal adhesive containing copper nanoparticles improves the stability of hybrid layer in a cariogenic oral environment: An in situ study. J Mech Behav Biomed Mater. 2022;126:105017. https://doi.org/10.1016/j.jmbbm.2021.105017.
15. Gutiérrez MF, Alegría-Acevedo LF, Méndez-Bauer L, Bermudez J, Dávila-Sánchez A, Buvinic S, Hernández-Moya N, Reis A, Loguercio AD, Farago PV, Martin J, Fernández E. Biological, mechanical and adhesive properties of universal adhesives containing zinc and copper nanoparticles. *J Dent*. 2019;82:45-55. https://doi.org/10.1016/j.jdent.2019.01.012
16. Basualdo Allende J, Nascimento FD, Damasceno E Souza Chiari M, Aliaga-Galvez R, Ñaupari-Villasante R, Miranda CB, Pardo-Díaz C, Gutiérrez MF, Covarrubias C, Loguercio AD, Fernández E. Evaluation of adhesive properties and enzymatic activity at the hybrid layer of a simplified adhesive loaded with 0.2 % Cu and 5 % ZnO nanoparticles: A Randomized Clinical Trial and ex vivo analysis. J Dent. 2024;149:105283.https://doi.org/10.1016/j.jdent.2024.105283
17. Skallevold HE, Rokaya D, Khurshid Z, & Zafar MS. Bioactive glass applications in dentistry. Int J Mol Sci. 2019;20(23):1–24. https://doi.org/10.3390/ijms20235960.
18. Abuna G, Campos P, Hirashi N, Giannini M, Nikaido T, Tagami J, Coelho Sinhoreti MA, Geraldeli S. The ability of a nanobioglass-doped self-etching adhesive to re-mineralize and bond to artificially demineralized dentin. *Dental materials : official publication of the Academy of Dent Mater. 2021; 37*(1):120–130. https://doi.org/10.1016/j.dental.2020.10.026
19. Nagarkar, S., Theis-Mahon, N., & Perdigão, J. (2019). Universal dental adhesives: Current status, laboratory testing, and clinical performance. J Biomed Mater Res B Appl Biomater. 2019;*107*(6):2121–2131. https://doi.org/10.1002/jbm.b.34305
20. Ferracane JL, Hilton TJ, Stansbury JW, Watts DC, Silikas N, Ilie N, Heintze S, Cadenaro M, Hickel R. Academy of Dental Materials guidance-Resin composites: Part II-Technique sensitivity (handling, polymerization, dimensional changes). Dent Mater. 2017;33(11):1171-91. https://doi.org/10.1016/j.dental.2017.08.188
21. Ilie N, Hilton TJ, Heintze SD, Hickel R, Watts DC, Silikas N, Stansbury JW, Cadenaro M, & Ferracane JL. Academy of Dental Materials guidance — Resin

composites: Part I — Mechanical properties. Dent Mater. 2017;33:880–894, https://doi.org/10.1016/j.dental.2017.04.013
22. Kokubo T, & Takadama H. How useful is SBF in predicting in vivo bone bioactivity? Biomaterials. 2006;27(15):2907–2915, https://doi.org/10.1016/j.biomaterials.2006.01.017.
23. Drago L, Toscano M, Bottagisio M. Recent evidence on bioactive glass antimicrobial and antibiofilm activity: A mini-review Materials (Basel). 2018;11(2):1–11, https://doi.org/10.3390/ma11020326.
24. Jun SK, Yang SA, Kim YJ, El-Fiqi A, Mandakhbayar N, Kim DS, Roh J, Sauro S, Kim HW, Lee JH, Lee HH. Multi-functional nano-adhesive releasing therapeutic ions for MMP-deactivation and remineralization. Sci Rep. 2018:8(1) 1–10, https://doi.org/10.1038/s41598-018-23939-6.
25. Catunda RQ, Vieira JRC, de Oliveira EB, da Silva EC, Brasil VLM, & Perez DE da C. Citotoxicity evaluation of three dental adhesives on vero cells in vitro. J Clin Exp Dent .2017:9(1) e61–e66, https://doi.org/10.4317/jced.53039.
26. Hench LL (2006) The story of Bioglass® J Mater Sci Mater Med. 2006;7(11):967–978, https://doi.org/10.1007/s10856-006-0432-z.
27. Schwendicke, F, Al-Abdi, A, Pascual Moscardó, A, Ferrando Cascales, A, & Sauro, S. Remineralization effects of conventional and experimental ion-releasing materials in chemically or bacterially-induced dentin caries lesions. Dent mater. 2019;35(5):772–779. https://doi.org/10.1016/j.dental.2019.02.021
28. Par M, Tarle Z, Hickel R, & Ilie N. Mechanical properties of experimental composites containing bioactive glass after artificial aging in water and ethanol. Clin Oral Investig. 2019;23(6):2733–2741, https://doi.org/10.1007/s00784-018-2713-6.
29. Carvalho EM, Ferreira PVC, Gutiérrez MF, Sampaio RF, Carvalho CN, Menezes AS, Loguercio AD, Bauer J. Development and characterization of self-etching adhesives doped with 45S5 and niobophosphate bioactive glasses: Physicochemical, mechanical, bioactivity and interface properties. Dent Mater 2021; 37:1030–45. https://doi.org/10.1016/j.dental.2021.03.004.
30. B. Van Meerbeek, M. Peumans, A. Poitevin, A. Mine, A. Van Ende, A. Neves, J. De Munck. Relationship between bond-strength tests and clinical outcomes. Dent. Mater., 26 (2010), pp. e100-e121, https://doi.org/10.1016/j.dental.2009.11.148

3.5 ARTIGO 5 EFFECTS OF ZNO/CU AND BIOACTIVE GLASS-MODIFIED UNIVERSAL ADHESIVES ON BIOLOGICAL PROPERTIES, BOND STRENGTH, AND INTERFACIAL STABILITY UNDER CARIOGENIC CHALLENGE

Carolina Pardo-Díaz[abc], Gabriel Cochinski[b], Pedro Moreira[b], Fabio Dupart Nascimiento[d], Marina Damasceno e Souza Chiari[de], Joatan Costa[f], Cristian Covarrubias[g], Alessandro D. Loguercio[b], Eduardo Fernández[af*]

[a] Faculty of Dentistry, Dental School, University of Chile, 8380544, Santiago, Chile.

[b] Department of Restorative Dentistry, School of Dentistry, State University of Ponta Grossa, 84030-900, Ponta Grossa, Brazil.
[c] Department of Operative Dentistry, School of Dentistry, University of Valparaíso, 2360004, Valparaíso, Chile.
[d] Molecular Biology Division, Department of Biochemistry, Paulista Medical School, Federal University of São Paulo, 04044-020, São Paulo, Brazil
[e] Dental Research Division, Paulista University, 04026-002, São Paulo, Brazil
[f] Instituto de Ciencias Biomédicas, Universidad Autónoma de Chile, Santiago, Chile
[g] Laboratory of Nanobiomaterials, Institute for Research in Dental Sciences, Faculty of Dentistry, University of Chile, Santiago, Chile
Eduardo Fernández Godoy (Fernández E, *Corresponding author). Faculty of Dentistry, Dental School, University of Chile, Santiago, Chile, zip code: 8380544; Department of Operative Dentistry, School of Dentistry and Instituto de Ciencias Biomédicas, Universidad Autónoma de Chile, Santiago, Chile, e-mail address: edofdez@yahoo.com.

STATUS: Publicado em 2026
REVISTA: The Journal Clinical Oral Investigations
DOI: 10.1007/s00784-026-06766-2

Abstract

Objectives: To evaluate the effect of incorporating zinc oxide (ZnO), copper (Cu), and bioactive glass (BG) nanoparticles into a universal adhesive on the resin–dentin bond stability under a cariogenic challenge. The influence of these nanoparticles on enzymatic activity, mineral deposition, nanoleakage (NL), and microtensile bond strength (μTBS) was assessed. Methods: Five experimental adhesives were formulated by adding nanoparticles to a commercial universal adhesive: Control (0%), ZnO/Cu (0.2 wt% Cu + 2.5 wt% ZnO), 5 wt% BG + ZnO/Cu, 10 wt% BG + ZnO/Cu, and 10 wt% BG. Human dentin specimens were bonded using etch-and-rinse (ER) or self-etch (SE) strategies and restored with resin composite. After 24 h, specimens were evaluated at baseline and following a 5-day Streptococcus mutans biofilm challenge (pH ≈ 4.0). μTBS and NL were measured before and after challenge. Matrix metalloproteinase (MMP) activity was analyzed via in situ zymography, and mineral

deposition was characterized by SEM-EDX after immersion in simulated body fluid. Data were analyzed using ANOVA and Tukey's post hoc test ($\alpha = 0.05$).
Results: Nanoparticle incorporation enhanced the biofunctional performance of the adhesive. The 10 wt% BG + ZnO/Cu formulation preserved μTBS and significantly reduced NL after the cariogenic challenge ($p < 0.05$), whereas the control lost than 40% of its initial bond strength. SEM-EDX revealed increased Ca and P deposition at the hybrid layer, approaching hydroxyapatite-like composition. Although MMP activity varied between bonding strategies, no consistent inhibitory effect was detected.

Significance: The synergistic incorporation of ZnO, Cu, and BG nanoparticles improved the biological and interfacial stability of the universal adhesive, supporting remineralization and resistance to biofilm-induced degradation.

Keywords: zinc oxide; copper; bioactive glass; microtensile bond strength; nanoleakage; remineralization; MMPs.

Introduction

The longevity of resin composite restorations depends largely on the stability of the resin–dentin interface. Resin composites are the gold standard for direct restorations due to their esthetics, conservative tooth preparation requirements, and favorable mechanical performance [1, 2]. However, clinical evidence indicates an average service life of approximately 7–10 years, with secondary caries and hybrid layer degradation being the main reasons for failure [3, 4]. Preserving the adhesive interface under functional and cariogenic stress therefore remains a key challenge in restorative dentistry.

Bonding to enamel is predictable due to its high mineral content and low organic composition, whereas dentin bonding is intrinsically more complex because of its hydrated collagen matrix and tubular structure [5]. Acid etching or acidic monomers partially demineralize dentin, exposing a collagen scaffold that must be effectively infiltrated by resin monomers to form the hybrid layer. Ideally, this structure creates a micromechanical seal that prevents fluid movement and bacterial penetration [6]. However, incomplete resin infiltration leaves collagen fibrils vulnerable to enzymatic degradation, while polymerized resin remains susceptible to hydrolysis [7]. Over time,

these mechanisms promote nanoleakage, reduce bond strength, and ultimately compromise the adhesive interface [7, 8].

Endogenous dentin proteases, particularly matrix metalloproteinases (MMPs) and cysteine cathepsins, play a central role in hybrid layer degradation [9]. These enzymes, naturally present in dentin, can be activated by acidic monomers or bacterial acids [10]. Once activated, they degrade exposed collagen fibrils, weakening the hybrid layer [11]. Concurrently, acids produced by cariogenic biofilms, predominantly Streptococcus mutans and lactobacilli, further demineralize dentin, amplifying interfacial breakdown. Thus, adhesive failure and secondary caries result from the combined effects of enzymatic and acidic challenge [12].

Universal adhesives, which can be applied using self-etch (SE), etch-and-rinse (ER), or selective enamel etching protocols, have gained popularity due to their versatility and simplified clinical use. Nonetheless, their long-term performance, particularly in dentin, remains a topic of concern [13]. Clinical studies have reported progressive loss of bond strength, marginal discoloration, and secondary caries at rates higher than those observed with multi-step systems [14, 15]. Consequently, strategies to improve the biological resilience and interfacial stability of universal adhesives are of increasing interest.

Attempts to improve resin–dentin bond durability include the use of MMP inhibitors such as chlorhexidine, although their effect diminishes over time [16], and collagen cross-linkers, which can enhance matrix stability but may introduce additional clinical steps and potential biocompatibility concerns. A promising alternative is the development of intrinsically biofunctional adhesives capable of inhibiting enzymes, reducing biofilm activity, and promoting remineralization. Incorporating functional nanoparticles into adhesive systems has emerged as a viable pathway to achieve these goals [17].

Zinc oxide (ZnO) and copper (Cu) nanoparticles exhibit complementary biological properties. Zinc stabilizes collagen by binding to protease-sensitive sites and promotes mineral nucleation [18], while copper inhibits MMP-2 activity, stimulates tissue inhibitors of metalloproteinases (TIMPs) expression, and activates lysyl oxidase, enhancing collagen cross-linking [13]. Both types of nanoparticles disrupt bacterial membranes, promote reactive oxygen species (ROS) generation, and release bioactive ions that selectively inhibit cariogenic bacteria while maintaining cytocompatibility, as demonstrated in recent mechanistic and translational studies [19,

20]. However, metallic nanoparticles alone do not guarantee sustained remineralization and their long-term stability within adhesives matrices remains to be determined. Bioactive glass (BG), first developed by Hench in the 1960s, is a silica-based material capable of forming hydroxycarbonate apatite upon exposure to physiological fluids. Through the release of Ca^{2+} and PO_4^{3-} ions, BG promotes remineralization, increases local pH, and exerts antibacterial effects. In adhesives, BG nanoparticles have been shown to enhance calcium–phosphate deposition, inhibit collagen degradation, and improve long-term interfacial stability [21, 22].

Combining ZnO/Cu nanoparticles with BG may yield a multifunctional universal adhesive capable of addressing multiple pathways of hybrid layer degradation. While ZnO and Cu contribute antibacterial and enzymatic modulation, BG provides sustained mineral release and buffering capacity. Such synergy could limit bacterial colonization, neutralize acidic conditions, stabilize collagen, and facilitate apatite formation, thereby enhancing the long-term durability of adhesive interface under cariogenic challenge.

Accordingly, this study evaluated the effects of incorporating ZnO/Cu and BG nanoparticles into a universal adhesive on MMP activity, mineral deposition, nanoleakage and bond strength under cariogenic challenge. The null hypotheses were that: (1) nanoparticle modification would not influence bond strength and nanoleakage after cariogenic challenge; (2) incorporation of ZnO/Cu and BG would not inhibit enzymatic activity within the hybrid layer; and (3) modified adhesives would not increase mineral deposition at the resin–dentin interface compared with the unmodified adhesive.

Materials and methods

Matrix metalloproteinase (MMP) activity was characterized using in situ enzymatic assays, while mineralization was characterized using simulated body fluid (SBF) immersion. NL and μTBS were assessed before and after cariogenic challenge to assess adhesive durability.

Preparation of nanoparticle-modified adhesives

A commercial universal adhesive (Ambar Universal, FGM Dental Group, Joinville, SC, Brazil) served as the base resin for all experimental formulations. Five groups were prepared: Control (0%) – unmodified adhesive; ZnO/Cu – 2.5 wt% ZnO + 0.2 wt% Cu; 5%BG + ZnO/Cu – 5 wt% BG + 2.5 wt% ZnO + 0.2 wt% Cu;

10%BG + ZnO/Cu – 10 wt% BG + 2.5 wt% ZnO + 0.2 wt% Cu; and 10%BG – 10 wt% BG. Nanoparticles were manually mixed and then ultrasonically dispersed at 25 °C for 10 min in light-protected conditions. Nanoparticles were manually premixed and subsequently ultrasonically dispersed using an ultrasonic bath (Ultrasonic Cleaner, Unique®, Indaiatuba, Brazil) operating at 40 kHz at room temperature (25 °C) for 10 min under light-protected conditions. Each experimental formulation was prepared using a standardized volume of adhesive sufficient for all specimens within the corresponding experimental group. Phase separation was visually monitored immediately after preparation and prior to application, and no macroscopic segregation was observed.

Tooth Preparation and bonding procedures

All third molars were erupted teeth extracted for orthodontic or prophylactic reasons. Donor age ranged between 18 and 30 years. Teeth presenting caries, restorations, cracks, or structural defects were excluded. Eighty sound human third molars extracted within the six months were disinfected in 0.5% chloramine and stored in distilled water. Occlusal enamel was removed using 180-grit silicon carbide (SiC) paper under continuous water irrigation in a polishing machine (Arotec APL-4, São Paulo, Brazil) operating at 300 rpm to expose flat mid-coronal dentin. Lateral enamel was removed with a #4137 cylindrical diamond bur (KG Sorensen, Barueri, SP, Brazil). The exposed dentin surfaces were further polished on wet # 600-grit silicon–carbide paper for 60 s to standardize the smear layer [13].

Teeth were randomly assigned to two bonding strategies: ER or SE (n = 8 per group). Adhesives were applied following the manufacturer's instructions (Table 18). In ER mode, dentin was etched with 37% phosphoric acid for 15 s (Condac, FGM Dental Group, Joinville, SC, Brazil), rinsed for 15 s, and gently air–dried to keep moist dentin. Composite increments were light-cured for 20 s using a multiwavelength LED curing unit (VALO, Ultradent, South Jordan, UT, USA) operated in standard mode. Irradiance output was periodically verified using a calibrated radiometer, and the reported energy values correspond to measured output at the curing tip [13]. Specimens were stored for 24 h at 37 °C and sectioned with a diamond saw (Isomet 1000, Buehler, Lake Bluff, IL, USA) into sticks with ~ 0.8 ± 0.1 mm² cross-sectional area verified by digital caliper (Mitutoyo, Tokyo, Japan). All bonding procedures were performed by a single calibrated operator to minimize technique-related variability. Incremental layering of 1 mm was intentionally selected to ensure optimal light

penetration, minimize polymerization stress, and standardize curing conditions across experimental groups.

Universal Adhesive/ Batch numbers	Composition	Adhesive strategy	
		Etch-and-rinse mode	Self-etch mode
Ambar Universal (FGM Dental Group, Joinville, Santa Catarina, Brazil) / (080622,070722,030321,0303, 210323)	10-MDP*, methacrylate monomers, APS**, co-initiators, stabilizers, inertload (silica particles) and ethanol. Density: 1.07 g/cm³.	1. Apply phosphoric acid for 15 s. 2. Wash the surface with plenty of water and dry the cavity so that the dentin does not get dehydrated, but without the accumulation of water on the surface. 3. Apply a first layer vigorously rubbing the adhesive with the micro applicator for 10 s. 4. Next, apply a second layer of adhesive for 10 s, spreading the product. 5. Evaporate excess solvent by thoroughly air-drying with an air syringe for 10 s. 6. Light cure for 10 s at 1200 mW/cm^2.	1. Apply a first layer vigorously rubbing the adhesive with the micro applicator for 10 s. 2. Apply a second layer of adhesive for 10 s, spreading the product. 3. Evaporate excess solvent by thoroughly air-drying with an air syringe for 10 s. 4. Light cure for 10 s at 1200 mW/cm^2.

Tabela 18. Universal adhesive system and batch number; composition and adhesive strategy.

**10-MDP: 10- metacryloyloxydecyldihidrogen phosphate; **APS: advanced photoinitiators complex.*

Cariogenic challenge

A validated in vitro cariogenic challenge was used [24]. Approximately 6 resin–dentin bonded sticks per tooth were sterilized (121 °C, 15 min) and immersed in 1.5 mL cariogenic medium (9.25 g BHI broth, 1.25 g yeast extract, and 5 g sucrose in 250 mL water) inoculated with 100 mL of Streptococcus mutans (ATCC 25175) adjusted to ~ 5.0×10^6 CFU/mL. Samples were incubated at 37 °C under microaerophilic conditions for five days; medium was replaced every 48 h. Final pH was ≈ 4.0. Autoclave sterilization was selected to ensure complete microbial inactivation prior to biofilm formation, as previously validated in resin–dentin bond durability studies [24]. Although high temperature may affect exposed collagen, all groups were subjected to identical conditions, and previous evidence indicates that relative intergroup comparisons remain valid under this protocol.

Microtensile bond strength (μTBS)

Resin-dentin bonded sticks were fixed to testing jigs with cyanoacrylate adhesive (Loctite Superbonder, Henckel, Brazil) and tested under tension at 0.5 mm/min, and a 20 Kgf load cell until failure in a universal testing machine (Kratos, Cotia, SP, Brazil). Bond strength was expressed in MPa. Ethical approval was granted from the institutional human research ethics committee of local university (Protocol No. 5.395.921). Sample size calculation followed Academy of Dental Materials guidelines [25, 26] and previous μTBS studies [27, 28]. Preparing at least 10 sticks per tooth and using eight teeth per group provided 80% statistical power to detect significant intergroup differences ($\alpha = 0.05$). All μTBS tests were performed under controlled laboratory conditions (23 ± 2 °C), and crosshead speed calibration was verified before testing.

Nanoleakage (NL)

Resin–dentin bonded sticks (n = 4/group/time-point) were coated with two nail-varnish layers leaving 1 mm around the bonded interfaces exposed. They were then immersed in a 50 wt% ammoniacal silver nitrate solution for 24 h in darkness, rinsed, and developed in photographic solution for 8 h under fluorescent light.

Samples were mounted on aluminum stubs and sequentially polished with 1000–4000 grit SiC papers, followed by polishing 1.0 μm and 0.25 μm diamond pastes

(Buehler Ltd., Lake Bluff, IL, USA). Specimens were then ultrasonically cleaned, air-dried, dehydrated in colloidal silica for 24 h, and gold-sputter coated (MED 010, Balzers Union, Balzers, Liechtenstein).

The resin–dentin interfaces were examined using a SEM in backscattered electron mode at 12 kV (VEGA 3, TESCAN, Shimadzu, Tokyo, Japan). Three images were captured per specimen: one at the center of the bonded interface and two images taken 0.3 mm to the left and right of this point. All images were analyzed by a blinded operator. Nanoleakage was quantified as the percentage of silver infiltration within the adhesive and hybrid layers using ImageJ software (NIH, Bethesda, MD, USA). This nanoleakage protocol and quantitative image analysis approach is consistent with previously established method [27, 29]. All images were analyzed by a blinded operator. Intraoperator repeatability was verified by repeated measurements in a subset of specimens, showing high consistency.

Inhibition of proteolytic activity (MMPs)

In situ zymography was performed to assess inhibition of endogenous MMPs. Thirty restored teeth (n = 3/group/ adhesive strategy) were sectioned into 0.4 mm discs (Isomet 5000, Buehler, IL, USA) and polished to a final thickness of 300 μm. Discs were incubated for 7 days in fluorescein-conjugated gelatin (EnzChek Gelatinolytic/Collagenolytic Kit, Thermo Fisher), following the protocol described by Mazzoni et al. [9]. Hydrolysis, indicating gelatinolytic activity, was analyzed using multiphoton confocal laser scanning microscopy (CLSM; Leica TCS SP8 MP, Leica Microsystems, Wetzlar, Germany; excitation 488 nm, emission > 530 nm). Optical Sect. (20 μm) was captured, and fluorescence intensity was quantified with LAS X software (Leica Microsystems, Wetzlar, Germany). Mean fluorescence values from eight discs per group was used to calculate MMPs inhibition rates. Untreated dentin surfaces were included as internal negative controls during CLSM acquisition. Detector gain and acquisition parameters were fixed and maintained constant for all specimens to allow valid intergroup comparisons.

Simulated body fluid assay

Discs from Sect. 2.4 (n = 2/group/ adhesive strategy) were immersed in SBF [30] for 14 or 28 days to evaluate mineral deposition. Surface characterization and elemental analysis were performed using SEM coupled with energy-dispersive X-ray spectroscopy (SEM-EDX, JSM-IT300LV, JEOL, Tokyo, Japan) to quantify Ca and P

content. Elemental composition was determined by averaging three random points per sample, and values were reported as mean weight percentages.

Statistical analysis

Statistical analyses were performed using SPSS 28.0 (IBM Corp., Armonk, NY, USA). Normality (Shapiro–Wilk) and variance homogeneity (Levene's test) were verified prior analysis. μTBS and NL data were analyzed using two-way ANOVA (factors: adhesive formulation and bonding strategy), followed by Tukey's post hoc test. Paired t-tests were used to compare baseline and post-challenge μTBS values within each group. In situ zymography and Ca/P data were analyzed by one-way ANOVA. Statistical significance was set at $p < 0.05$.

Results

At baseline, all experimental adhesives successfully established resin–dentin bonds. Under the SE strategy, no significant differences in μTBS were observed among groups ($p > 0.05$). Mean baseline μTBS values are reported in Table 19 and showed no significant differences among groups under the SE strategy ($p > 0.05$).

Tabela 19. Microtensile bond strength (μTBS) at baseline and after cariogenic challenge

Groups	SE			ER		
	μTBS (MPa)			μTBS (MPa)		
	Baseline	Challenged	Reduction (%)	Baseline	Challenged	Reduction (%)
Control	40 ± 1.5 A	26.6 ± 1.0 B	-33.5*	44,8 ±0.52 A	25.8 ± 3.6 B	-42.4*
ZnO/Cu	44.1 ± 10.7 A	34.3 ± 4.3 A	-22.2	51,9 ± 5,9 A	32.6 ± 1.7 A	-37.1*
5%BG+ZnO/ Cu	49,1 ± 2.9 A	36.8 ± 1.7 A	-25.0*	46.8 ± 2.4 A	35 ± 2.7 A	-25.4*
10%BG+ZnO/ Cu	37.4 ± 3.8 A	32.6 ± 5.2 AB	-12.8	35.2 ± 3.7 B	32.8 ± 2.6 A	-6.9
10%BG	39.9 ± 1.3 A	30.8 ± 4.6 AB	-23.0*	37.3 ± 2.17 B	29.9 ± 2.5 A	-19.8*

Legend: Different capital letters indicate statistically significant differences among groups within each adhesive strategy and time condition ($p < 0.05$). * Indicates statistically significant reduction of μTBS after cariogenic challenge. ($p < 0.05$). No

statistically significant differences were found among SE and ER strategies ($p > 0.05$). Mean ± SD: standard deviation; SE: self-etch; ER: etch and rinse

Microtensile bond strength after cariogenic challenge

After five days of cariogenic biofilm exposure, a marked decrease in μTBS was observed for the control group. ER specimens lost 42.4% of their initial μTBS, while SE specimens decreased by 33.5% (Table 2).

Adhesives containing nanoparticles exhibited significantly better preservation of μTBS. The ZnO/Cu group retained higher μTBS values than the control, maintaining values in ER mode (− 22.2%), although a significant reduction was still observed under SE mode (− 37.1%).

The 5%BG + ZnO/Cu group maintained μTBS values close to baseline, with reductions of approximately 25%. The 10%BG showed moderate but significant decreases (− 23.0% SE; −19.8% ER). Notably, the 10BG + ZnO/Cu adhesive preserved μTBS almost entirely, with decreases of only 6.9% (ER) and 12.8% (SE), which did not differ significantly from baseline ($p > 0.05$).

Nanoleakage (NL) at baseline

At baseline, with the SE strategy, significant differences were detected among groups ($p = 0.001$). The control and ZnO/Cu groups exhibited the lowest NL values (1.93 ± 0.4% and 2.05 ± 1.2%, respectively). The 5%BG + ZnO/Cu and 10%BG + ZnO/Cu groups demonstrated intermediate values (2.93 ± 0.6% and 3.14 ± 0.4%), while 10%BG exhibited significantly higher NL (4.05 ± 0.6%) (Table 20). For the ER strategy, no significant differences were found among groups at baseline ($p = 0.053$). Representative SEM images of nanoleakage patterns and nanoparticle characterization (SEM, EDX, and FTIR) are provided as Supplementary Figures.

Tabela 20. Nanoleakage (NL) at baseline and after cariogenic challenge.

Groups	SE			ER		
	NL (%)			NL (%)		
	Baseline	Challenged	Increase (%)	Baseline	Challenged	Increase (%)
Control	1.93 ± 0.4 B	9.62 ± 1.1 A	+398.4	2.09 ±0.6 A	9.06 ± 0.8 A	+333.5
ZnO/Cu	2.05 ± 1.2 B	7.41 ± 1.1 AB	+261.5	2.52 ± 1.4 A	7.69 ± 1.6 AB	+205.28
5%BG+ZnO/Cu	2.93 ± 0.6 AB	5.52 ± 0.7 C	+88.4	2.87 ± 0.6 A	5.87 ± 0.8 C	+104.5
10%BG+ZnO/Cu	3.14 ± 0.4 AB	6.49 ± 1.9 BC	+106.6	3.17 ± 0.9 A	6.57 ± 0.6 BC	+107.3
10%BG	4.05 ± 0.6 A	7.38 ± 1.6 AB	+82.2	3.60 ± 0.5 A	7.33 ± 1.5 AB	+103,6

Legend: Different capital letters indicate statistically significant differences among groups within each adhesive strategy and time condition ($p < 0.05$). No statistically significant differences were found among SE and ER strategies ($p > 0.05$). Mean ± SD: standard deviation; SE: self-etch; ER: etch and rinse.

Nanoleakage (NL) after cariogenic challenge

After cariogenic challenge, significant differences in NL were observed among groups for both application strategies. For SE, the control group exhibited the highest NL (9.62 ± 1.1%)., whereas 5%BG + ZnO/Cu group showed the lowest NL (5.52 ± 0.7%; $p < 0.001$). The 10%BG + ZnO/Cu, ZnO/Cu, and 10%BG groups presented intermediate values (Table 20).

A similar trend was observed under ER ($p < 0.001$). All group showed significant increases in NL after the cariogenic challenge ($p < 0.05$). The magnitude of increase varied: BG-containing groups displayed consistently lower NL increments. The 10%BG-SE group demonstrated the lowest NL increase (82.2%), followed by 5%BG + ZnO/Cu-SE (88.4%) and 10%BG + ZnO/Cu (106.6%). ZnO/Cu showed higher increases (205.2-261.5%), while the control group exhibited the greatest rise (333.5-398.4%) (Table 20).

Inhibition of Enzymatic Proteolytic Activity

Under SE, all groups exhibited high enzymatic activity, with only a slight reduction for 10%BG group. Under ER strategy, intense gelatinolytic activity was observed in the control and BG-only groups. The ZnO/Cu and 10%BG + ZnO/Cu groups showed visibly reduced fluorescence within the hybrid layer and adjacent dentin, suggesting partial, but not complete, MMP inhibition (Fig. 1). One-way ANOVA

revealed significant differences in gelatinolytic activity among groups under the ER strategy ($p < 0.01$), but not under the SE strategy ($p = 0.21$). Post hoc analysis showed that the ZnO/Cu and 10%BG + ZnO/Cu groups exhibited significantly lower fluorescence intensity compared with the control under ER mode ($p < 0.05$), whereas no statistically significant inhibition was observed for BG-only formulations.

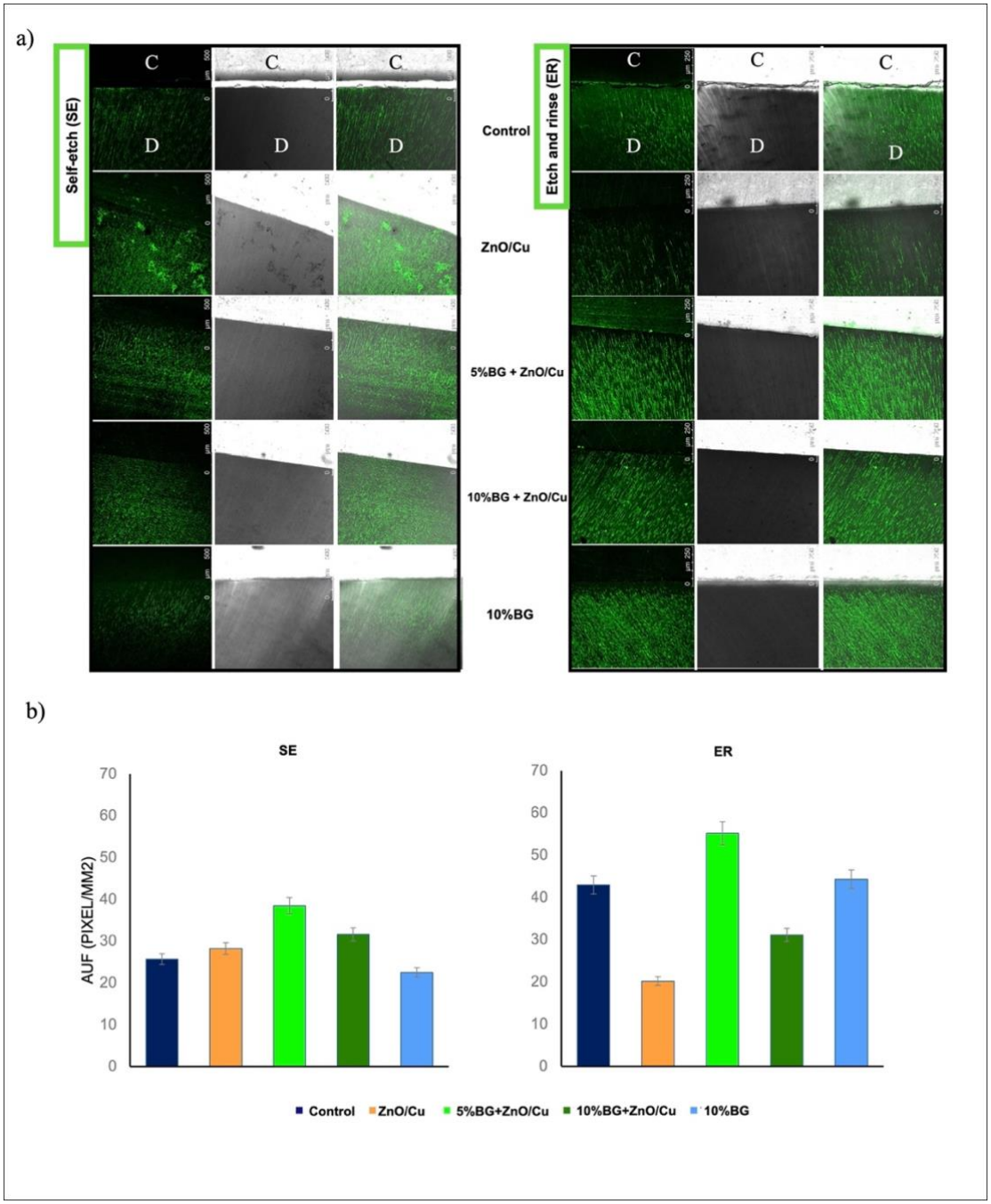

Figura 16. Confocal laser scanning microscopy (CLSM) images of resin-dentin adhesive interfaces

Confocal laser scanning microscopy (CLSM) images of resin-dentin adhesive interfaces (a) Representative CLMS images after 7 days of incubation in fluorescein-labeled gelatin. The left column shows green fluorescence indicating gelatinolytic activity; the middle column presents differential interference contrast (DIC) images identifying dentin; and the right column displays merged images. Two adhesive strategies were evaluated: ER = etch-and-rinse; SE = self-etch. High enzymatic activity was observed in all groups, although fluorescence intensity was reduced in the ZnO/Cu and 10% BG + ZnO/Cu groups under ER mode. (b) Relative fluorescence quantification corresponding to CLSM images, expressed as mean ± standard deviation in arbitrary fluorescence units (AFU; n = 3). Only the ZnO/Cu and 10% BG + ZnO/Cu groups showed lower fluorescence intensity within the hybrid layer and adjacent dentin.

Mineral deposition at the hybrid layer

SEM after immersion in SBF revealed clear differences after 28 days. Control and ZnO/Cu groups exhibited smooth hybrid layers without noticeable mineral clusters. In contrast, BG-containing adhesives showed progressive deposition of calcium–phosphate (Ca–P) nodules. Small spherical deposits were present in the 5%BG + ZnO/Cu and 10%BG groups, whereas dense, fused mineral layers resembling apatite were observed in the 10%BG + ZnO/Cu group. EDX confirmed increased Ca and P levels at the adhesive–dentin interface, with the highest Ca/P ratios in the 10%BG + ZnO/Cu group, approaching hydroxyapatite stoichiometry (Fig. 2).

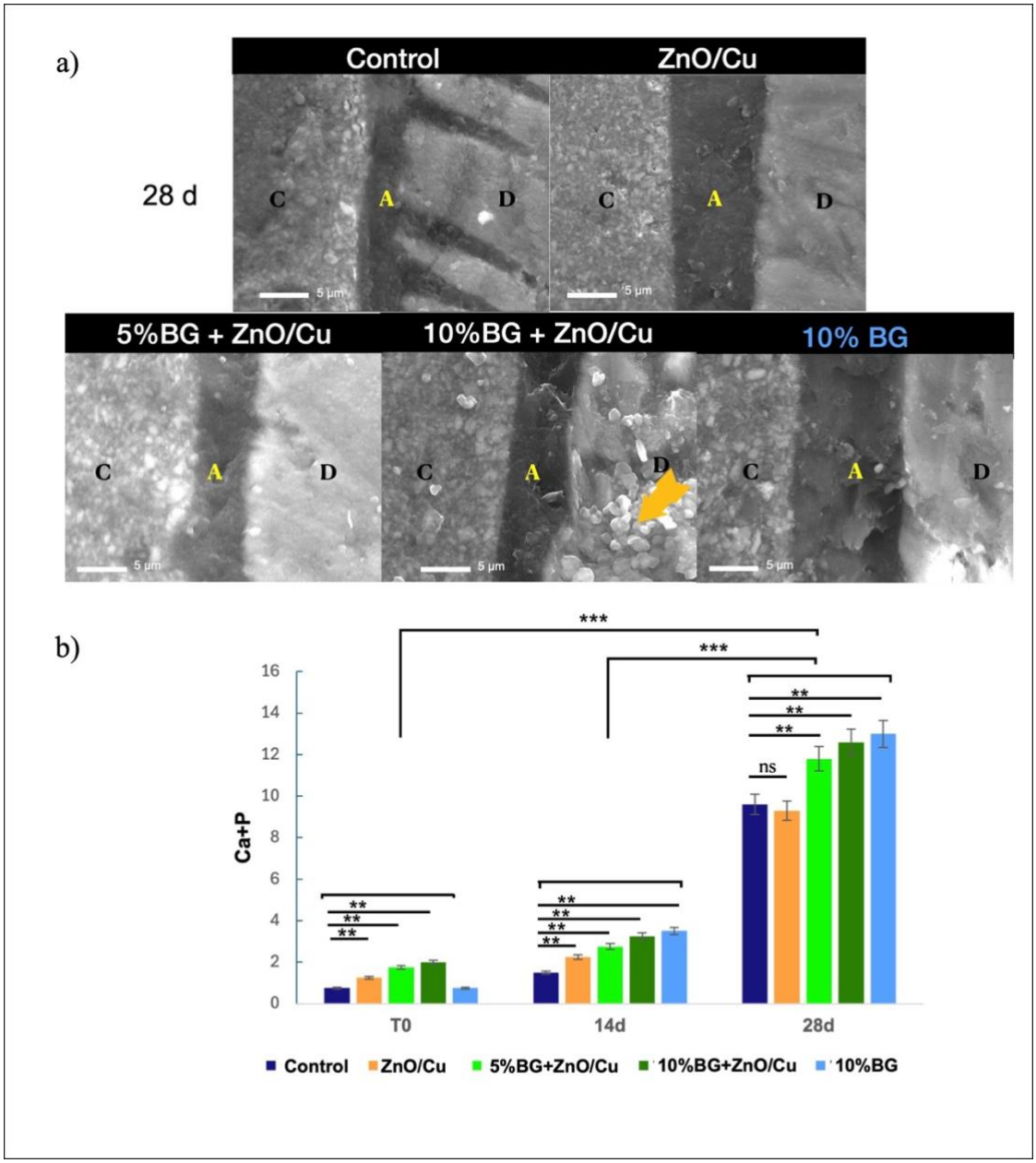

Figura 17. Mineralization at the hybrid layer evaluated by SEM and EDX

Mineralization at the hybrid layer evaluated by SEM and EDX. (a) SEM micrographs (4000×) showing the resin–dentin adhesive interface after 28 days of immersion in simulated body fluid. A: adhesive; D: dentin; C: resin composite. Yellow arrows indicate mineral deposits within the hybrid layer. (b) Calcium (Ca%) and phosphorus (P%) content at the hybrid layer surface at baseline (T_0), 14 days and 28 days. Data are expressed as mean ± standard deviation. Significant differences were detected among time points and between experimental groups at 14 and 28 days ($p < 0.05$*, $p < 0.001$**, $p < 0.0001$***), compared with the control group at the same time point.

Discussion

The first and third null hypotheses were rejected, whereas the second hypothesis regarding consistent MMP inhibition could not be rejected. Incorporating ZnO, Cu, and BG nanoparticles into the universal adhesive improved its biological performance, as evidenced by increased mineral deposition at resin–dentin bonded interface, improved preservation of bond strength, and reduced nanoleakage after the cariogenic challenge compared with the control group. Although variations in MMPs activity were observed depending on the adhesive strategy, a consistent inhibitory effect was not detected. Overall, these modifications contributed to greater interfacial stability, suggesting improved resistance to hydrolytic and acid-mediated degradation.

The mechanical properties of resin-based materials are strongly influenced by filler-related parameters, including concentration, morphology, and particle size[31]. In this study, μTBS was affected by the interaction between adhesive strategy, and composition, as well as resistance to acidic challenge. These findings align with previous studies highlighting the role of nanoparticles in reinforcing adhesives and improving their resistance to degradation[33].

Regarding adhesive strategies and μTBS, the ER technique appeared more sensitive to adhesive composition, likely due to deeper demineralization and increased exposure of collagen fibrils, which accentuate compositional differences 7, 8, 32]. Conversely, the SE approach produced no significant differences among groups at baseline, suggesting that milder demineralization reduces the effect of compositional variations [33].

While fillers typically reinforce resin matrices by improving stress distribution and crack deflection [31]. BG nanoparticles behave differently because they are not chemically bond to the resin matrix. Their contribution is therefore concentration-dependent and may become detrimental at excessive levels [34]. In this study, BG was limited to 10 wt% in accordance with previous recommendations [31]. Similarly, ZnO content was reduced compared with earlier studies [27, 33] to optimize dispersion and minimize aggregation.

Under the ER strategy, the ZnO/Cu and 5%BG + ZnO/Cu groups maintained initial μTBS values comparable to the control. Conversely, higher BG concentrations (10%BG and 10%BG + ZnO/Cu) reduced initial μTBS in the ER strategy, indicating potential weakening of the interface at elevated concentrations. The superior

performance of ZnO/Cu and 5%BG + ZnO/Cu may be attributed to the catalytic effect of Cu, which promotes collagen cross-linking and polymer network reinforcement [19]; however, this effect may be attenuated at higher BG due to ion chelation.

After cariogenic challenge, the 10%BG + ZnO/Cu formulation demonstrated the most favorable balance between initial performance and long-term stability. This effect can be attributed to the capacity of BG to buffer acidic conditions and induce localized remineralization, forming an apatite-like layer similar to dentin that reinforces the hybrid layer [35]. These findings support a synergistic interaction between nanoparticles. The same BG concentration alone also improved long-term outcomes, although less consistent manner. Meanwhile, the ZnO/Cu formulation maintained μTBS under the SE conditions but showed reduced performance under ER, reinforcing the influence of the bonding strategy on the behavior of nanoparticle-modified adhesives.

NL findings paralleled the μTBS results. At baseline, significant differences were found only under the SE strategy, with the 10% BG group showing higher NL. This underscores the relevance of ZnO/Cu in achieving immediate interfacial integrity, as previously reported [33]. Following the cariogenic challenge, BG-containing adhesives exhibited lower NL values and greater stability, whereas the control group showed extensive silver uptake. These findings suggest distinct yet complementary protective mechanisms: ZnO/Cu nanoparticles preserve structural integrity through synergistic antimicrobial and enzymatic modulation, while BG promotes mineral precipitation, sealing microdefects over time. The statistical similarity between SE and ER strategies reinforces that the protective effects are not dependent on the bonding approach, supporting their clinical versatility.

Together, μTBS and NL results indicate that ZnO and Cu nanoparticles provide mechanical and biological reinforcement, including antibacterial benefits [30], while BG, provides sustained remineralization, acid buffering, and micro-defect sealing [36]. The combined action in the 10%BG + ZnO/Cu formulation created a ion-releasing microenvironment capable of integrating complementary protective mechanisms and delivering durable performance. The slightly lower baseline μTBS observed for the 10%BG + ZnO/Cu group under the ER strategy is likely related to the higher filler content, which may partially interfere with initial resin infiltration and polymer network formation. Importantly, despite this initial reduction, this formulation demonstrated the greatest resistance to degradation after cariogenic challenge, indicating a trade-off between immediate bond strength and long-term interfacial stability.

MMPs are zinc-dependent endopeptidases implicated in hybrid layer degradation and loss of bond durability [11]. Controlling MMP activity therefore represents a promising strategy [37]. Although metallic ions, particularly Cu and Zn, have been shown to modulate MMPs activity [18, 27, 36], and BG may indirectly inhibit these enzymes by increasing the local pH beyond their optimal activity range [36]. In this study the in situ zymography results revealed high MMP activity across all groups. Only the ZnO/Cu and 10%BG + ZnO/Cu groups under the ER strategy showed a slight reduction. The absence of a consistent inhibitory effect likely reflects concentration- and time-dependent limitations. BG requires ionic release, and the short-term evaluation period may not have reached the critical pH threshold (> 8.5necessary for substantial enzymatic suppression [36].

Similarly, the ZnO concentration used (2.5 wt%) was probably insufficient for effective enzymatic inhibition, as higher concentrations (≥ 5 wt%) have shown dose-dependent suppression [27, 33]. In addition, possible chelation interactions between BG and metallic ions may have reduced the availability of Cu and Zn, thereby limiting their bioactivity. Future formulations should therefore optimize nanoparticle ratios and extend evaluation periods to more accurately assess enzymatic modulation.

The mineralization assays further supported the biologically mediated potential of BG-modified adhesives. SEM and EDX analyses showed increased Ca and P deposition within the hybrid layer, especially after 28 days, confirming ionic release and mineral nucleation. Although mineral precipitates were not consistently observed on the adhesive surface, the localized accumulation at the interface suggests inward ion migration and effective biomimetic remineralization [38].

Clinically, these results are relevant because secondary caries remain the primary cause of restoration replacement, responsible for over 50% of failures [4]. The enhanced bond stability and reduced nanoleakage observed in BG- and ZnO/Cu-modified adhesives support their potential to extend restoration longevity, particularly in patients at increased caries risk. Adhesive formulations that integrate antibacterial effects, modulation of endogenous enzymatic activity, and sustained ion release may reduce the frequency of retreatment, limit associated biological and economic costs and improve long-term clinical outcomes. The use of a universal adhesive platform further increases clinical applicability by enabling both self-etch and etch-and-rinse strategies. Although higher BG loadings resulted in a modest reduction in initial μTBS

under etch-and-rinse conditions, this effect was offset by superior bond preservation over time. Collectively, these findings suggest that optimizing adhesive formulations for long-term interfacial stability, rather than maximizing immediate bond strength alone, may offer greater clinical benefit.

This study has limitations. It was conducted in vitro using a simplified S. mutans biofilm model, whereas clinical biofilms are polymicrobial and more complex. The cariogenic challenge lasted only five days; extended or cyclic challenges would better replicate intraoral conditions. Although SEM/EDX confirmed mineral deposition, complementary methods such as X-ray diffraction or Raman spectroscopy would help confirm apatite crystallinity. Additionally, only short-term μTBS was assessed; future studies should include thermocycling or prolonged water storage to assess aging effects. The degree of conversion, water sorption, and solubility were not assessed in the present study and therefore represent additional limitations that should be addressed in future investigations. Finally, optimal nanoparticle concentrations remain to be established, as excessive loadings may influence viscosity, monomer diffusion, and polymerization behavior.

Future investigations should refine nanoparticle ratios to maximize synergistic effects without compromising handling or interfacial infiltration. Experimental models incorporating multispecies biofilms, extended cariogenic cycles, and mechanical aging will yield more clinically relevant outcomes. In vivo studies and ion-release kinetics analyses are also necessary to confirm translational potential and elucidate the underlying bioactive mechanisms.

Conclusion

This in vitro study demonstrated that incorporating ion-modified nanoparticles into a universal adhesive improved resin–dentin bond durability after five days of Streptococcus mutans biofilm exposure. The 10 wt% BG + ZnO/Cu formulation preserved bond strength, reduced nanoleakage, modulated enzymatic activity, and promoted calcium–phosphate deposition at the hybrid layer. These ion-mediated effects enhanced interfacial stability and resistance to hydrolytic and biofilm-induced degradation.

References

[1] Ferracane JL. Resin composite—state of the art. Dent Mater. 2011;27(1):29–38. https://doi.org/10.1016/j.dental.2010.10.020

[2] Josic U, D'Alessandro C, Miletic V, Maravic T, Mazzitelli C, Jacimovic J, Sorrentino R, Zarone F, Mancuso E, Delgado AH, Breschi L, Mazzoni A (2023) Clinical longevity of direct and indirect posterior resin composite restorations: an updated systematic review and meta-analysis. Dent Mater 39(12):1085–1094. https://doi.org/10.1016/j.dental.2023.10.009

[3] Demarco FF, Collares K, Coelho-de-Souza FH, Correa MB, Cenci MS, Moraes RR, Opdam NJ (2015) Anterior composite restorations: a systematic review on long-term survival and reasons for failure. Dent Mater 31(10):1214–1224. https://doi.org/10.1016/j.dental.2015.07.005

[4] Askar H, Krois J, Göstemeyer G, Schwendicke F (2021) Secondary caries risk of different adhesive strategies and restorative materials in permanent teeth: systematic review and network meta-analysis. J Dent 104:103541. https://doi.org/10.1016/j.jdent.2020.103541

[5] Matos AB, Trevelin, LT, Silva BTFD, Francisconi-Dos-Rios LF, Siriani LK, Cardoso MV(2017) Bonding efficiency and durability: current possibilities. Braz Oral Res. 31(Suppl 1):e57. https://doi.org/10.1590/1807-3107BOR-2017.vol31.0057

[6] Nakabayashi N, Nakamura M, Yasuda N (1991) Hybrid layer as a dentin-bonding mechanism. J Esthet Dent 3(4):133–138. https://doi.org/10.1111/j.1708-8240.1991.tb00985.x

[7] Van Meerbeek B, Yoshihara K, Van Landuyt K, Yoshida Y, Peumans M (2020) From buonocore's pioneering acid-etch technique to self-adhering restoratives: a status perspective of rapidly advancing dental adhesive technology. J Adhes Dent 22(1):7–34. https://doi.org/10.3290/j.jad.a43994

[8] Pashley DH, Tay FR, Breschi L, Tjäderhane L, Carvalho RM, Carrilho M, Tezvergil-Mutluay A (2011) State of the Art etch-and-rinse adhesives. Dent Mater 27(1):1–16. https://doi.org/10.1016/j.dental.2010.10.016

[9] Mazzoni A, Mannello F, Tay FR, Tonti GA, Papa S, Mazzotti G, Di Lenarda R, Pashley DH, Breschi L (2007) Zymographic analysis and characterization of MMP-2 and −9 forms in human sound dentin. J Dent Res 86(5):436–440. https://doi.org/10.1177/154405910708600509

[10] Mazzoni A, Tjäderhane L, Checchi V, Di Lenarda R, Salo T, Tay FR, Pashley DH, Breschi L (2015) Role of dentin MMPs in caries progression and bond stability. J Dent Res 94(2):241–251. https://doi.org/10.1177/0022034514562833

[11] Tjäderhane L, Nascimento FD, Breschi L, Mazzoni A, Tersariol IL, Geraldeli S, Tezvergil-Mutluay A, Carrilho MR, Carvalho RM, Tay FR, Pashley DH (2013) Optimizing dentin bond durability: control of collagen degradation by matrix metalloproteinases and cysteine cathepsins. Dent Mater 29(1):116–135. https://doi.org/10.1016/j.dental.2012.08.004

[12] Schwendicke F, Al-Abdi A, Pascual Moscardó A, Ferrando Cascales A, Sauro S (2019) Remineralization effects of conventional and experimental ion-releasing materials in chemically or bacterially-induced dentin caries lesions. Dent Mater 35(5):772–779. https://doi.org/10.1016/j.dental.2019.02.021

[13] Vidal O, de Paris Matos T, Núñez A, Méndez-Bauer L, Sutil E, Ñaupari-Villasante R, Souta MC, Pitlovanciv M, Gutiérrez MF, Loguercio AD (2022) A

universal adhesive containing copper nanoparticles improves the stability of hybrid layer in a cariogenic oral environment: an in-situ study. J Mech Behav Biomed Mater 126:105017. https://doi.org/10.1016/j.jmbbm.2021.105017

[14] Reis A, Carrilho M, Breschi L, Loguercio AD (2013) Overview of clinical alternatives to minimize the degradation of the resin-dentin bonds. Oper Dent 38(4):E1–E25. https://doi.org/10.2341/12-258-LIT

[15] Cadenaro M, Josic U, Maravić T, Mazzitelli C, Marchesi G, Mancuso E, Breschi L, Mazzoni A (2023) Progress in dental adhesive materials. J Dent Res 102(3):254–262. https://doi.org/10.1177/00220345221145673

[16] Breschi L, Mazzoni A, Nato F, Carrilho M, Visintini E, Tjäderhane L, Ruggeri A Jr, Tay FR, Dorigo Ede S, Pashley DH (2010) Chlorhexidine stabilizes the adhesive interface: a 2-year in vitro study. Dent Mater 26(4):320–325. https://doi.org/10.1016/j.dental.2009.11.153

[17] Jandt KD, Watts DC (2020) Nanotechnology in dentistry: present and future perspectives on dental nanomaterials. Dent Mater 36(11):1365–1378. https://doi.org/10.1016/j.dental.2020.08.006

[18] Toledano M, Yamauti M, Ruiz-Requena ME, Osorio R (2012) A ZnO-doped adhesive reduced collagen degradation favouring dentine remineralization. J Dent 40(9):756–765. https://doi.org/10.1016/j.jdent.2012.05.007

[19] Gutiérrez MF, Alegría-Acevedo LF, Méndez-Bauer L, Bermudez J, Dávila-Sánchez A, Buvinic S, Hernández-Moya N, Reis A, Loguercio AD, Farago PV, Martin J, Fernández E (2019) Biological, mechanical and adhesive properties of universal adhesives containing zinc and copper nanoparticles. J Dent 82:45–55. https://doi.org/10.1016/j.jdent.2019.01.012

[20] Josic U, Teti G, Ionescu A, Maravic T, Mazzitelli C, Cokic S, Van Meerbeek B, Falconi M, Brambilla E, Mazzoni A, Breschi L (2024) Cytotoxicity and Microbiological behavior of universal resin composite cements. Dent Mater 40(10):1515–1523. https://doi.org/10.1016/j.dental.2024.07.004

[21] Skallevold HE, Rokaya D, Khurshid Z, Zafar MS (2019) Bioactive glass applications in dentistry. Int J Mol Sci 20(23):5960. https://doi.org/10.3390/ijms20235960

[22] Abuna G, Campos P, Hirashi N, Giannini M, Nikaido T, Tagami J, Coelho Sinhoreti MA, Geraldeli S (2021) The ability of a nanobioglass-doped self-etching adhesive to re-mineralize and bond to artificially demineralized dentin. Dent Mater 37(1):120–130. https://doi.org/10.1016/j.dental.2020.10.026

[23] Covarrubias C, Arroyo F, Balanda C, Neira M, von Marttens A, Caviedes P, Rodríguez JP, Urra C (2015) The effect of the nanoscale structure of nanobioceramics on their in vitro bioactivity and cell differentiation properties. J Nanomater 526230. https://doi.org/10.1155/2015/526230

[24] de Alencar NA, Fidalgo TK, Cajazeira MR, Maia LC (2014) Influence of the number of adhesive layers on adhesive interface properties under cariogenic challenge using Streptococcus mutans. J Adhes Dent 16(4):339–346. https://doi.org/10.3290/j.jad.a32569

[25] Ferracane JL, Hilton TJ, Stansbury JW, Watts DC, Silikas N, Ilie N, Heintze S, Cadenaro M, Hickel R (2017) Academy of dental materials guidance-Resin composites: part II-Technique sensitivity (handling, polymerization, dimensional changes). Dent Mater 33(11):1171–1191. https://doi.org/10.1016/j.dental.2017.08.188

[26] Ilie N, Hilton TJ, Heintze SD, Hickel R, Watts DC, Silikas N, Stansbury JW, Cadenaro M, Ferracane JL (2017) Academy of dental materials guidance-Resin

composites: part I-Mechanical properties. Dent Mater 33(8):880–894. https://doi.org/10.1016/j.dental.2017.04.013

[27] Basualdo Allende J, Nascimento FD, Damasceno E, Souza Chiari M, Aliaga-Galvez R, Ñaupari-Villasante R, Miranda CB, Pardo-Díaz C, Gutiérrez MF, Covarrubias C, Loguercio AD, Fernández E (2024) Evaluation of adhesive properties and enzymatic activity at the hybrid layer of a simplified adhesive loaded with 0.2% Cu and 5% ZnO nanoparticles: A randomized clinical trial and ex vivo analysis. J Dent 149:105283. https://doi.org/10.1016/j.jdent.2024.105283

[28] Sahadi BO, Sebold M, André CB, Nima G, Dos Santos A, Chiari MDESC, Nascimento FD, Tersariol ILDS, Giannini M (2024) Effect of experimental dentin etchants on dentin bond strength, metalloproteinase inhibition, and antibiofilm activity. Dent Mater 40(4):e12–e23. https://doi.org/10.1016/j.dental.2024.02.017

[29] Hass V, Dobrovolski M, Zander-Grande C, Martins GC, Gordillo LA, Rodrigues Accorinte Mde L, Gomes OM, Loguercio AD, Reis A (2013) Correlation between degree of conversion, resin-dentin bond strength and Nanoleakage of simplified etch-and-rinse adhesives. Dent Mater 29(9):921–928. https://doi.org/10.1016/j.dental.2013.05.001

[30] Kokubo T, Takadama H (2006) How useful is SBF in predicting in vivo bone bioactivity? Biomaterials 27(15):2907–2915. https://doi.org/10.1016/j.biomaterials.2006.01.017

[31] Carvalho EM, Ferreira PVC, Gutiérrez MF, Sampaio RF, Carvalho CN, Menezes AS, Loguercio AD, Bauer J (2021) Development and characterization of self-etching adhesives doped with 45S5 and niobophosphate bioactive glasses: Physicochemical, mechanical, bioactivity and interface properties. Dent Mater 37(6):1030–1045. https://doi.org/10.1016/j.dental.2021.03.004

[32] Melo MAS, Garcia IM, Mokeem L, Weir MD, Xu HHK, Montoya C, Orrego S (2023) Developing bioactive dental resins for restorative dentistry. J Dent Res 102(11):1180–1190. https://doi.org/10.1177/00220345231182357

[33] Gutiérrez MF, Bermudez J, Dávila-Sánchez A, Alegría-Acevedo LF, Méndez-Bauer L, Hernández M, Astorga J, Reis A, Loguercio AD, Farago PV, Fernández E (2019) Zinc oxide and copper nanoparticles addition in universal adhesive systems improve interface stability on caries-affected dentin. J Mech Behav Biomed Mater 100:103366. https://doi.org/10.1016/j.jmbbm.2019.07.024

[34] Par M, Tarle Z, Hickel R, Ilie N (2019) Mechanical properties of experimental composites containing bioactive glass after artificial aging in water and ethanol. Clin Oral Investig 23(6):2733–2741. https://doi.org/10.1007/s00784-018-2713-6

[35] Yao C, Ahmed MH, Li X, Nedeljkovic I, Vandooren J, Mercelis B, Zhang F, Van Landuyt KL, Huang C, Van Meerbeek B (2020) Zinc-Calcium-Fluoride Bioglass-Based innovative multifunctional dental adhesive with Thick adhesive resin film thickness. ACS Appl Mater Interfaces 12(27):30120–30135. https://doi.org/10.1021/acsami.0c06865

[36] Osorio R, Yamauti M, Sauro S, Watson TF, Toledano M (2012) Experimental resin cements containing bioactive fillers reduce matrix metalloproteinase-mediated dentin collagen degradation. J Endod 38(9):1227–1232. https://doi.org/10.1016/j.joen.2012.05.011

[37] Josic U, Mazzitelli C, Maravic T, Comba A, Cadenaro M, Radovic I, Sebold M, Turco G, Breschi L, Mazzoni A (2023) The effect of carbodiimide on push-out bond strength of fiber posts and endogenous enzymatic activity. BMC Oral Health 16(1):399. https://doi.org/10.1186/s12903-023-03067-y

[38] Nosrati R, Kheirouri S, Ghodsi R, Ojaghi H (2019) The effects of zinc treatment on matrix metalloproteinases: A systematic review. J Trace Elem Med Biol 56:107–115. https://doi.org/10.1016/j.jtemb.2019.08.001

4 DISCUSSÃO

A estabilidade da união adesiva à dentina é um fator crítico para assegurar a durabilidade das restaurações dentárias, especialmente em ambientes intraorais propensos à presença de cárie e à degradação do substrato dentinário[7]. A incorporação de nanopartículas em adesivos dentários representa uma tendência inovadora para potencializar suas propriedades, promovendo não apenas melhor adesão, mas também maior resistência frente a processos de degradação biológica e química[13]. Nesta investigação, explorou-se o potencial da incorporação de nanopartículas de vidro bioativo (VB) em adesivos universais modificados com nanopartículas (NPs) de óxido de zinco (ZnO) e cobre (Cu), como uma estratégia inovadora para favorecer a estabilidade da interfase adesiva e, consequentemente, promover uma maior longevidade das restaurações dentárias.

Mecanismos moleculares de citotoxicidade dos adesivos universais

Neste estudo, inicialmente foram abordadas as bases biológicas relacionadas à segurança dos adesivos universais, por meio da investigação dos mecanismos moleculares de citotoxicidade de adesivos universais comerciais em células osteoblásticas Saos-2, *in vitro*. Observou-se que, embora todos os adesivos tenham induzido morte celular, os mecanismos subjacentes variaram significativamente: o Single Bond Universal promoveu predominantemente apoptose, enquanto o Ambar Universal e o Prime & Bond Universal induziram necrose. Essa distinção é relevante, uma vez que a necrose, ao contrário da apoptose, está associada à lise celular e à indução de resposta inflamatória, podendo comprometer a integridade dos tecidos circundantes[10]. A compreensão desses mecanismos é fundamental não apenas para subsidiar o desenvolvimento para o desenvolvimento de adesivos mais seguros, mas também para fornecer uma base interpretativa robusta para os resultados de citocompatibilidade de adesivos modificados com nanopartículas em estudos subsequentes.

Incorporação de NPs de ZnO/Cu em adesivos universais: avaliação in vitro

Na etapa seguinte, avaliou-se, *in vitro*, o efeito da incorporação de NPs de ZnO/Cu (5/0,1% e 5/0,2% p/p) em dois adesivos universais — Prime&Bond Active (PBA) e Ambar Universal (AMB) — sobre a resistência de união à microtração (μTBS), a nanoinfiltração (NL) e a presença de NPs na camada híbrida em condição imediata e após dois anos de armazenamento em água. Os resultados demonstraram que a

adição de NPs de ZnO/Cu não comprometeu a μTBS imediata em nenhuma das estratégias adesivas avaliadas. Após dois anos, os grupos AMB modificados com NPs de ZnO/Cu (5/0,2%) apresentaram μTBS significativamente superiores ao grupo controle, enquanto os grupos PBA mantiveram valores estáveis ao longo do tempo.

A diminuição da nanoinfiltração observada nos grupos contendo NPs de ZnO/Cu, tanto no período imediato quanto após dois anos, pode ser atribuída a múltiplos mecanismos. Entre eles, destacam-se a inibição da atividade das MMPs-2 e -9 pelos íons Cu e Zn, o estímulo ao entrecruzamento do colágeno mediado pela lisil-oxidase (LOX)[19], enzima dependente de Cu, e a indução da formação de depósitos minerais nas fibras colágenas pelo ZnO[21]. A análise por espectroscopia de energia dispersiva de raios X (EDX) confirmou a presença de ZnO e CuNPs na camada híbrida após dois anos de armazenamento, sugerindo que essas NPs podem atuar como reservatório de longa duração, com liberação controlada e progressiva de íons[22,24]. Essa persistência dos efeitos protetores após período prolongado reforça o potencial clínico dessa estratégia.

Não obstante, a degradação progressiva da interface — evidenciada pelo aumento da nanoinfiltração ao longo do tempo em todos os grupos — indica que as NPs metálicas, por si sós, não são suficientes para impedir completamente os processos de degradação hidrolítica e enzimática[20,21]. Esse achado justifica a adição de VB como uma alternativa complementar para potencializar a ação protetora das NPs de ZnO/Cu frente a desafios ácidos e favorecer a estabilidade da interface adesiva.

Incorporação de NPs de ZnO/Cu em adesivos universais: avaliação ex vivo

No ensaio clínico randomizado *ex vivo* de boca dividida, avaliou-se o efeito de um adesivo carregado com 0,2% de NPs de Cu e 5% de NPs de ZnO sobre as propriedades adesivas e a atividade gelatinolítica na camada híbrida em dentes extraídos após um mês de uso clínico. Consistentemente com outros estudos in vitro, os resultados demonstraram que a adição de NPs não comprometeu a μTBS nem o grau de conversão[19,20]. O achado mais relevante desse estudo foi a redução significativa da atividade enzimática — avaliada por zimografia in situ — no grupo experimental em comparação com o grupo controle. Essa redução foi acompanhada pela detecção de Cu e Zn na camada híbrida, validando a incorporação e retenção das nanopartículas no substrato dentinário após o procedimento restaurador realizado em condição clínica. Esses achados forneceram a base para a etapa seguinte da tese,

na qual se investigou se a adição de VB poderia complementar os efeitos protetores das NPs metálicas.

Incorporação de NPs de ZnO/Cu e VB em adesivos universais: avaliação in vitro

A etapa seguinte buscou ampliar essa estratégia por meio da incorporação de nanopartículas de VB a um adesivo universal, modificado com nanopartículas de ZnO a 2,5% e Cu a 0,2%. Foram analisados seu impacto na estabilidade da união adesiva à dentina, bem como sua resistência frente a um desafio cariogênico in vitro, com o objetivo de simular as condições agressivas do ambiente bucal. A adição de VB melhorou principalmente as propriedades biológicas do adesivo, especialmente a atividade antimicrobiana e o potencial mineralizante, sem comprometer de forma relevante a integridade da união adesiva. No entanto, Embora não tenha sido observado um efeito inibitório generalizado em todos os grupos e estratégias adesivas, reduções significativas da atividade proteolítica foram detectadas em condições específicas, especialmente na estratégia ER.

A caracterização do tamanho das nanopartículas de VB sintetizadas em laboratório confirmou que todas apresentavam diâmetro inferior a 100 nm, o que permite classificá-las como nanopartículas. A confirmação dessa característica é fundamental, pois garante alta reatividade química e potencializa sua eficácia nos ensaios subsequentes[28]. Além disso, as NPs de VB foram caracterizadas como vidros amorfos, ressaltando seu potencial mineralizante e sua capacidade de favorecer processos biológicos de interesse na aplicação clínica[19,26,29]. Este estudo demonstrou que os adesivos modificados com NPs exerceram uma ação antibacteriana efetiva e significativa contra Streptococcus mutans, um microrganismo-chave no desenvolvimento da cárie dentária[19]. Esses achados são consistentes com estudos prévios em que as NPs de VB, ZnO e Cu, incorporadas de forma individual, também mostraram efeito antibacteriano relevante[20,22].

Os grupos modificados com NPs de VB apresentaram efeito antibacteriano superior, especialmente na maior concentração de VB (10%). Esse resultado indica que a matriz de VB proporciona uma atividade antimicrobiana notável, atribuída provavelmente à sua capacidade de elevar o pH do meio[27,30]. Essa alcalinização compromete a integridade da membrana citoplasmática bacteriana e pode promover dano celular, reduzindo a viabilidade bacteriana e a formação de biofilme[29,30].

O mecanismo antibacteriano do VB é impulsionado por um aumento sustentado do pH local e pela liberação de íons como Na^+, Ca^{2+} e PO_4^{3-}[31]. Esse ambiente alcalino

é hostil para bactérias acidófilas como S. mutans, inibindo seu metabolismo e crescimento. Adicionalmente, a alta concentração iônica gera uma pressão osmótica que desestabiliza o potencial de membrana, contribuindo para a lise bacteriana[29,31-33].

Em contraste, as NPs metálicas dependem unicamente da liberação de íons Cu^{2+} ou Zn^{2+}. Embora esses íons sejam antibacterianos, ao gerarem espécies reativas de oxigênio (ROS)[34,35], danificarem a membrana e inibirem enzimas, não alteram de forma significativa o pH e, neste estudo, seu efeito foi mais limitado. Contrariamente à hipótese de um efeito aditivo ou sinérgico evidente, os grupos que combinaram VB com ZnO/CuNPs exibiram efeito antibacteriano intermediário, inferior ao observado no grupo contendo 10% de VB isoladamente. Esse comportamento sugere que o mecanismo de alcalinização promovido pelo VB foi predominante e que pode ter havido interferência na biodisponibilidade dos íons metálicos.

Uma possível explicação para esse achado é a ocorrência de um fenômeno de quelação superficial, em que a camada de gel de sílica do VB, com abundantes grupos silanol (Si-OH), teria sequestrado os íons Cu^{2+} e Zn^{2+} liberados[34]. Essa imobilização iônica na superfície do VB reduziria a concentração de íons metálicos biodisponíveis para exercer sua ação antibacteriana, explicando assim a ausência de efeito aditivo evidente[36]. A redução na contagem de colônias, corroborada pelas imagens de microscopia eletrônica de varredura (MEV) que evidenciam uma diminuição notável da biopelícula nos grupos modificados, reforça o potencial clínico desses materiais para limitar a colonização bacteriana na interface das restaurações dentárias.

Os adesivos dentários atualmente utilizados possuem monômeros resinosos em sua composição[13,37], e estes podem ser liberados mesmo após a fotopolimerização, em contato com fluidos orais, gerando efeitos citotóxicos[37]. Neste estudo, observou-se redução significativa da viabilidade celular aos 14 dias em todos os grupos avaliados. No entanto, essa redução também ocorreu no grupo controle, indicando que a incorporação de NPs de ZnO/Cu e VB, nas concentrações estudadas, não aumentou a citotoxicidade do adesivo em relação à formulação não modificada, o que está em consonância com estudos prévios[22,30], ressaltando seu potencial uso clínico de forma segura.

A bioatividade é caraterizada pela capacidade que um material tem de interagir favoravelmente com os tecidos biológicos, promovendo respostas específicas que conduzem à integração e regeneração tecidual[25]. A capacidade mineralizante do vidro bioativo é uma propriedade fundamental relacionada à sua liberação iônica e à

formação de depósitos cálcio-fosfato na superfície do material[38-40]. Esse processo inicia-se por sua hidrólise no meio aquoso, na qual ocorre uma troca iônica. Íons Ca^{2+} e Na^{+} são liberados para o meio, enquanto os prótons (H^{+}) do meio ingressam na estrutura do vidro, provocando um aumento no pH local[25,33]. O incremento no pH favorece a precipitação de uma camada de sílica na superfície do vidro, que atua como matriz de difusão para outros íons, permitindo a migração de Ca^{2+} e PO_4^{3-}, os quais inicialmente precipitam na forma de cristais amorfos de carbonato de cálcio[25]. Com o tempo, o aumento sustentado do pH continua degradando a rede de sílica, facilitando a formação de hidroxiapatita na superfície do material.

Neste estudo, a capacidade mineralizante foi evidenciada pela formação de depósitos de Ca-P e depósitos ricos em cálcio e fósforo, compatíveis com mineralização apatita-like na superfície dos adesivos modificados com VB. A morfologia em camadas e em formas esféricas desses depósitos é compatível com relatos prévios de formação de depósitos minerais em materiais contendo vidro bioativo. Embora a caracterização por EDX permita identificar a composição elementar da amostra em nível microscópico, ela não fornece informação direta sobre a estrutura cristalina, nem permite determinar propriedades dos cristais, como tamanho, tipo ou orientação. Essas características poderiam ser avaliadas por difração de raios X (XRD)[41]. Portanto, os achados devem ser interpretados como evidência indireta de mineralização cálcio-fosfato, e não como confirmação cristalográfica de hidroxiapatita.

O grau de conversão (GC) é uma propriedade fundamental dos adesivos dentários. Um GC elevado associa-se a melhores propriedades mecânicas, contribuindo significativamente para o sucesso a longo prazo de um tratamento restaurador[42]. Neste estudo, o GC obtido foi superior a 60% em todos os grupos, o que indica uma polimerização efetiva do adesivo[42]. Portanto, a incorporação das NPs, tanto metálicas quanto de VB, não afetou a porcentual de conversão do adesivo. O grupo 10%VB foi o único que apresentou diferenças em relação aos demais grupos, exibindo GC maior que o grupo 10%VB+ZnO/Cu.

Os resultados deste estudo são coerentes com estudos prévios[22], nos quais se assinala que as NPs metálicas costumam apresentar estado químico neutro e não influenciam na reação de polimerização, ao menos nas concentrações utilizadas neste estudo. Do mesmo modo, estudos prévios relataram que o VB, nas concentrações empregadas, não reduz o GC dos adesivos[43]. Isso pode ser explicado porque, embora

a presença de NPs possa restringir a mobilidade das cadeias monoméricas, também reduz o espaço intersticial quando ocorre a copolimerização de cadeias opostas, o que pode aumentar o GC, dependendo de sua morfologia e concentração[44].

Os resultados deste estudo indicaram que, após a incorporação de nanopartículas de VB, os percentuais de Ca e P na superfície da camada híbrida aumentaram significativamente em comparação com o controle. Esse aumento, mais notável para Ca aos 28 dias, indica uma tendência à mineralização favorecida pelo VB. Embora depósitos minerais não tenham sido detectados de forma homogênea em todos os grupos modificados com VB após o ensaio em SBF, esse achado pode estar relacionado à limitada área disponível para nucleação mineral na interface adesiva e à possível migração dos íons liberados em direção à camada híbrida, contribuindo na mineralização e fortalecendo a união adesiva na dentina[45].

As metaloproteinases da matriz (MMPs) são enzimas dependentes de zinco, responsáveis pela degradação do colágeno dentinário, comprometendo a durabilidade das restaurações adesivas[46,47]. A regulação de sua atividade representa um objetivo terapêutico de grande relevância em odontologia restauradora. A capacidade dos íons metálicos Cu e Zn de modular a atividade das MMPs tem sido amplamente documentada na literatura científica[19-21,48]. Por sua vez, ao VB também têm sido atribuídas propriedades inibitórias sobre essas enzimas, principalmente pela geração de um ambiente alcalino que se encontra fora da faixa ótima de atividade das MMPs[45]. Neste estudo, embora a atividade enzimática tenha mostrado variações nos grupos avaliados, dependente da estratégia adesiva empregada, os resultados da zimografia in situ revelaram atividade enzimática elevada das MMPs em todos os grupos analisados, incluindo aqueles que continham NPs, embora tenham sido observadas diferenças na atividade dependentes da modalidade de preparação do substrato.

Na modalidade autocondicionante (SE), a ausência de condicionamento ácido prévio e o uso de um adesivo de acidez moderada promovem desmineralização mais superficial e, potencialmente, menor ativação das MMPs. Essa condição poderia explicar o efeito mais limitado das NPs, já que neste estudo não se observou redução significativa da atividade enzimática em comparação com o grupo controle nessa estratégia adesiva. Em contraste, na modalidade de condicionamento total (TE), os grupos ZnO/Cu e 10%VB+ ZnO/Cu conseguiram reduzir significativamente a atividade proteolítica, de maneira equivalente. Esse achado sugere um potencial inibitório, ainda

que limitado nas condições avaliadas, das nanopartículas metálicas e de sua associação com VB em alta concentração.

Esse efeito pode ser explicado pelas condições físico-químicas específicas dessa técnica: o pH baixo do ácido ortofosfórico a 37% utilizado para o tratamento da superfície, que pode favorecer maior ativação das MMPs e maior exposição de fibras de colágeno[29]. Nesse ambiente, os íons metálicos de ZnO/Cu podem atuar diretamente sobre as enzimas ativadas, enquanto o VB teria condições mais favoráveis para a liberação de íons. Além disso, a combinação de nanopartículas de VB em maior concentração (10%) e ZnO/Cu favoreceu um efeito inibitório em comparação com o grupo 10%VB, mostrando um efeito inibitório da atividade enzimática das MMPs que pode ter sido promovido principalmente pela incorporação das NPs metálicas de Cu e ZnO. No entanto, ao comparar diferentes concentrações de VB (5% e 10%) em combinação com NPs metálicas na estratégia TE, a maior concentração de VB promoveu efeito inibitório significativamente maior. Isso sugere que, em certas condições de pH, o vidro bioativo pode contribuir para um efeito inibitório da atividade enzimática, embora a possível existência de um efeito sinérgico evidente com as NPs metálicas exija avaliação em outras condições experimentais, como as que serão descritas ao discutir o desafio cariogênico.

Alguns fatores experimentais podem explicar as variações na atividade enzimática detectada pela zimografia in situ, bem como a ausência de um efeito inibitório efetivo neste estudo. O efeito inibitório do VB depende da dissolução de sua superfície vítrea e da liberação de íons que aumentam o pH local[33]. Em condições de avaliação imediata, a dissolução pode ter sido insuficiente para alcançar o pH crítico (>8,5) necessário para inibir de forma efetiva a atividade das MMPs, mesmo com concentrações de 10% de VB, previamente relatadas como efetivas de maneira individual[48]. Em relação às NPs metálicas, é provável que a concentração reduzida de ZnO (2,5%) tenha sido insuficiente, considerando estudos que empregaram concentração de 5% e relataram efeitos inibitórios[19,22]. A inibição das MMPs também tem sido documentada como um efeito dose-dependente[40]. Além disso, assim como o VB, é possível que as NPs metálicas tenham requerido maior tempo de exposição para liberar quantidade suficiente de íons ativos. Esses resultados sugerem que futuras formulações devem considerar concentrações otimizadas de nanopartículas metálicas e avaliações temporais estendidas para permitir liberação efetiva de íons que estabeleçam um efeito inibitório mais consistente.

As propriedades mecânicas dos materiais resinosos estão estreitamente associadas a fatores relacionados às partículas de carga, como sua concentração, forma e tamanho[41]. A RU neste estudo foi influenciada significativamente pela interação entre a estratégia adesiva, a composição do material e a resistência ao ambiente ácido, sendo consistente com estudos prévios que demonstraram a influência das nanopartículas no comportamento dos sistemas adesivos[49].

Quanto à técnica empregada para preparar o substrato dentinário, de TE (condicionamento total) e SE (autocondicionante), a técnica de condicionamento total foi a que mostrou maior sensibilidade à composição do material, possivelmente mediada por sua capacidade de criar padrões de desmineralização mais profundos, que permitiram maior expressão das propriedades intrínsecas de cada formulação adesiva[31,47], assim como na avaliação da atividade enzimática das MMPs. Em contraste, a estratégia SE não apresentou diferenças entre os grupos na condição inicial (sadio), sugerindo um efeito modulador da técnica sobre a expressão das propriedades do material[19].

Em termos gerais, a resistência mecânica dos materiais melhora com a incorporação de partículas de carga, o que se explica por um empacotamento denso da fase dispersa e consequente deflexão da fratura como mecanismo de resistência[41]. No entanto, as NPs de VB não possuem papel de reforço como as partículas de vidro silanizado ou sílica (inertes) utilizadas comumente em materiais resinosos odontológicos, uma vez que uma vez que apresentam menor capacidade de interação química com a matriz resinosa, quando comparadas a partículas de vidro silanizado ou sílica inerte convencionalmente utilizadas como carga e podem afetar suas propriedades mecânicas de maneira dependente de sua concentração[51,52].

Considerando o possível impacto de concentrações elevadas de VB sobre as propriedades mecânicas e a dispersão das partículas, não foram utilizadas concentrações superiores a 10% de VB. não foram utilizadas concentrações superiores a 10% de VB, conforme recomendado em estudos prévios. Adicionalmente, a concentração de ZnO foi reduzida em relação a outros estudos, com o objetivo de favorecer melhor distribuição das partículas e minimizar efeitos adversos associados à aglomeração.

Inicialmente, na estratégia TE, a incorporação de nanopartículas metálicas nos grupos ZnO/Cu e 5%VB+ZnO/Cu não resultou em diminuição da RU inicial em comparação com o grupo controle. Contudo, os grupos modificados com VB em maior

concentração (10%VB+ZnO/Cu e 10%VB) evidenciaram igualmente diminuição da RU para a estratégia ER antes do desafio cariogênico, em comparação com os demais grupos.

O efeito observado no grupo com menor concentração de VB (5%) e no grupo ZnO/Cu poderia ser explicado principalmente pelo efeito catalisador do cobre, que facilita a formação de ligações químicas entre as moléculas, favorecendo o entrecruzamento e resultando em uma estrutura mais resistente do adesivo. Esse efeito foi relatado por Gutiérrez et al.[16], embora esse efeito possa ter sido atenuado quando existiam concentrações elevadas de vidro bioativo, possivelmente devido aos efeitos de quelação dos íons metálicos descritos anteriormente.

Quando se avaliou a estabilidade adesiva após o desafio cariogênico, a incorporação de nanopartículas, particularmente na formulação 10%VB+ZnO/Cu, demonstrou o melhor equilíbrio entre desempenho inicial e resistência ao desafio. Esse comportamento pode ser explicado pela capacidade do vidro bioativo de neutralizar parcialmente o ambiente ácido e promover a remineralização local, protegendo assim a interface[52]. Além disso, essa camada mineral, bioquimicamente semelhante ao mineral dentário natural, facilita a união química entre o material adesivo e a estrutura dentinária, promovendo mineralização biomimética[52].

Os resultados sugerem uma interação funcional entre os diferentes tipos de nanopartículas, embora essa interação não tenha sido uniformemente sinérgica em todos os desfechos avaliados. Enquanto o VB apresentou efeito mais expressivo sobre a atividade antibacteriana e o potencial mineralizante, as ZnO/CuNPs pareceram contribuir de forma mais relevante para a modulação da atividade enzimática em determinadas condições, especialmente na estratégia ER. Portanto, a combinação entre VB e ZnO/CuNPs deve ser interpretada como uma estratégia multifuncional, e não necessariamente como um efeito sinérgico universal para todos os parâmetros analisados.

Esses achados sugerem que as nanopartículas de ZnO e Cu podem otimizar a resistência de união inicial por meio de mecanismos que incluem melhora das propriedades mecânicas da matriz polimérica e atividade antimicrobiana[19]. Por outro lado, as nanopartículas de vidro bioativo parecem fornecer proteção a longo prazo por meio da liberação controlada de íons, que podem neutralizar ácidos e facilitar a remineralização[34,41]. A combinação desses três tipos de nanopartículas na formulação 10%VB+ZnO/Cu parece gerar um microambiente bioativo na interface híbrida,

integrando mecanismos antibacterianos, mineralizantes e potencialmente moduladores da atividade enzimática, o que resulta em um material com propriedades funcionalmente balanceadas.

A incorporação de nanopartículas de zinco e cobre em sistemas adesivos demonstrou melhorar parâmetros críticos como resistência de união, atividade antimicrobiana e viabilidade celular, conforme documentado por Gutiérrez et al. (2019)[19]. No entanto, a funcionalização exclusiva com metais não aborda de forma integral a necessidade de induzir remineralização sustentada na interface híbrida, nem garante a formação de um selamento biológico duradouro. Nesse contexto, a adição de VB representa uma estratégia complementar altamente promissora. Esse material atua como fonte controlada de íons Ca^{2+}, PO_4^{3-} e Si^{4+}, capazes de promover a nucleação de hidroxiapatita carbonatada sobre a dentina desmineralizada, favorecendo processos de remineralização intrafibrilar e estabilização biomimética da matriz colagênica[46,47]. Diferentemente dos mecanismos redox mediados por Cu e Zn, o VB não depende de estresse oxidativo, mas interage diretamente com o ambiente iônico e proteico, promovendo a estabilização estrutural da interface sem comprometer a viabilidade celular. Além disso, os produtos iônicos liberados pelo VB têm demonstrado modular a expressão gênica relacionada à osteogênese, angiogênese e diferenciação celular, o que sugere um efeito bioindutivo para além da remineralização passiva[34].

Neste estudo, a incorporação de nanopartículas de ZnO, Cu e VB ao sistema adesivo universal conferiu propriedades multifuncionais relevantes para a preservação da interface adesiva. A interação entre esses componentes aborda diferentes desafios associados ao fracasso das restaurações dentárias. Por um lado, a capacidade antibacteriana das nanopartículas de ZnO, Cu e VB oferece defesa contra a colonização bacteriana e a formação de biofilme, particularmente por microrganismos cariogênicos como S. mutans, contribuindo para a prevenção da cárie secundária[47,48]. De forma complementar, as nanopartículas metálicas, embora não tenham inibido completamente a atividade enzimática, promoveram diminuição da atividade das MMPs em condições específicas, especialmente quando o substrato foi tratado pela estratégia ER. Somado a isso, a adição de VB introduziu capacidade mineralizante, promovendo a formação de depósitos ricos em Ca-P na interface. Esses benefícios funcionais foram alcançados mantendo citocompatibilidade adequada, indicando que o material modificado não induziu toxicidade adicional em

relação ao controle. Em conjunto, essas propriedades: antibacterianas, bioativas, citocompatíveis e potencialmente moduladoras da atividade proteolítica, posicionam o adesivo modificado como um material biomimético avançado, com potencial para criar uma interface adesiva mais estável, durável e biologicamente ativa.

As principais limitações deste estudo incluem sua natureza *in vitro*, que não replica completamente a complexidade do ambiente oral, e a avaliação predominantemente imediata ou de curtu prazo. Adicionalmente, embora o desafio cariogênico simulado tenha sido padronizado, ele não reproduz integralmente a variabilidade do ambiente oral, no qual saliva, biofilme bacteriano, forças mastigatórias e ciclos de pH interagem de maneira dinâmica. Além disso, o estudo concentrou-se na resistência de união imediata e após desafio cariogênico, sem avaliar o comportamento a longo prazo sob condições de envelhecimento térmico e mecânico, que poderiam revelar padrões diferentes de degradação. Do mesmo modo, o uso de uma única linhagem celular para análise de citocompatibilidade limita a extrapolação da resposta biológica para outros tipos celulares relevantes, como células pulpares ou odontoblastos. Ademais, a liberação iônica a partir da matriz adesiva não foi quantificada, de modo que ainda não se conhece a cinética de difusão nem a estabilidade funcional do sistema a longo prazo. Outra limitação relevante é a ausência de caracterização cristalográfica dos depósitos minerais por técnicas como XRD, o que impede confirmar a formação de hidroxiapatita cristalina diretamente. Frente a esses aspectos, investigações futuras deveriam considerar validação cruzada in vitro e in vivo. Seria particularmente relevante incorporar modelos tridimensionais ou de microambiente dentino-pulpar para analisar a resposta de células-tronco, osteoblastos e odontoblastos em contato com os sistemas propostos. A caracterização da liberação iônica, em meio condicionado a pH fisiológico e/ou cariogênico, por meio de técnicas como espectrometria de emissão óptica com plasma indutivamente acoplado (ICP-OES) ou espectrometria de massas, permitiria correlacionar os perfis de liberação com os efeitos biológicos observados. Finalmente, estudos de envelhecimento acelerado por termociclagem, carga mecânica ou imersão em soluções desmineralizantes permitirão avaliar a estabilidade estrutural, química e funcional do adesivo a longo prazo, avançando rumo à sua futura validação pré-clínica.

Apesar das limitações deste estudo, os resultados obtidos indicam que a modificação de um adesivo universal com nanopartículas de ZnO, Cu e VB promove

uma resposta multifuncional favorável na interface resina-dentina. Essa resposta resulta da interação entre mecanismos antimicrobianos, mineralizantes e potencialmente moduladores da atividade proteolítica, ainda que tais efeitos não tenham sido uniformes entre todos os desfechos avaliados. Assim, a incorporação de VB a adesivos modificados com nanopartículas metálicas representa uma estratégia promissora para favorecer a estabilidade da interface adesiva, especialmente em condições de maior desafio ácido ou risco cariogênico. Entretanto, sua validação translacional requer estudos adicionais que incluam quantificação da liberação iônica, envelhecimento mecânico e térmico, caracterização mineralógica dos depósitos formados e avaliação em modelos biológicos mais complexos, antes de sua aplicação clínica.

5 CONCLUSÃO

Com base nos resultados obtidos nos estudos que compõem esta tese, podem-se estabelecer as seguintes conclusões:

- Os adesivos universais comerciais exibem diferentes mecanismos de citotoxicidade em células osteoblásticas Saos-2, incluido apoptose e necrose, o que ressalta a importância de uma avaliação biológica abragente durante o desenvolvimento e a modificação de novos materiais dentários.

- A incorporação de nanopartículas de VB, especialmente na concentração de 10%, melhorou significativamente a atividade antibacteriana contra *Streptococcus mutans*, sem aumentar a citotoxicidade do adesivo em relação ao adesivo não modificado.

- Os adesivos modificados com VB evidenciaram potencial mineralizante por meio da formação de depósitos ricos em cálcio e fósforo em sua superfície, sugirindo liberação iônica partir da matriz adhesiva.

- A adição de nanopartículas de VB e ZnO/Cu não compromete o grau de conversão dos adesivos, que se manteve superior a 60% em todos os grupos experimentais.

- Foi observada inibição significativa da atividade enzimática das metaloproteinases da matriz nos adesivos modificados com NPs de ZnO/Cu (5/0,2%), em prejuízo da resistência de união ou do grau de conversão.

- Quando VB e NPs metálicas foram combinados, a atividade enzimática das MMPs apresentou redução estratégia-dependente. Na modalidade TE, os grupos ZnO/Cu e 10%VB+ZnO/Cu reduziram a atividade proteolítica em comparação ao controle; entretanto, esse efeito não foi observado de forma consistente em todos os grupos nem na estratégia SE. Assim, as concentrações avaliadas parecem exercer efeito modulador limitado sobre as MMPs, sendo necessárias condições experimentais adicionais para confirmar seu potencial inibitório.

- A resistência de união inicial foi reduzidanos grupos com concentração de VB de 10%. De forma relevante, após o desafio cariogênico, o grupo 10%VB+ZnO/Cu manteve sua resistência de união sem mudanças significativas em ambas as estratégias de preparação do substrato, enquanto o grupo controle mostrou redução importante. Esse achado sugere que o VB contribui para a estabilidade da interface adesiva frente a condições ácidas, especialmente quando combinado com ZnO/Cu na formulação 10%VB+ZnO/Cu.
- Este estudo apresenta uma abordagem inovadora ao combinar VB com nanopartículas metálicas de ZnO/Cu em adesivos dentários, demonstrando que a formulação 10%VB+ZnO/Cu representa uma alternativa promissora para favorecer a estabilidade da interface adesiva frente a desafios cariogênicos, com potencial aplicação futura em situações clínicas associadas a maior risco cariogênico.
- Os resultados obtidos justificam a realização de estudos adicionais de liberação iônica, envelhecimento térmico e mecânico, caracterização mineralógica e validação em modelos biológicos mais complexos, como etapas prévias à realização de estudos clínicos controlados.

REFERÊNCIAS

1. Kassebaum NJ, Bernabé E, Dahiya M, Bhandari B, Murray CJL, Marcenes W. Global burden of untreated caries: a systematic review and metaregression. J Dent Res. 2015;94(5):650-658. doi:10.1177/0022034515573272.

2. Schwendicke F, Dörfer CE, Schlattmann P, Foster Page L, Thomson WM, Paris S. Socioeconomic inequality and caries: a systematic review and meta-analysis. J Dent Res. 2015;94(1):10-18. doi:10.1177/0022034514557546.

3. Bayne SC, Ferracane JL, Marshall GW, Marshall SJ, van Noort R. The evolution of dental materials over the past century: silver and gold to tooth color and beyond. J Dent Res. 2019;98(3):257-265. doi:10.1177/0022034518822808.

4. Ferracane JL. Resin composite—state of the art. Dent Mater. 2011;27(1):29-38. doi:10.1016/j.dental.2010.10.020.

5. Tagle EL. Disminución gradual de amalgama dental en el programa de salud bucal en Chile 2015. Organización Panamericana de la Salud. Disponible en: https://www.paho.org/hq/dmdocuments/2015/amalgama-dental-chile-e-tagle.pdf.

6. Mjör IA, Dahl JE, Moorhead JE. Age of restorations at replacement in permanent teeth in general dental practice. Acta Odontol Scand. 2000;58(3):97-101. doi:10.1080/000163500429208.

7. Cadenaro M, Josic U, Maravić T, Mazzitelli C, Marchesi G, Mancuso E, et al. Progress in dental adhesive materials. J Dent Res. 2023;102(3):254-262. doi:10.1177/00220345221145673.

8. Nakabayashi N. Hybrid layer as a dentin-bonding mechanism. J Esthet Dent. 1991;3(4):133-8. doi: 10.1111/j.1708-8240.1991.tb00985.x. PMID: 1817582.

9. Demarco FF, Collares K, Coelho-de-Souza FH, Correa MB, Cenci MS, Moraes RR, et al. Anterior composite restorations: a systematic review on long-term survival and reasons for failure. Dent Mater. 2015;31(10):1214-1224. doi:10.1016/j.dental.2015.07.005.

10. Wawrzynkiewicz A, Rozpedek-Kaminska W, Galita G, Lukomska-Szymanska M, Lapinska B, Sokolowski J, et al. The cytotoxicity and genotoxicity of three dental universal adhesives—an in vitro study. Int J Mol Sci. 2020;21(11):3950. doi:10.3390/ijms21113950.

11. de Alencar NA, Fidalgo TK, Cajazeira MR, Maia LC. Influence of the number of adhesive layers on adhesive interface properties under cariogenic challenge using *Streptococcus mutans*. J Adhes Dent. 2014;16(4):339-346. doi:10.3290/j.jad.a32569.

12. Cohn N, Bradtmüller H, Zanotto E, von Marttens A, Covarrubias C. Novel organic–inorganic nanocomposite hybrids based on bioactive glass nanoparticles and their enhanced osteoinductive properties. Biomolecules. 2024;14(4):482. doi:10.3390/biom14040482.

13. Reis A, Carrilho M, Breschi L, Loguercio AD. Overview of clinical alternatives to minimize the degradation of the resin-dentin bonds. Oper Dent. 2013;38(4):E1-E25. doi:10.2341/12-258-LIT.

14. Mazzoni A, Tjäderhane L, Checchi V, Di Lenarda R, Salo T, Tay FR, et al. Role of dentin MMPs in caries progression and bond stability. J Dent Res. 2015;94(2):241-251. doi:10.1177/0022034514562833.

15. Maske TT, Kuper NK, Cenci MS, Huysmans MC. Minimal gap size and dentin wall lesion development next to resin composite in a microcosm biofilm model. Caries Res. 2017;51(5):475-481. doi:10.1159/000478536.

16. Askar H, Krois J, Göstemeyer G, Schwendicke F. Secondary caries risk of different adhesive strategies and restorative materials in permanent teeth: systematic review and network meta-analysis. J Dent. 2021;104:103541. doi:10.1016/j.jdent.2020.103541.

17. Breschi L, Mazzoni A, Nato F, Carrilho M, Visintini E, Tjäderhane L, et al. Chlorhexidine stabilizes the adhesive interface: a 2-year in vitro study. Dent Mater. 2010;26(4):320-325. doi:10.1016/j.dental.2009.11.153.

18. Carrilho MR, Tay FR, Donnelly AM, Agee KA, Tjäderhane L, Mazzoni A, et al. Host-derived loss of dentin matrix stiffness associated with solubilization of collagen. J Biomed Mater Res B Appl Biomater. 2009;90(1):373-380. doi:10.1002/jbm.b.31295.

19. Gutiérrez MF, Bermúdez J, Dávila-Sánchez A, Alegría-Acevedo LF, Méndez-Bauer L, Hernández M, et al. Zinc oxide and copper nanoparticles addition in universal adhesive systems improve interface stability on caries-affected dentin. J Mech Behav Biomed Mater. 2019;100:103366. doi:10.1016/j.jmbbm.2019.07.024.

20. Toledano-Osorio M, Osorio R, Aguilera FS, Medina-Castillo AL, Toledano M, Osorio E, et al. Polymeric nanoparticles protect the resin-dentin bonded interface from cariogenic biofilm degradation. Acta Biomater. 2020;111:316-326. doi:10.1016/j.actbio.2020.05.002.

21. Toledano M, Yamauti M, Ruiz-Requena ME, Osorio R. A ZnO-doped adhesive reduced collagen degradation favouring dentine remineralization. J Dent. 2012;40(9):756-765. doi:10.1016/j.jdent.2012.05.007.

22. Gutiérrez MF, Alegría-Acevedo LF, Méndez-Bauer L, Bermudez J, Dávila-Sánchez A, Buvinic S, et al. Biological, mechanical and adhesive properties of universal adhesives containing zinc and copper nanoparticles. J Dent. 2019;82:45-55. doi:10.1016/j.jdent.2019.01.012.

23. Wang L, D'Alpino PHP, Lopes LG, Pereira JC. Mechanical properties of dental restorative materials: relative contribution of laboratory tests. J Appl Oral Sci. 2003;11(3):162-167. doi:10.1590/S1678-77572003000300002.

24. Marelli B, Le Nihouannen D, Hacking SA, Tran S, Li J, Murshed M, et al. Newly identified interfibrillar collagen crosslinking suppresses cell proliferation and remodelling. Biomaterials.2015;54:126-135. doi: 10.1016/j.biomaterials.2015.03.018.

25. Hench LL. The story of Bioglass®. J Mater Sci Mater Med. 2006;17(11):967-978. doi:10.1007/s10856-006-0432-z.

26. Abbassy MA, Bakry AS, Alshehri NI, Alghamdi TM, Rafiq SA, Aljeddawi DH, et al. 45S5 Bioglass paste is capable of protecting the enamel surrounding orthodontic brackets against erosive challenge. J Orthod Sci. 2019;8:5. doi:10.4103/jos.JOS_93_18.

27. Aponso S, Ummadi JG, Davis H, Ferracane J, Koley D. A chemical approach to optimizing bioactive glass dental composites. J Dent Res. 2019;98(2):194-199. doi:10.1177/0022034518809086.

28. Jandt KD, Watts DC. Nanotechnology in dentistry: present and future perspectives on dental nanomaterials. Dent Mater. 2020;36(11):1365-1378. doi:10.1016/j.dental.2020.08.006.

29. Bauer J, Silva e Silva A, Carvalho EM, Ferreira PVC, Carvalho CN, Manso AP, et al. Dentin pretreatment with 45S5 and niobophosphate bioactive glass: effects on pH, antibacterial, mechanical properties of the interface and microtensile bond strength. J Mech Behav Biomed Mater. 2019;90:374-380. doi:10.1016/j.jmbbm.2018.10.029.

30. Schwendicke F, Al-Abdi A, Pascual Moscardó A, Ferrando Cascales A, Sauro S. Remineralization effects of conventional and experimental ion-releasing materials in chemically or bacterially-induced dentin caries lesions. Dent Mater. 2019;35(5):772-779. doi:10.1016/j.dental.2019.02.021.

31. Abuna G, Campos P, Hirashi N, Giannini M, Nikaido T, Tagami J, et al. The ability of a nanobioglass-doped self-etching adhesive to re-mineralize and bond to artificially demineralized dentin. Dent Mater. 2021;37(1):120-130. doi:10.1016/j.dental.2020.10.026.

32. Jun SK, Yang SA, Kim YJ, El-Fiqi A, Mandakhbayar N, Kim DS, et al. Multi-functional nano-adhesive releasing therapeutic ions for MMP-deactivation and remineralization. Sci Rep. 2018;8:5663. doi:10.1038/s41598-018-23939-6.

33. Melo MAS, Garcia IM, Mokeem L, Weir MD, Xu HHK, Montoya C, et al. Developing bioactive dental resins for restorative dentistry. J Dent Res. 2023;102(11):1180-1190. doi:10.1177/00220345231182357.

34. Palza H, Escobar B, Bejarano J, Bravo D, Diaz-Dosque M, Perez J. Designing antimicrobial bioactive glass materials with embedded metal ions synthesized by the sol-gel method. Mater Sci Eng C Mater Biol Appl. 2013;33(7):3795-3801. doi:10.1016/j.msec.2013.05.012.

35. Correa S, Matamala L, González JP, de la Fuente M, Miranda H, Olivares B, et al. Development of novel antimicrobial acrylic denture modified with copper nanoparticles. J Prosthodont Res. 2024;68(1):156-165. doi:10.2186/jpr.JPR_D_22_00227.

36.Drago L, Toscano M, Bottagisio M. Recent evidence on bioactive glass antimicrobial and antibiofilm activity: a mini-review. Materials (Basel). 2018;11(2):326. doi:10.3390/ma11020326.

37. Catunda RQ, Vieira JRC, de Oliveira EB, da Silva EC, Brasil VLM, Perez DEC. Citotoxicity evaluation of three dental adhesives on Vero cells in vitro. J Clin Exp Dent. 2017;9(1):e61-e66. doi:10.4317/jced.53039.

38. Jung JH, Kim DH, Yoo KH, Yoon SY, Kim Y, Bae MK, et al. Dentin sealing and antibacterial effects of silver-doped bioactive glass/mesoporous silica nanocomposite: an in vitro study. Clin Oral Investig. 2019;23(1):253-266. doi: 10.1007/s00784-018-2432-z.

39. Carvalho EM, Ferreira PVC, Gutiérrez MF, Sampaio RF, Carvalho CN, Menezes AS, et al. Development and characterization of self-etching adhesives doped with 45S5 and niobophosphate bioactive glasses: physicochemical, mechanical, bioactivity and interface properties. Dent Mater. 2021;37(6):1030-1045. doi:10.1016/j.dental.2021.03.004.

40. Zhou X, Sahai N, Qi L, Mankoci S, Zhao W. Biomimetic and nanostructured hybrid bioactive glass. Biomaterials. 2015;50:1-9. doi:10.1016/j.biomaterials.2015.01.024.

41. Bunaciu AA, Udriştioiu EG, Aboul-Enein HY. X-ray diffraction: instrumentation and applications. Crit Rev Anal Chem. 2015;45(4):289-99. doi: 10.1080/10408347.2014.949616.

42. Ferracane JL, Hilton TJ, Stansbury JW, Watts DC, Silikas N, Ilie N, et al. Academy of Dental Materials guidance—resin composites: Part II—technique sensitivity. Dent Mater. 2017;33(11):1171-1191. doi:10.1016/j.dental.2017.08.188.

43. Moldovan M, Balazsi R, Soanca A, Roman A, Sarosi C, Prodan D, et al. Evaluation of the degree of conversion, residual monomers and mechanical properties of some light-cured dental resin composites. Materials (Basel). 2019;12(13): 2109. doi: 10.3390/ma12132109.

44. Han X, Chen Y, Jiang Q, Liu X, Chen Y. Novel bioactive glass-modified hybrid composite resin: mechanical properties, biocompatibility, and antibacterial and remineralizing activity. Front Bioeng Biotechnol. 2021;9:661734. doi:10.3389/fbioe.2021.661734.

45. Osorio R, Yamauti M, Sauro S, Watson TF, Toledano M. Experimental resin cements containing bioactive fillers reduce matrix metalloproteinase-mediated dentin collagen degradation. J Endod. 2012;38(9):1227-1232. doi:10.1016/j.joen.2012.05.011.

46. Tjäderhane L, Nascimento FD, Breschi L, Mazzoni A, Tersariol IL, Geraldeli S, et al. Optimizing dentin bond durability: control of collagen degradation by matrix metalloproteinases and cysteine cathepsins. Dent Mater. 2013;29(1):116-135. doi:10.1016/j.dental.2012.08.004.

47. Sahadi BO, Sebold M, André CB, Nima G, Dos Santos A, Chiari MDESC, et al. Effect of experimental dentin etchants on dentin bond strength, metalloproteinase inhibition, and antibiofilm activity. Dent Mater. 2024;40(4):e12-e26. doi: 10.1016/j.dental.2024.02.017.

48. Nosrati R, Kheirouri S, Ghodsi R, Ojaghi H. The effects of zinc treatment on matrix metalloproteinases: a systematic review. J Trace Elem Med Biol. 2019;56:107-115.doi:10.1016/j.jtemb.2019.08.001.

49. Vidal O, de Paris Matos T, Núñez A, Méndez-Bauer L, Sutil E, Ñaupari-Villasante R, et al. A universal adhesive containing copper nanoparticles improves the stability of hybrid layer in a cariogenic oral environment: an in situ study. J Mech Behav Biomed Mater. 2022;126:105017. doi:10.1016/j.jmbbm.2021.105017.

50. Par M, Tarle Z, Hickel R, Ilie N. Mechanical properties of experimental composites containing bioactive glass after artificial aging in water and ethanol. Clin Oral Investig. 2019;23(6). DOI: 10.1007/s00784-018-2713-6.

51. Yao C, Ahmed MH, Li X, Nedeljkovic I, Vandooren J, Mercelis B, et al. Zinc-calcium-fluoride bioglass-based innovative multifunctional dental adhesive with thick adhesive resin film thickness. ACS Appl Mater Interfaces. 2020;12(27):30120-30135. doi:10.1021/acsami.0c06865.

52. Krishnan V, Lakshmi T. Bioglass: a novel biocompatible innovation. J Adv Pharm Technol Res. 2013;4(2):78-83. doi:10.4103/2231-4040.111523.

ANEXO A – APROVAÇÃO DO COMITÊ DE ÉTICA

UNIVERSIDADE ESTADUAL DE PONTA GROSSA - UEPG

Plataforma Brasil

PARECER CONSUBSTANCIADO DO CEP

DADOS DO PROJETO DE PESQUISA

Título da Pesquisa: Efeito da adição de biovidro (45S5) e nanopartículas de cobre e zinco em um sistema adesivo universal na perda de mineral, na atividade das MMPs, e nas propriedades mecânicas da interface adesiva em dentes restaurados com resina composta: um estudo in vitro.

Pesquisador: Alessandro Dourado Loguercio

Área Temática:

Versão: 2

CAAE: 57283022.2.0000.0105

Instituição Proponente: Universidade Estadual de Ponta Grossa

Patrocinador Principal: Financiamento Próprio

DADOS DO PARECER

Número do Parecer: 5.395.921

Apresentação do Projeto:

Este projeto visa aumentar a estabilidade da união adesiva à dentina controlando as MMPs e protegendo a interfase da desmineralização com um adesivo contendo nanopartículas metálicas (NPs) e Biovidro (BG). Objetivo: Avaliar o efeito da adição de Biovidro (BG) num sistema adesivo universal contendo nanoparticulas de cobre e zinco (Cu/ZnNPs), na redução da atividade das MMP-2 e MMP-9, e na perda mineral na região adjacente à interface dente-restauração. Metodologia: será determinada a possível concentração de BG a ser incorporado num adesivo universal com 5 / 0,2% em peso de Cu / Zn NPs, caracterizando suas propriedades. Posteriormente, 160 dentes humanos serão restaurados com RCs utilizando as estratégias adesivas: autocondicionamento (SE), e condicionamento e lavagem (E&R),
separadamente; divididos em grupos (n = 10, grupos; n = 5 subgrupos): grupo 1, controle negativo, adesivo sem carga: SE (C-SE) e E&R (C-ER); grupo 2, ligado com NPs metálicos de Cu / Zn 5 / 0,2% em peso: SE (M-SE) e E&R (M-ER); grupo 3, adesivo carregado com BG: SE (BG-SE) e E&R (BG-ER); e grupo 4, adesivo carregado com NPs Cu / Zn 5 / 0,2% em peso e BG: SE (MBG-SE) e E&R (MBG-ER). Os dentes serão seccionados em blocos quadrangulares (palitos) de 8mm x 3,2mm x 3,2mm. Posteriormente, serão realizadas provas de viabilidade celular, microdureza, Microrradiografia Independente do Comprimento de

Endereço: Av. Gen. Carlos Cavalcanti, nº 4748. UEPG, Campus Uvararanas, Bloco da Reitoria, sala 22
Bairro: Uvaranas **CEP:** 84.030-900
UF: PR **Município:** PONTA GROSSA
Telefone: (42)3220-3282 **E-mail:** propespsecretaria@uepg.br

Onda Transversal (T-WIM), Microtomografia (Micro-CT), Espectroscopia Raman, Microscopia Eletrônica de Emissão de Campo (FESEM) e Zimografia. A distribuição normal dos dados será avaliada. As comparações serão feitas com o teste t de student, ANOVA de medidas repetidas e teste post-hoc (ou seus respectivos testes para análise não paramétrica), serão
calculadas com o teste de Wilcoxon ou correlação ($p < 0,05$). As informações elencadas nos campos "Apresentação do Projeto", "Objetivos da Pesquisa" e "Avaliação
dos Riscos e Benefícios" foram retiradas do arquivo Informações Básicas da Pesquisa
PB_INFORMAÇÕES_BÁSICAS_DO_PROJETO: Título da Pesquisa: Efeito da adição de biovidro (45S5) e nanopartículas de cobre e zinco em um sistema adesivo universal na perda de mineral, na atividade das MMPs, e nas propriedades mecânicas da interface adesiva em dentes restaurados com resina composta: um estudo in vitro. CAAE: 57283022.2.0000.0105
Submetido em: 28/03/2022

Objetivo da Pesquisa:

Objetivo Primário:

Determinar se a adição de biovidro (45S5) em um sistema adesivo universal contendo Cu/ZnNp reduz a atividade das MMP-2 e MMP-9, e a perda de mineral; aumentado as propriedades mecânicas da interfase dente-restauração.

Objetivo Secundário:

1. Desenvolver e caracterizar um sistema adesivo universal contendo Biovidro (45S5) e nanopartículas de cobre e zinco (5/0,2 Zn/Cu % peso) in
vitro.2. Determinar os efeitos mecânicos, bioquímicos e funcionais de um adesivo universal carregado com Biovidro (45S5) juntamente com nanopartículas de cobre e zinco (5 / 0,2 Zn / Cu% peso), em comparação com um adesivo universal convencional in vitro.3. Comparar o efeito do uso de adesivo dental universal carregado com nanopartículas de cobre e zinco (5 / 0,2 Zn / Cu% em peso) e Biovidro (45S5) na viabilidade bacteriana na interfase dente-restauração em dentes restaurados com resina composta submetidos ao desafio cariogênico in vitro.4. Comparar o efeito do uso de adesivo dental universal carregado com nanopartículas de cobre e zinco (5 / 0,2 Zn / Cu% em peso) e Biovidro (45S5) na redução
perda mineral em dentes restaurados com resina composta submetidos ao desafio cariogênico in vitro.5. Comparar o efeito do uso de adesivo dental universal carregado com nanopartículas de cobre e zinco (5 / 0,2 Zn / Cu% em peso) e Biovidro (45S5) na redução da atividade das MMPs 2
e 9 em dentes restaurados com resina composta in vitro.

UNIVERSIDADE ESTADUAL DE PONTA GROSSA - UEPG

Continuação do Parecer: 5.395.921

Avaliação dos Riscos e Benefícios:

Riscos:

-Há riscos para os pesquisadores de contaminação, ferimento com instrumentos cortantes e alergia a materiais utilizados, que devem ser minimizados com a utilização de equipamento de proteção individual (EPI).

Benefícios:

A pesquisa contribuirá para um melhor entendimento sobre a degradação da interface dente-restauração e como controlá-la, isso permitirá acrescentar conhecimento par aumentar a longevidade das restaurações com resina composto, evitando tratamentos repetitivos e gerando um menor gasto no tratamento da doença de cárie dental.

Comentários e Considerações sobre a Pesquisa:

Será uma pesquisa In Vitro , para obtenção do Título de Doutor, do POGRAMA DE PÓS-GRADUAÇÃO STRICTO SENSU EM ODONTOLOGIA / PPGO ÁREAS DE CONCENTRAÇÃO: CLÍNICA INTEGRADA E DENTÍSTICA RESTAURADORA . Serão utilizados 160 dentes do Banco de Dente Humano, do Departamento de Odontologia, da UEPG

Considerações sobre os Termos de apresentação obrigatória:

Conclusões ou Pendências e Lista de Inadequações

Recomendações:

Conclusões ou Pendências e Lista de Inadequações

Conclusões ou Pendências e Lista de Inadequações:

Todos os documentos obrigatórios foram corretamente anexados, como também as demais etapas da pesquisa

Considerações Finais a critério do CEP:

Este parecer foi elaborado baseado nos documentos abaixo relacionados:

Tipo Documento	Arquivo	Postagem	Autor	Situação
Informações Básicas do Projeto	PB_INFORMAÇÕES_BÁSICAS_DO_PROJETO_1915714.pdf	17/04/2022 21:08:29		Aceito
Folha de Rosto	folha_de_rosto_assinada.pdf	17/04/2022	Alessandro	Aceito

Endereço: Av. Gen. Carlos Cavalcanti, nº 4748. UEPG, Campus Uvararanas, Bloco da Reitoria, sala 22
Bairro: Uvaranas **CEP:** 84.030-900
UF: PR **Município:** PONTA GROSSA
Telefone: (42)3220-3282 **E-mail:** propespsecretaria@uepg.br